This pdf file consists of all figures and photographs, and their captions, scanned from Chapters 1 and 2 of:

EXPERIMENTAL GROWTH OF FIBERS AND FIBROUS VEINS

by

Taohong Li

A Dissertation

Submitted to the University at Albany, State University of New York

in Partial Fulfillment of

the Requirements for the Degree of

Doctor of Philosophy

College of Arts & Sciences

Department of Earth & Atmospheric Sciences

2000

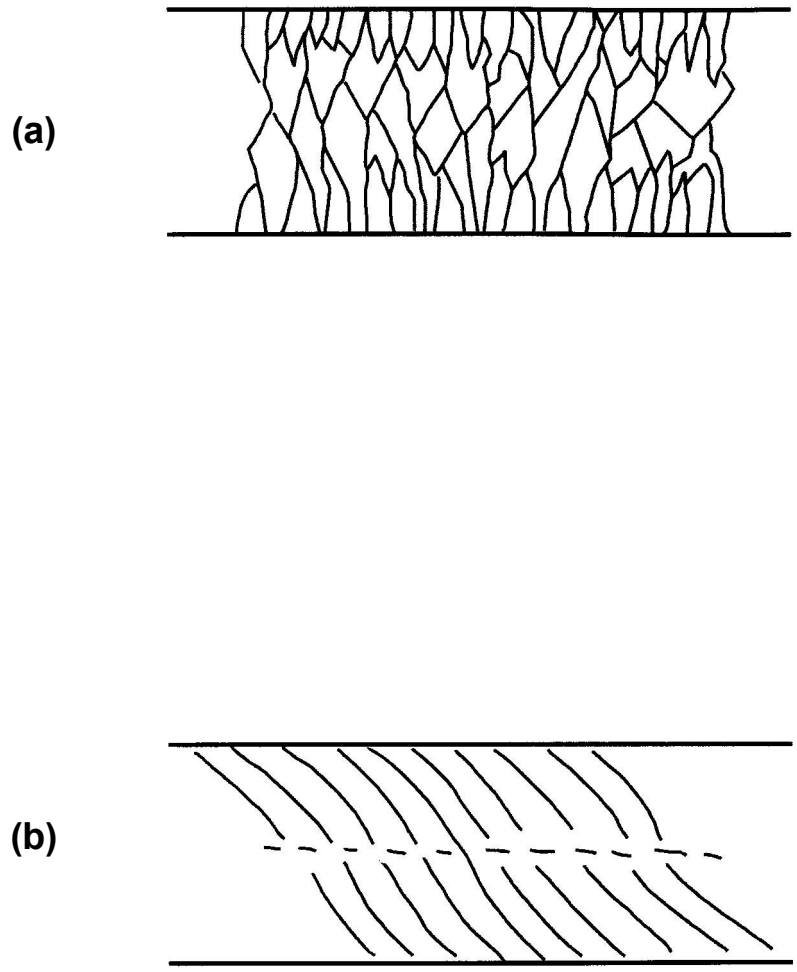

Fig. 1.1 Sketches illustrating two different types of texture of elongated crystals in veins. (**a**) Drusy or comb texture. (**b**) Fibrous texture. See text for discussion.

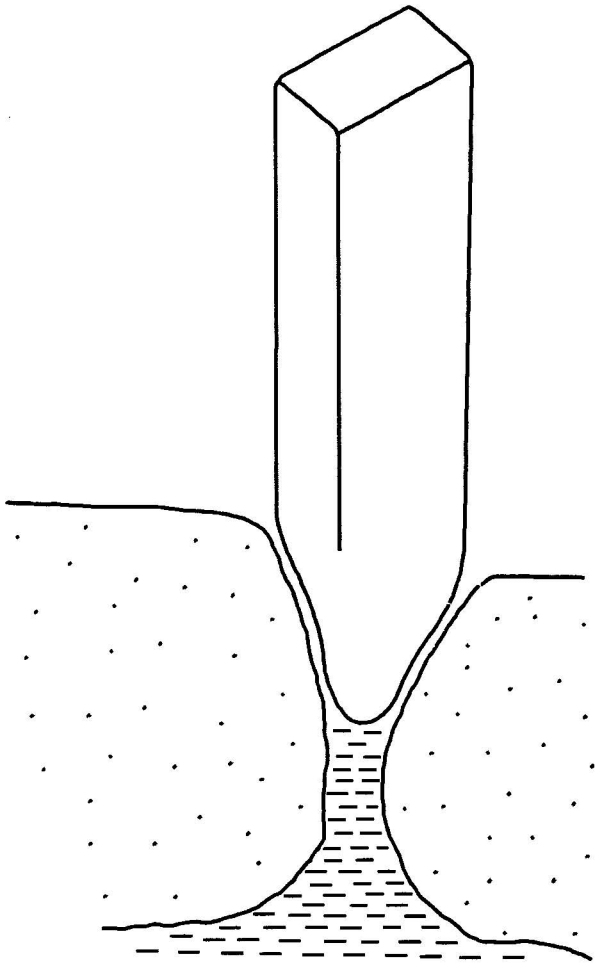

Fig. 1.2 Sketch showing a model of fiber growth on a porous substrate proposed by Berezhkova & Rozhanskii (1963) (see also Givargizov 1987, p.232).

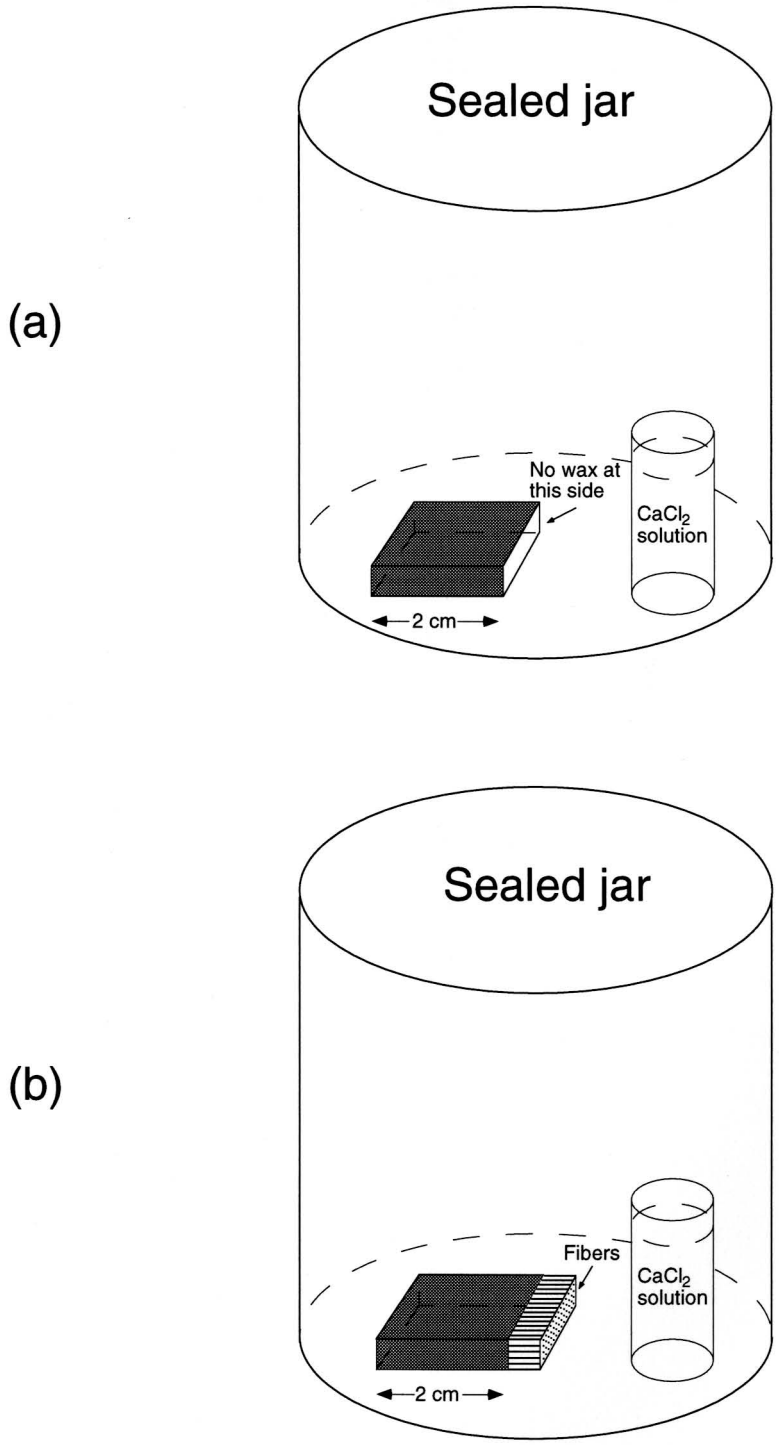

Fig. 2.1 Basic experimental setup for growth of fibers. (**a**) A single ceramic block coated with paraffin wax (shading) with one side uncoated (white) and soaked with a solution of ammonium thiocyanate (NH_4SCN) drying in a closed jar together with a $CaCl_2$ solution. (**b**) The same ceramic block with newly grown fibers on its uncoated side.

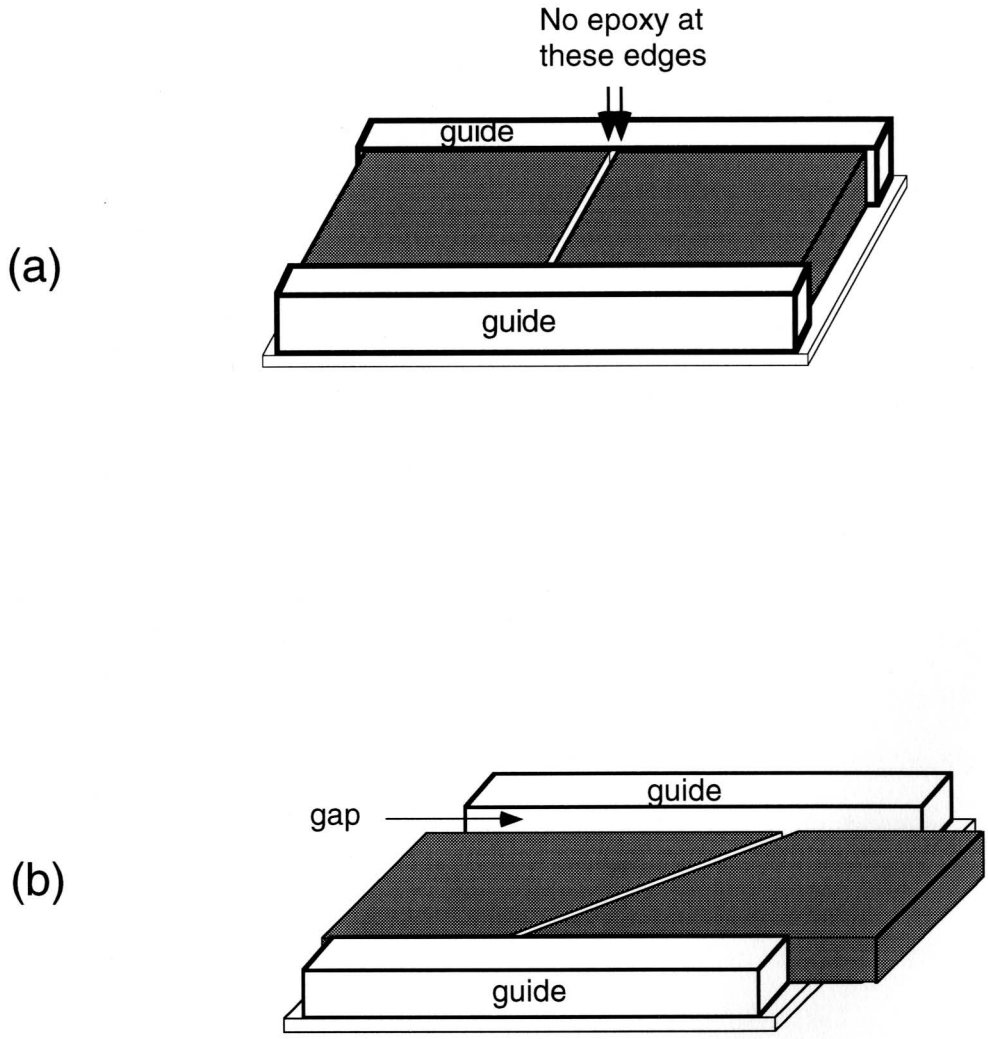

Fig. 2.2 Experimental setups for growth of fibrous veins. (**a**) Two ceramic blocks, coated with epoxy (shaded) and saturated with an inorganic salt solution, are placed against each other on their uncoated sides to form a narrow crack normal to the pair of "guides" cemented to a glass plate below the ceramic blocks. Total length of ceramic blocks is about 3 cm; vertical thickness about 3mm. (**b**) Same as above except the "crack" runs oblique to the guides in order to grow veins of oblique or curved fibers.

(a)

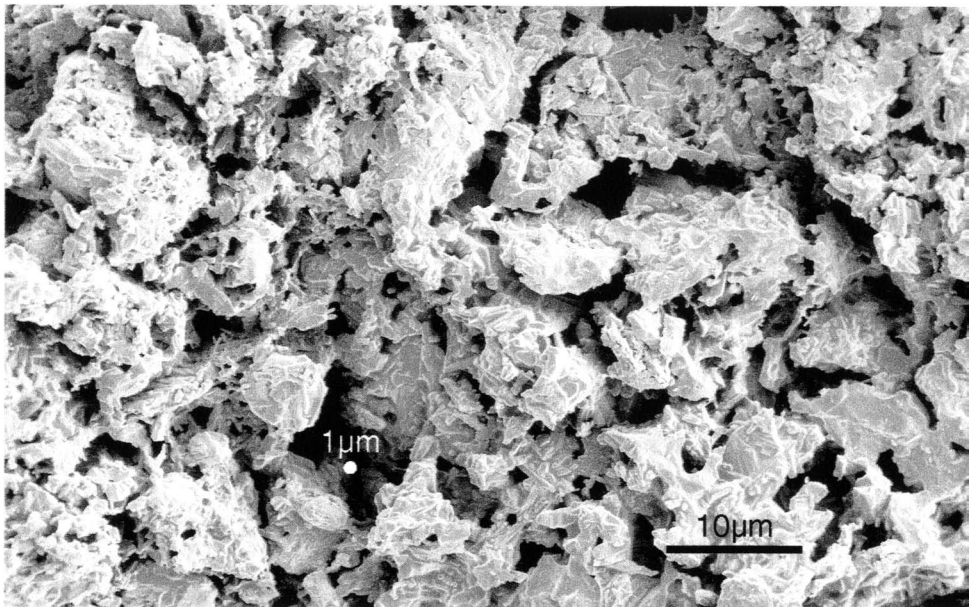

(b)

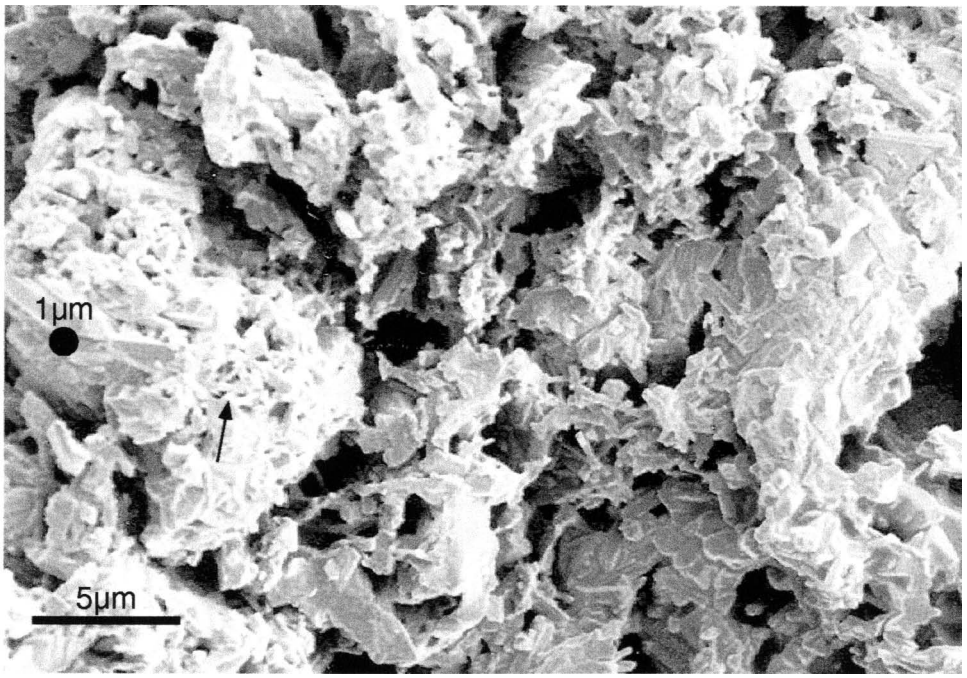

Fig. 2.3 SEM photomicrographs of the fractured surface of the porous material *P-3-C* from Coors Ceramics Co. (**a**) Scale bar is 10μm. (**b**) Scale bar is 5μm. A dot 1μm across is also shown in each picture for visual comparison. Note that besides the large pores in the range of about 1-8μm, there are also abundant minute pores (0.2-1.0μm) within the clumps of grains (one such clump pointed to by arrow).

(a)

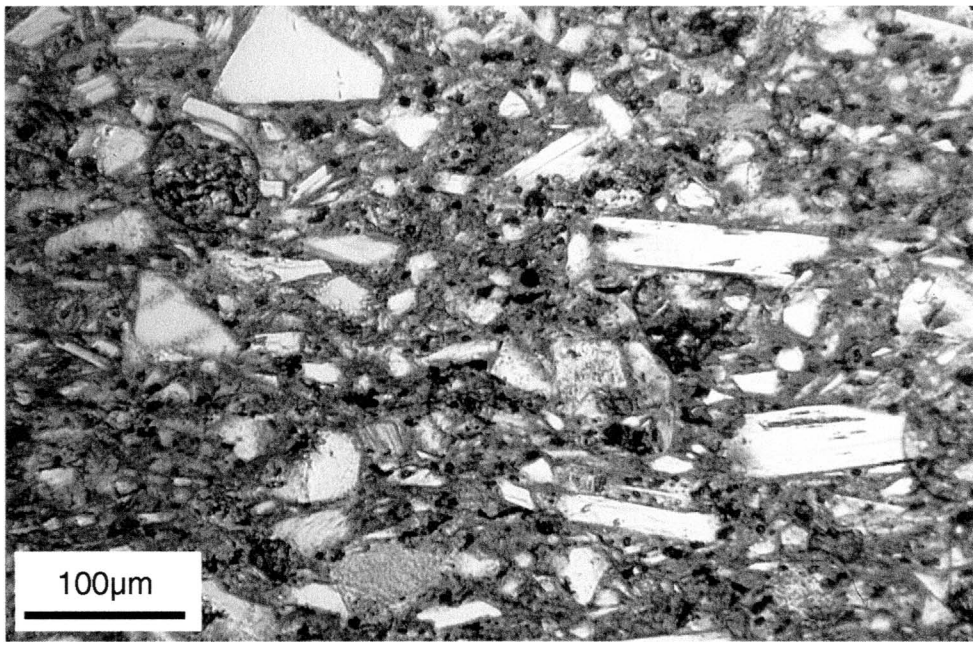

(b)

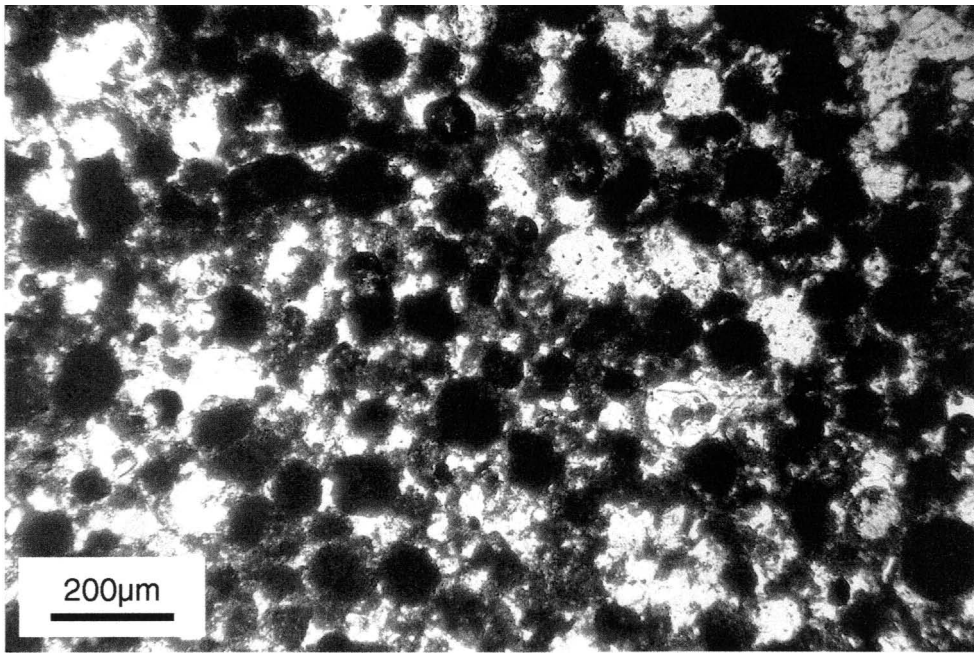

Fig. 2.4 (a) Photomicrograph of the *Big Disc* showing larger angular fragments set in a finer-grained porous matrix. Scale bar is 100μm. (b) Phtomicrograph of *P-20-C* from Coors Ceramics. Scale bar is 200μm. Both are taken in plain transmitted light.

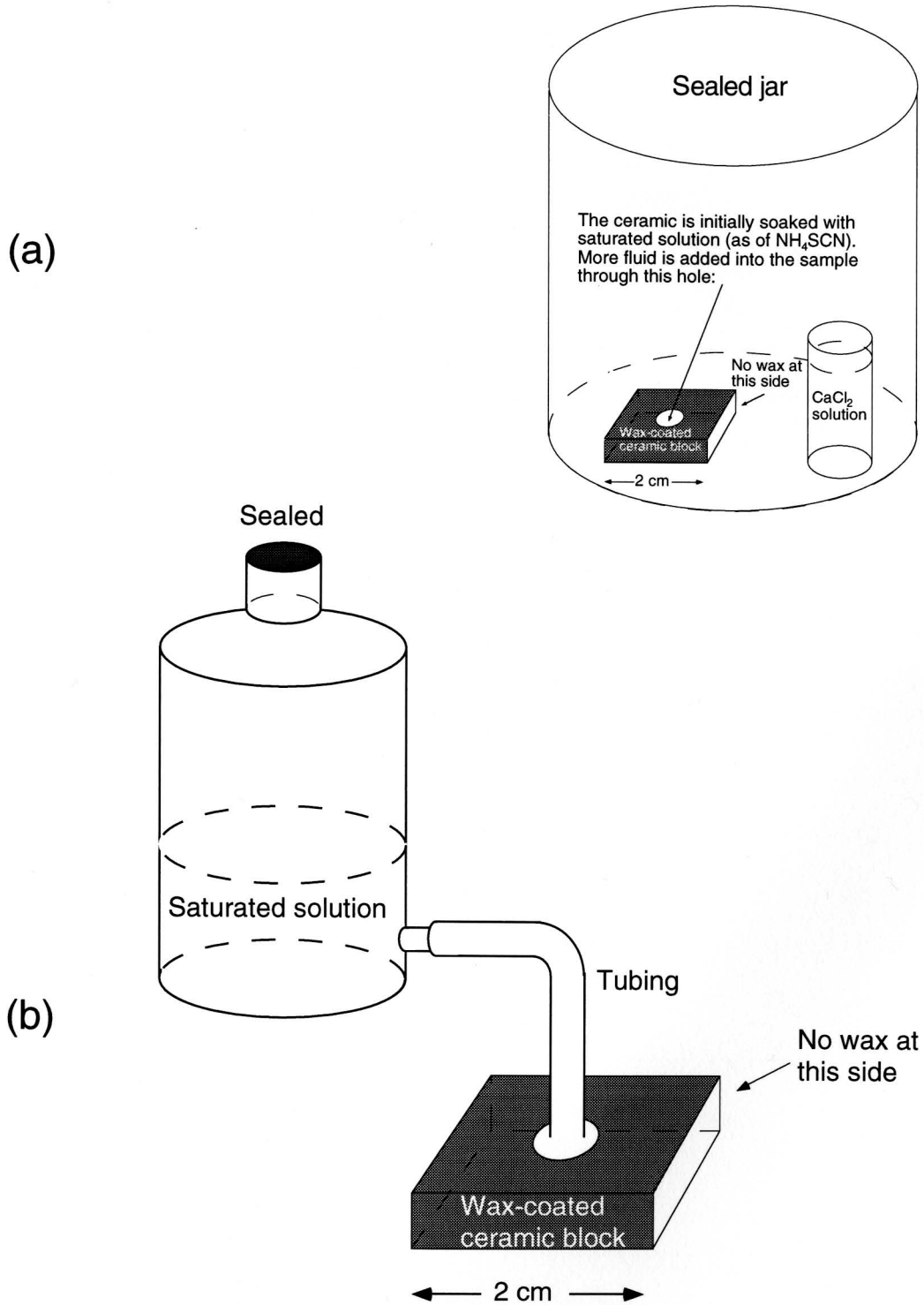

Fig. 2.5 Experimental set-ups for adding more nutrient into the sample during the experiment. In (**a**), a hole is drilled in the top of the sample, through which drops of solution can be added as needed or at a certain time interval during the experiment. In (**b**), the ceramic block is connected through a piece of tubing to a reservoir of the saturated solution of the crystallizing material so the nutrient is continuously supplied to the sample and the degree of saturation is kept constant.

(a)

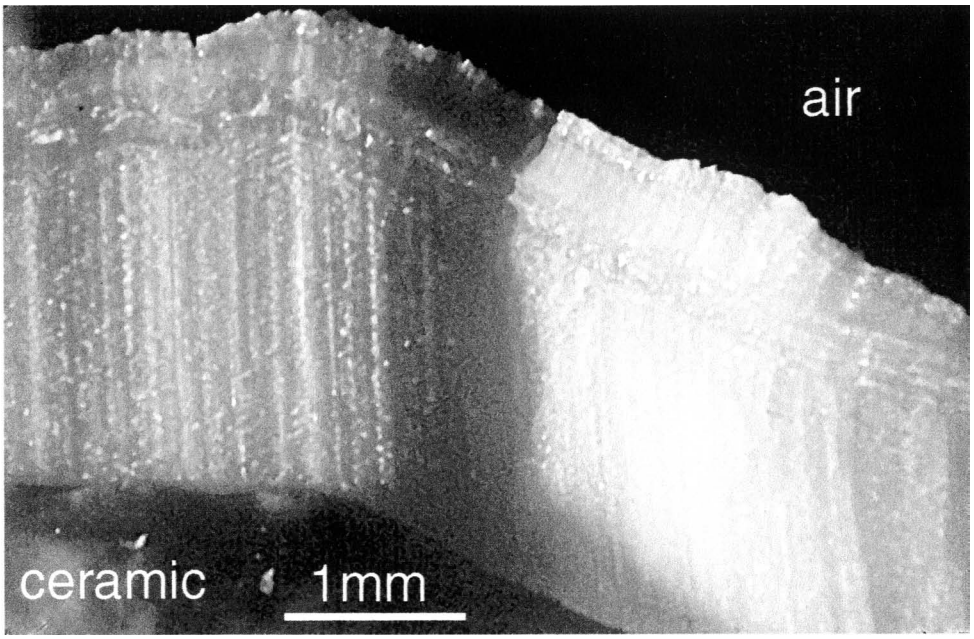

(b)

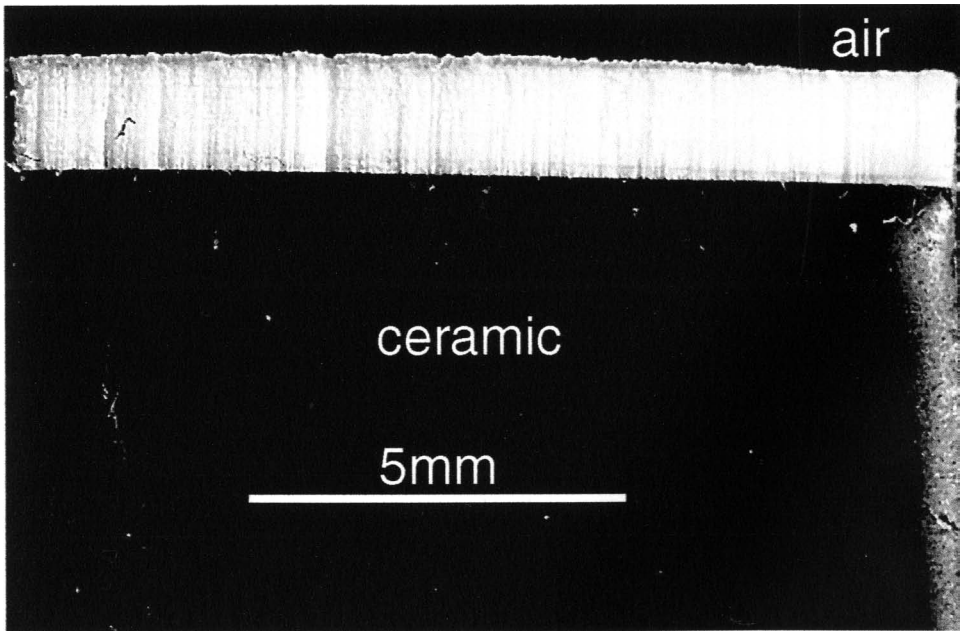

Fig. 2.6 (a) Growth of fibers of ammonium thiocyanate into open space in a single-block experiment (*NFB14*). Ceramic block (*Big Disc*) is coated with wax and growth occurred in an ambient air with a relative humidity of 35-40%. Notice that there is a local step intentionally cut on the growth side of the ceramic block, but overall the fibers are perpendicular to the general outline of the substrate. (b) Growth of ammonium thiocyanate fibers into open space in a single-block experiment (*TB6a*). Ceramic block (*P-3-C*) was painted black and coated with epoxy and growth occurred over a period of about 4 days in an ambient relative humidity of about 20-25%.

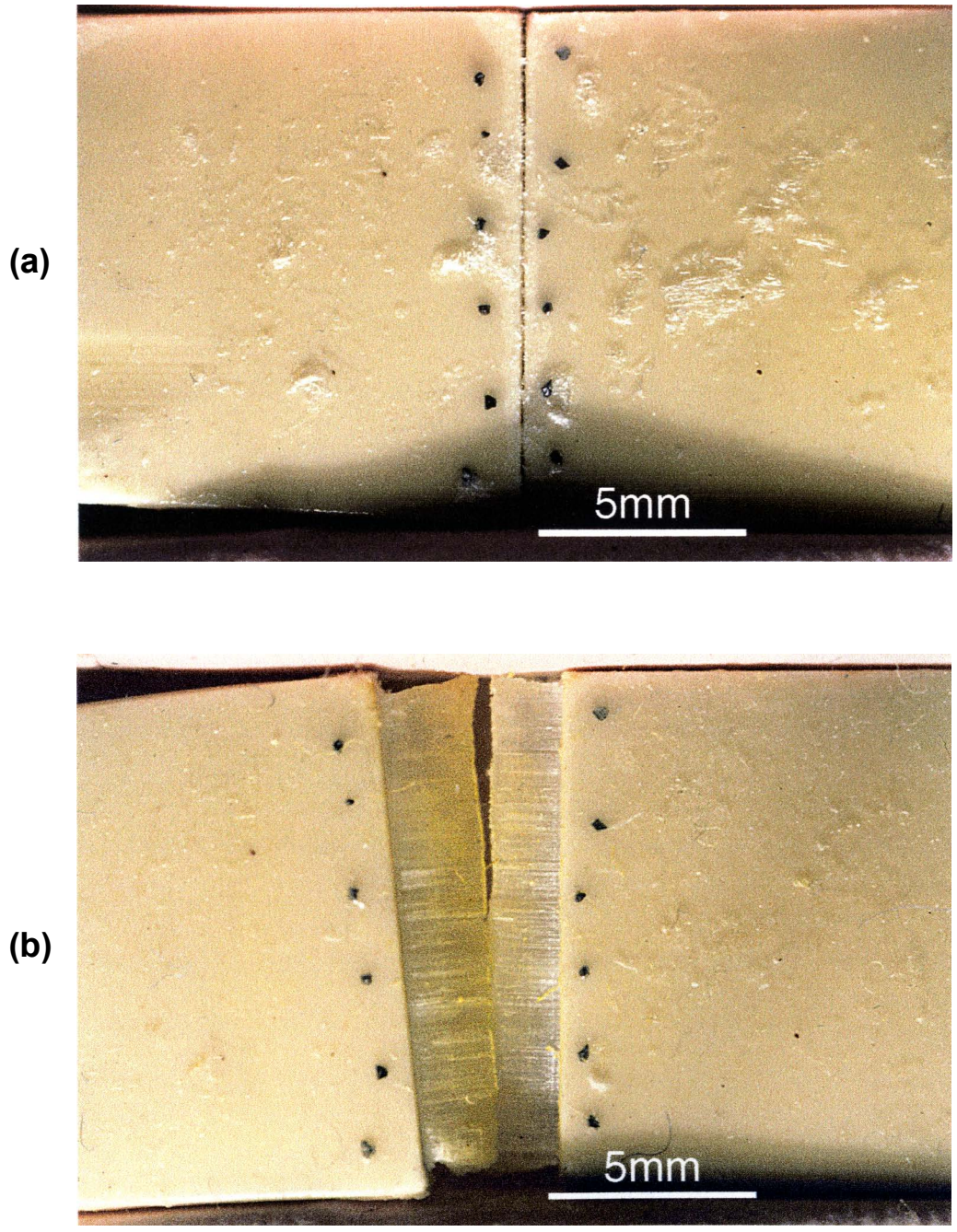

Fig. 2.7 An experimental fibrous vein of ammonium thiocyanate (*CFB-25*) grown into narrow space by pushing apart the enclosing walls. The blocks of ceramic (*Square*) were coated with epoxy together with some tiny black spots embedded alongside of the uncoated edges as markers for the purpose of reconstructing the displacement history of the vein. (a) The initial state of the sample showing only a narrow crack between the blocks. (b) A widened vein of fibers after 85 days of growth in an ambient air of about 20% of relative humidity. Notice a gap exists between the two halves of vein at the top of the vein.

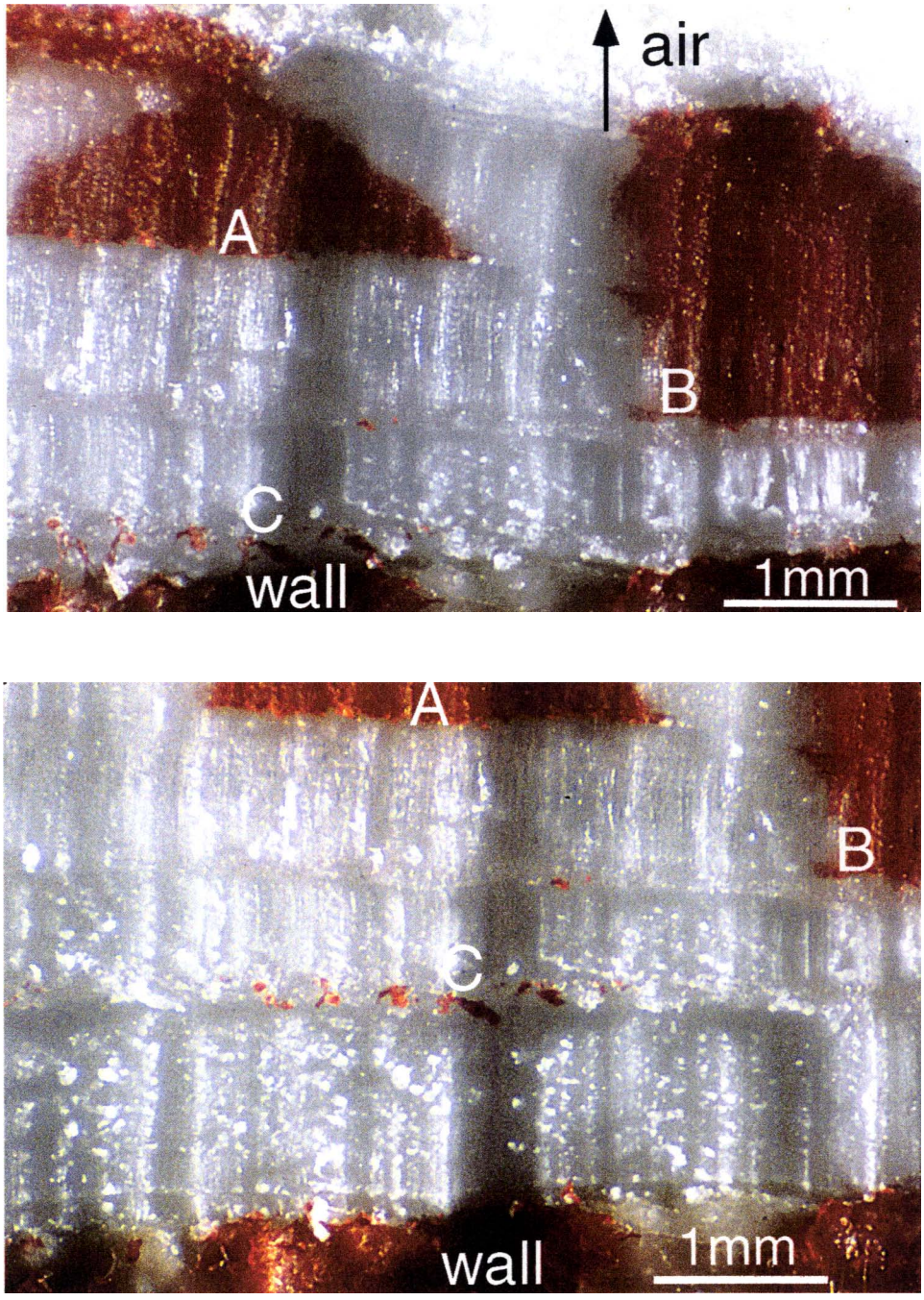

Fig. 2.8 Antitaxial growth of fibers of ammonium thiocyanate in single-block experiment *FB28*. Sample (*Big Disc*) is coated with wax and growth occurred in an ambient air with a relative humidity of 35-40%. **A** is a red ink marker placed across the fiber/wall interface on the 3rd day of the fiber growth stage of experiment. **B** is another ink marker placed on the 4th day of fiber growth and **C** is a piece of ink and/or wax broken off and displaced away from the wall by fiber growth. (a) shows the fibers seen on the 12th day since fibers first started to grow, when **B** and **C** were closer to the wall. (b) shows more growth three days later which has rifted all the older features away from the wall.

(a)

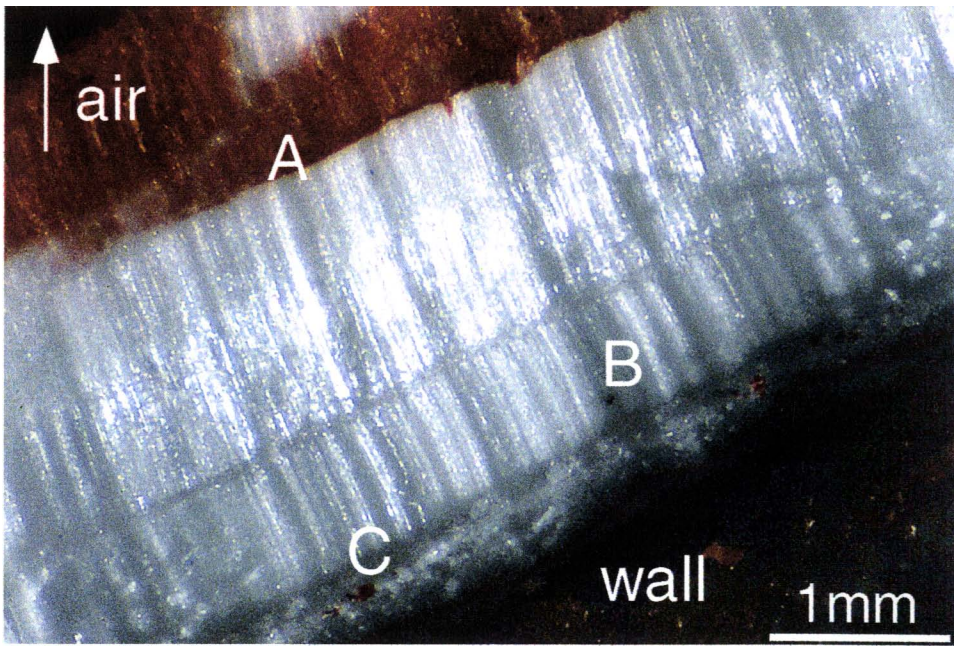

(b)

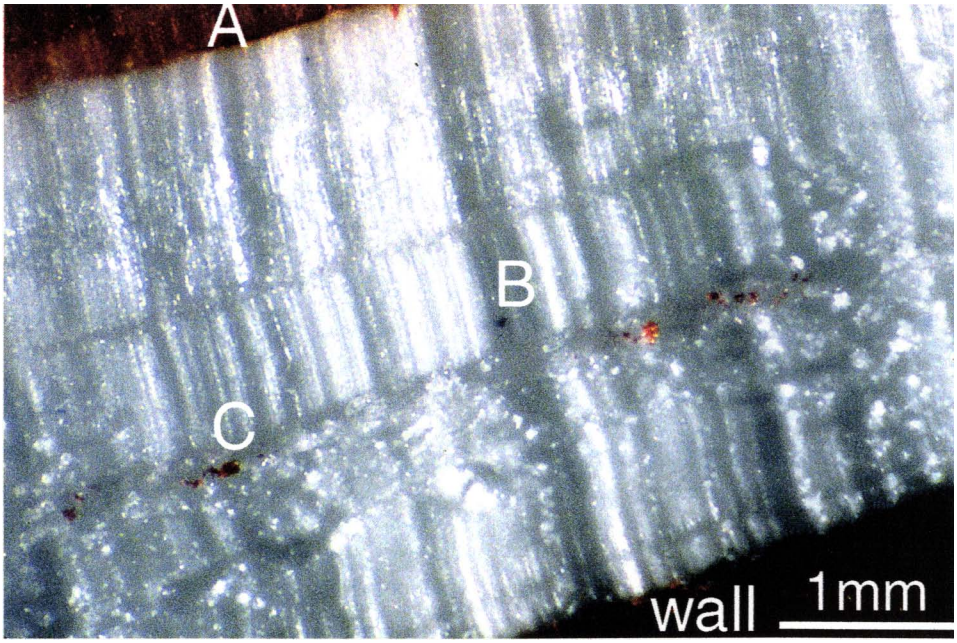

Fig. 2.9 Antitaxial growth of fibers of ammonium thiocyanate in single-block experiment *FB28*. Sample (*Big Disc*) is coated with wax except on the growth side. Growth occurred in an ambient air of 35-40% RH. **A** represents a red ink marker placed across the fiber/wall interface on the 2nd day of the fiber growth stage. **B** and **C** are pieces of red ink and/or wax broken off and displaced away from the wall by fiber growth. (a) shows fibers of good quality seen on the 12th day since fibers first started to grow, when **B** and **C** were closer to the wall. (b) shows more fiber growth of poorer character 3 days later which has rifted all the older features away from the wall.

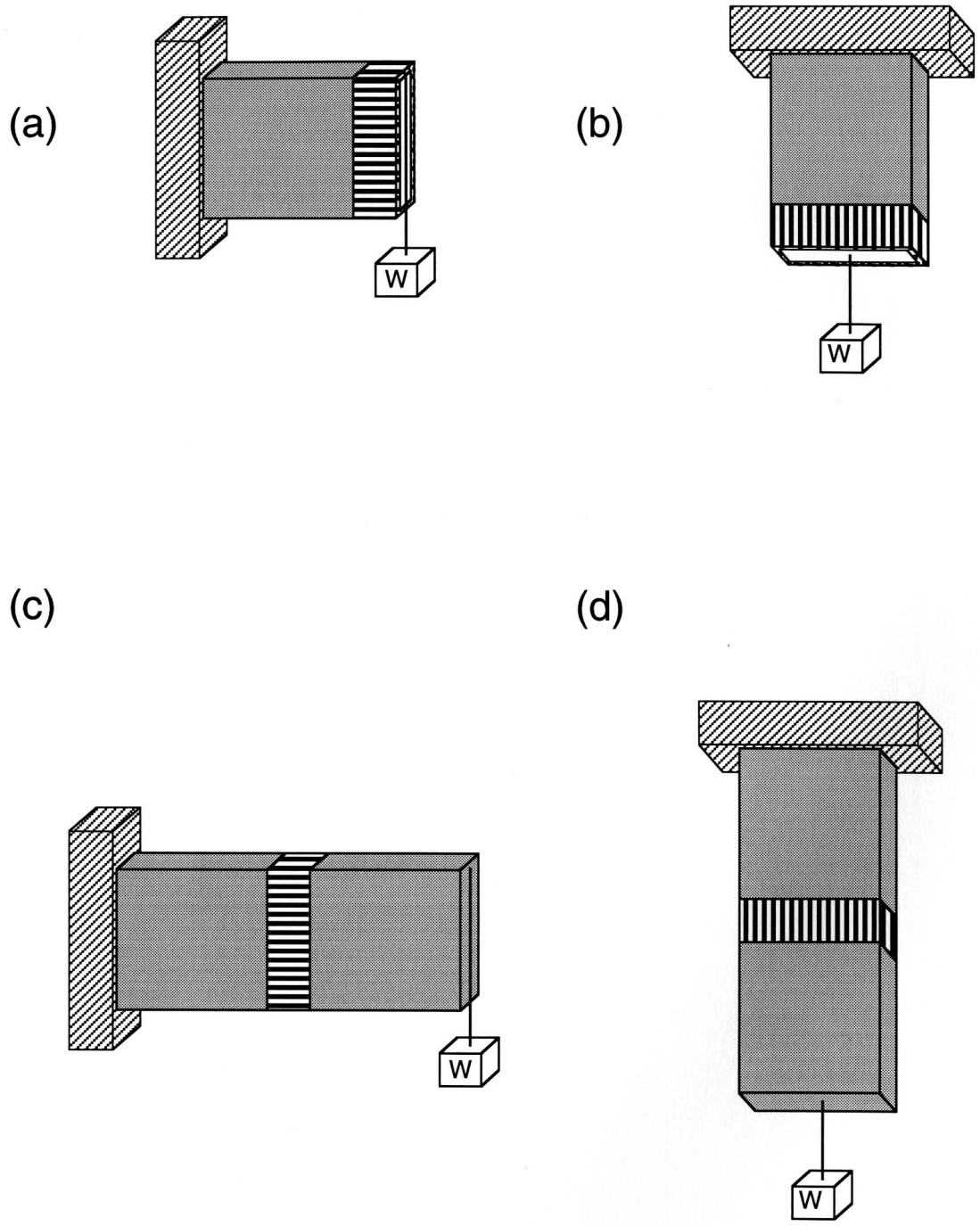

Fig. 2.10 Single-block (a and b) and two-block (c and d) fiber growth experiments with shear (a and c) and extensional (b and d) loading. Ceramic block (shaded) is fixed on some object (hatched) while a dead weight (**W**) is imposed on the fiber ends or the other ceramic block when fibers have started to grow. To ensure homogeneous loading in (a) and (b), the fiber ends are glued or taped together before the dead weight is imposed on the sample. If the dead weight is not too heavy, fibers will continue to grow without any fracture or detachment occurring at the fiber-ceramic interface. Length of ceramic block is about 2 cm.

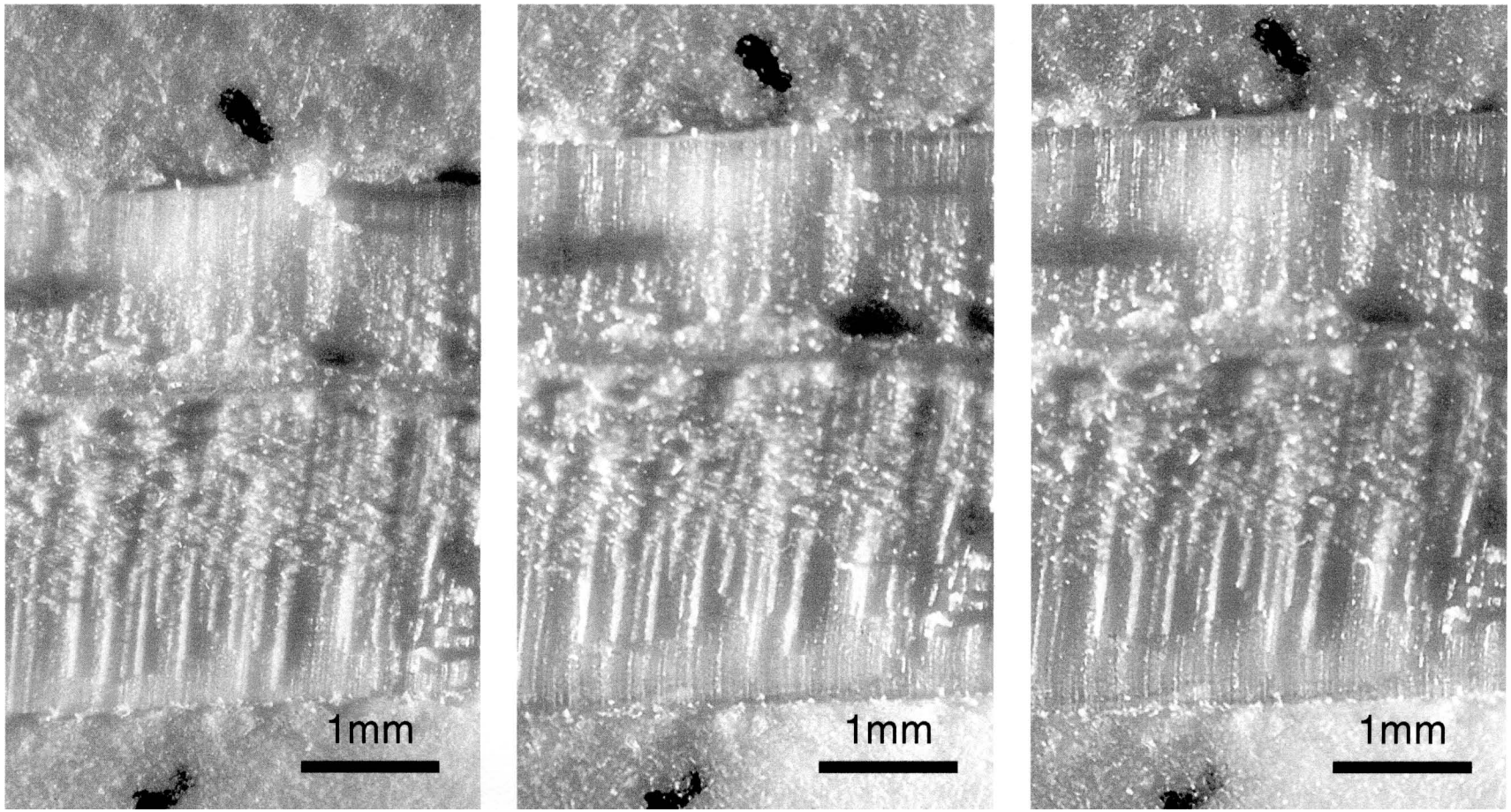

Fig. 2.11 Cohesive growth of fibers of sodium nitrate (*$NaNO_3$*) in a two-block experiment (*DW-20*) with dead-weight loading. Ceramic (*Square*) blocks were coated with epoxy except on the growth side and growth occurred at room air humidity. Shown in (a) through (c) are three later successive stages of shear and extensional loading and vein growth. From (a) to (b) sample was subjected to a shear loading of 150 g/cm^2 for about 68 hours while from (b) to (c) it was subjected to an extensional loading (same magnitude as shear) for 44 hours. No discontinuities or cracks are seen in the younger growth (fresh fibers near ceramic wall) in (b) or (c). Black spots on ceramic blocks are ink markers placed on them for the purpose of reconstructing vein displacement histories.

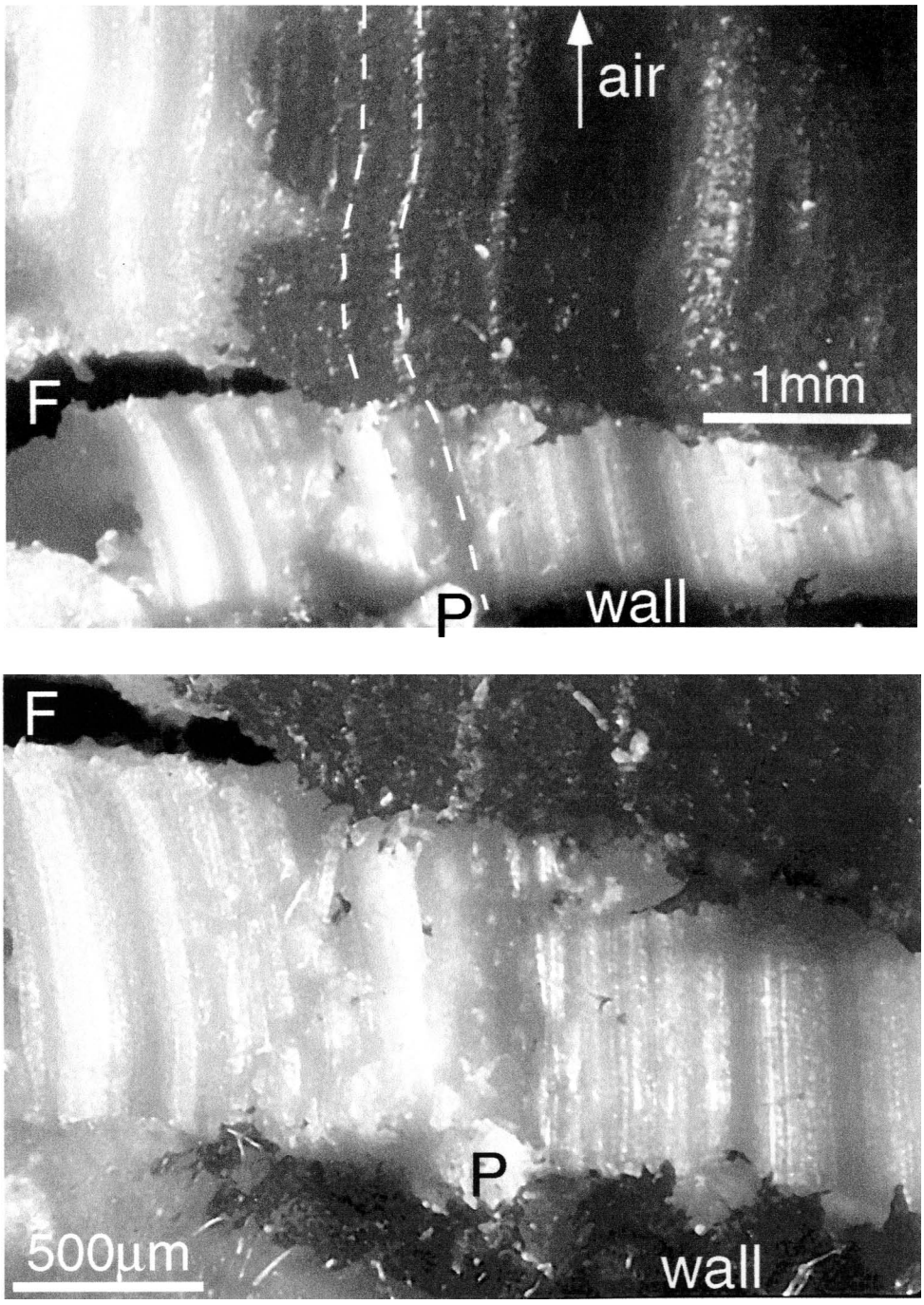

Fig. 2.12 Growth of curved fibers of NH_4SCN on fixed points in ceramic wall (*Big Disc*, coated with wax) under shear conditions in a single-block experiment (*NFB-7a*). Shear was imposed on older fibers (wax-painted) by other growing fibers (out of picture on the right) competing for space and pushing from right to left, causing younger fibers (clean without wax) to grow in oblique or curved patterns and giving rise to a fracture (**F**) between the older and younger fibers. Notice that the fracture occurs in the already formed fibers and is still propagating from left to right, whereas the growth interface is always cohesive so that fibers always grow on the same points in the wall. Outlined in (a) is one such fiber or fiber aggregate (dashed lines) which has always grown from the point marked by a small mass of granular growth (**P**) in the wall. (b) is a close-up view of the younger growth part of (a).

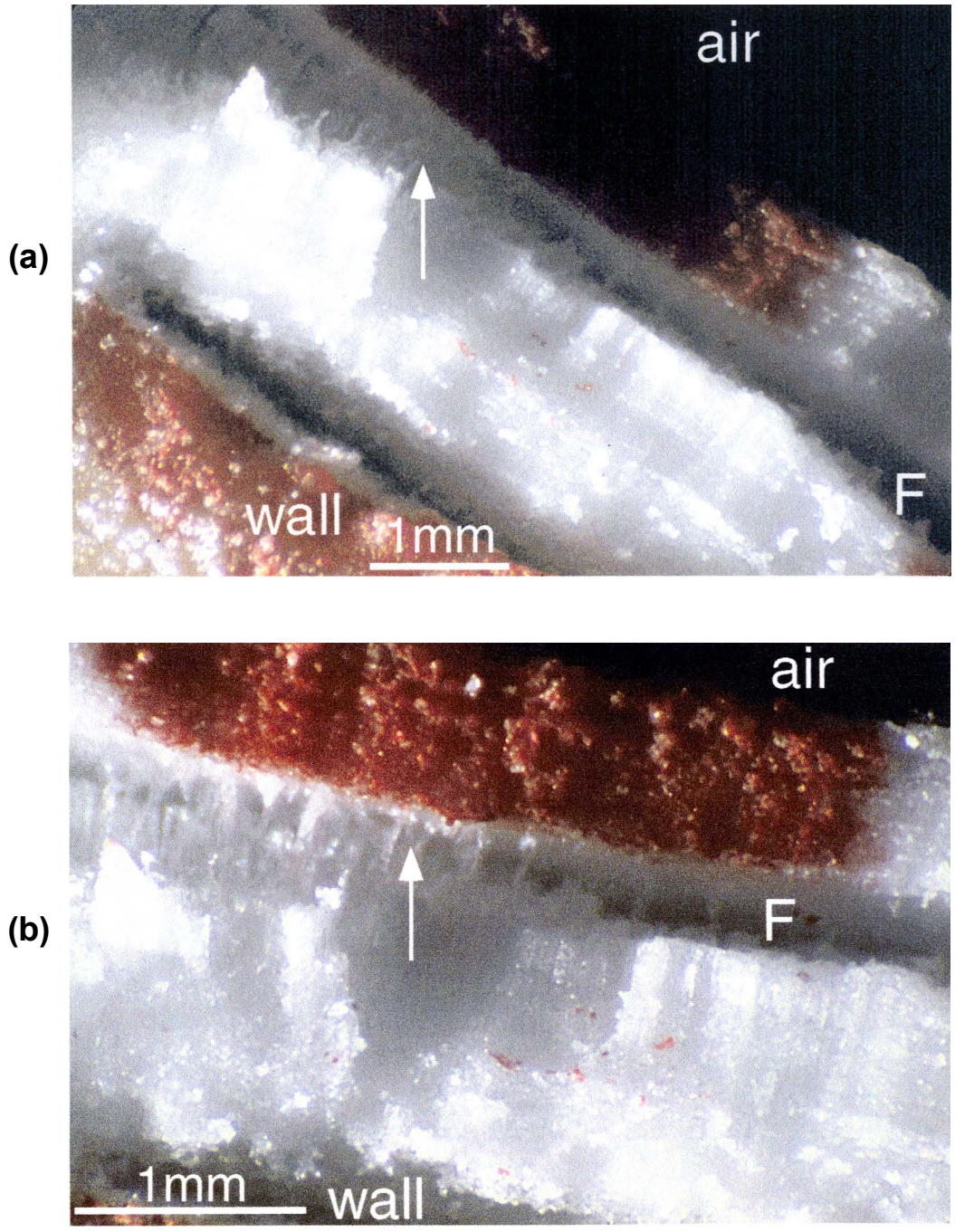

Fig. 2.13 A pronounced transverse discontinuity (F) across the fibers of NH_4SCN of a single-block experiment (*FB27*) which appeared 6 days before at the old fiber-wall contact due to too rapid injection of fluid into the sample and a small left-lateral shear loading (ca. 2 gm/cm^2) imposed on the older fibers (ink-marked, dark). The fracture has now been pushed away from the wall by younger fibers (bright, without ink). Although some younger fibers appear to be connected with the older fibers (arrow) in the crack, most fibers were completely broken and the crack was not filled with any further growth. (b) is a close-up of the same view as in (a).

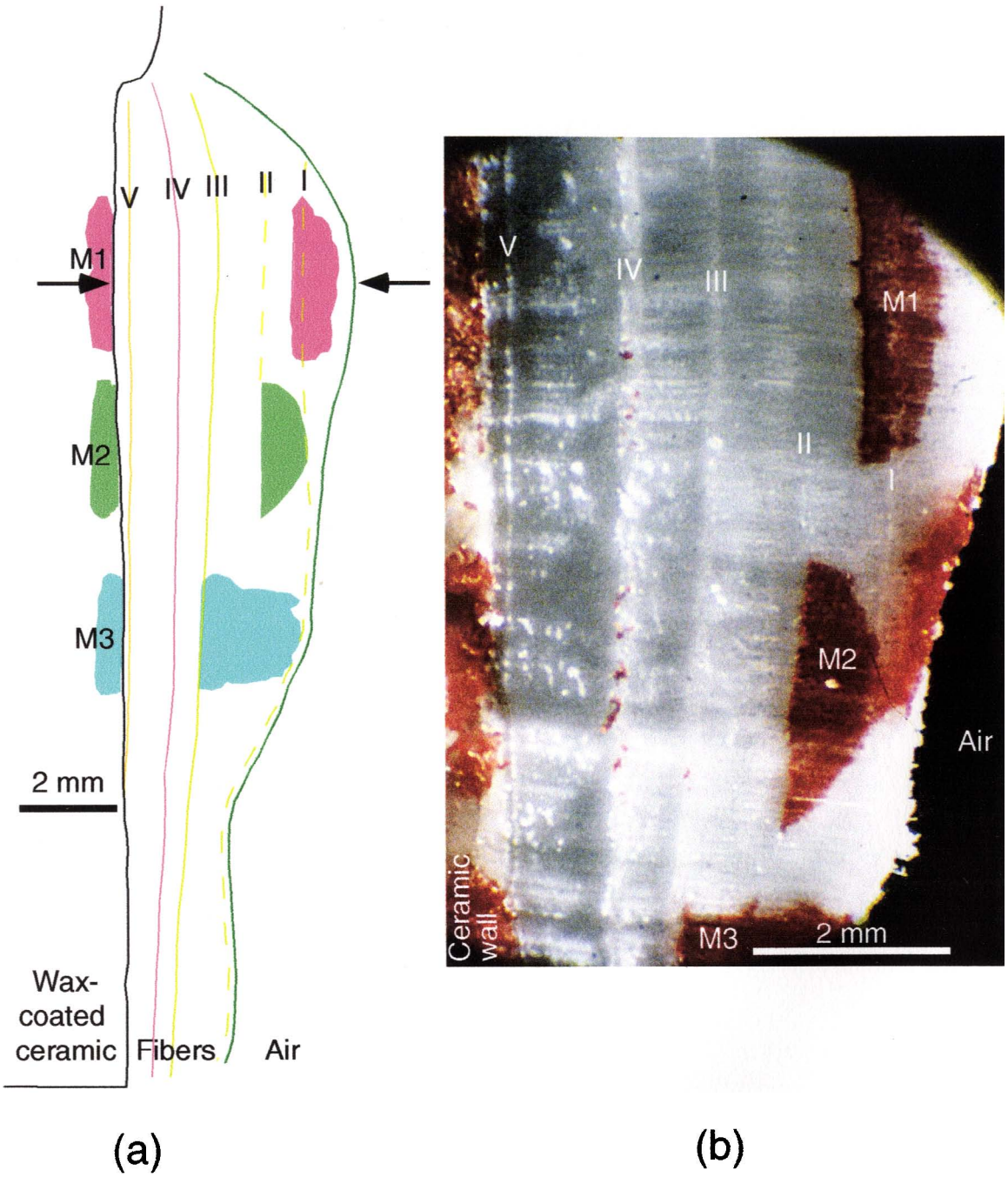

Fig. 2.14 (a) Sketch of sample of single-block experiment (*FB-28*) on the 14th day since the first appearance of fibers. Ink markers (**M1**, **M2**, **M3**) were placed across the fiber/wall interface at three different times, **M1** on the 2nd day, **M2** on the third day and **M3** on the fourth day since fibers first started to grow. They have now all been broken apart by fiber growth and displaced by varying distances away from the wall as shown. Five major transverse discontinuities are seen across the fibers (**I**, **II**, **III**, **IV** & **V**) , developed as a result of temporary interruption of fiber growth due mainly to too much crystallizing fluid added into sample during experiment (see Fig. 2.15). Arrows indicate the position at which measurements of thicknesses of the six fiber growth increments were made. (b) Photograph showing the main part of sample on a larger scale. Of the 5 tranverse discontinuities, the fourth one (**IV**) is the most conspicuous, marked by a thick seam of granular material as well as a line of solid inclusions (aligned black spots) which are actually pieces of pen ink and/or wax derived from the wax-coated and ink-marked wall during the antitaxial fiber growth.

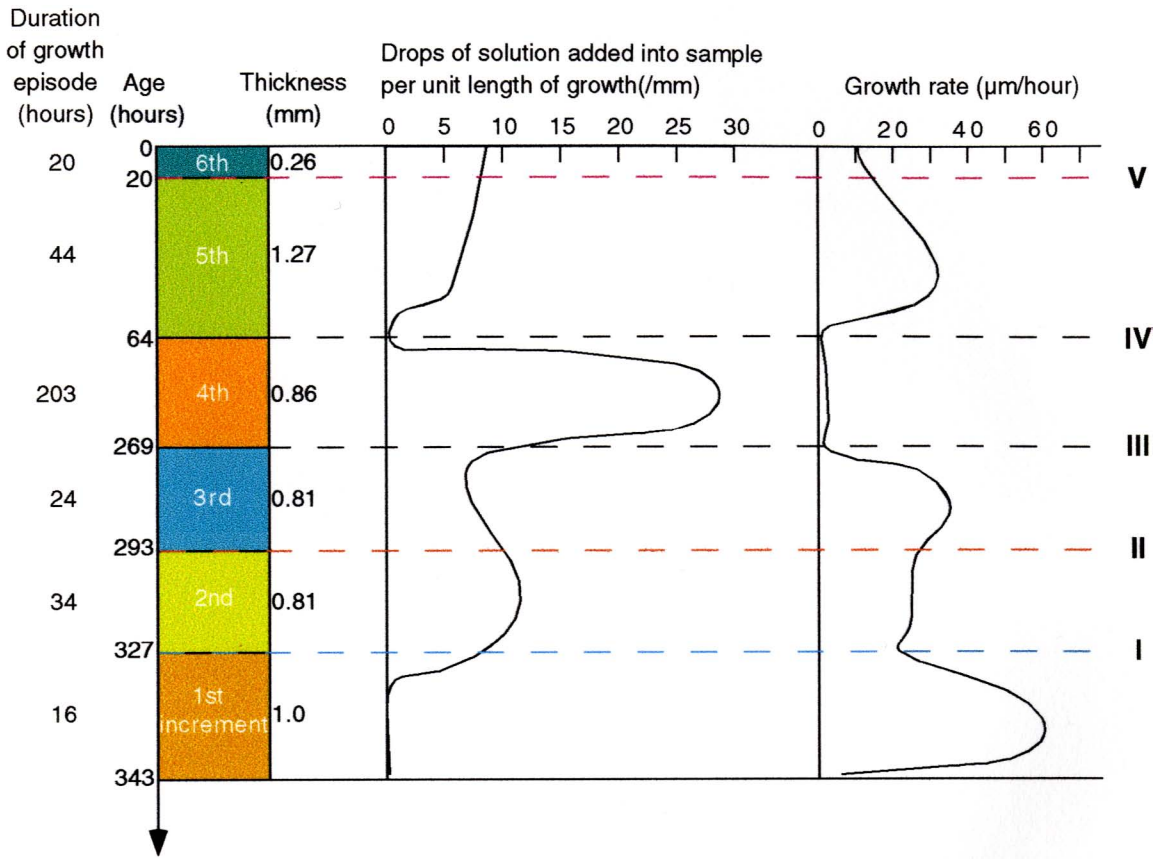

Fig. 2.15 'Stratigraphy' of the fibers of sample *FB28* shown in Fig. 2.14 compared with the histories of addition of crystallizing fluid and fiber linear growth rate. The divisions of the columnar section represent the six major fiber growth increments separated by the five transverse discontinuities numbered **I**, **II**, **III**, **IV** and **V** as shown in Fig. 2.14. Their different thicknesses are drawn to scale, and the corresponding numbers are given on the right side, as measured through the fibers at the position shown in Fig. 2.14. On the left side of the column are the ages of the boundaries and the durations of the growth bands. The first curve on the right shows the history of addition of more fluid into sample during the experiment in terms of the number of drops of fluid added over a certain interval of time divided by the corresponding growth length, while the second curve shows the growth length divided by the corresponding duration of time. Since the measurements were made over intervals of at least 6~10 hours, the details across the minor discontinuities (**I**, **II** and **V**) could not be resolved so the curves may not show the true values at these positions. However, the pauses of fiber growth at the two major discontinuities **III** and **IV** are clearly represented and the correlation is clearly shown between intervals of relatively fast fluid addition and relativly slow rate of fiber growth (e.g. band 4 and band 2). In particular, both of the two most prominant discontinuities (**III** and **IV**) were preceded by a period of fast fluid addition but relatively slow fiber growth.

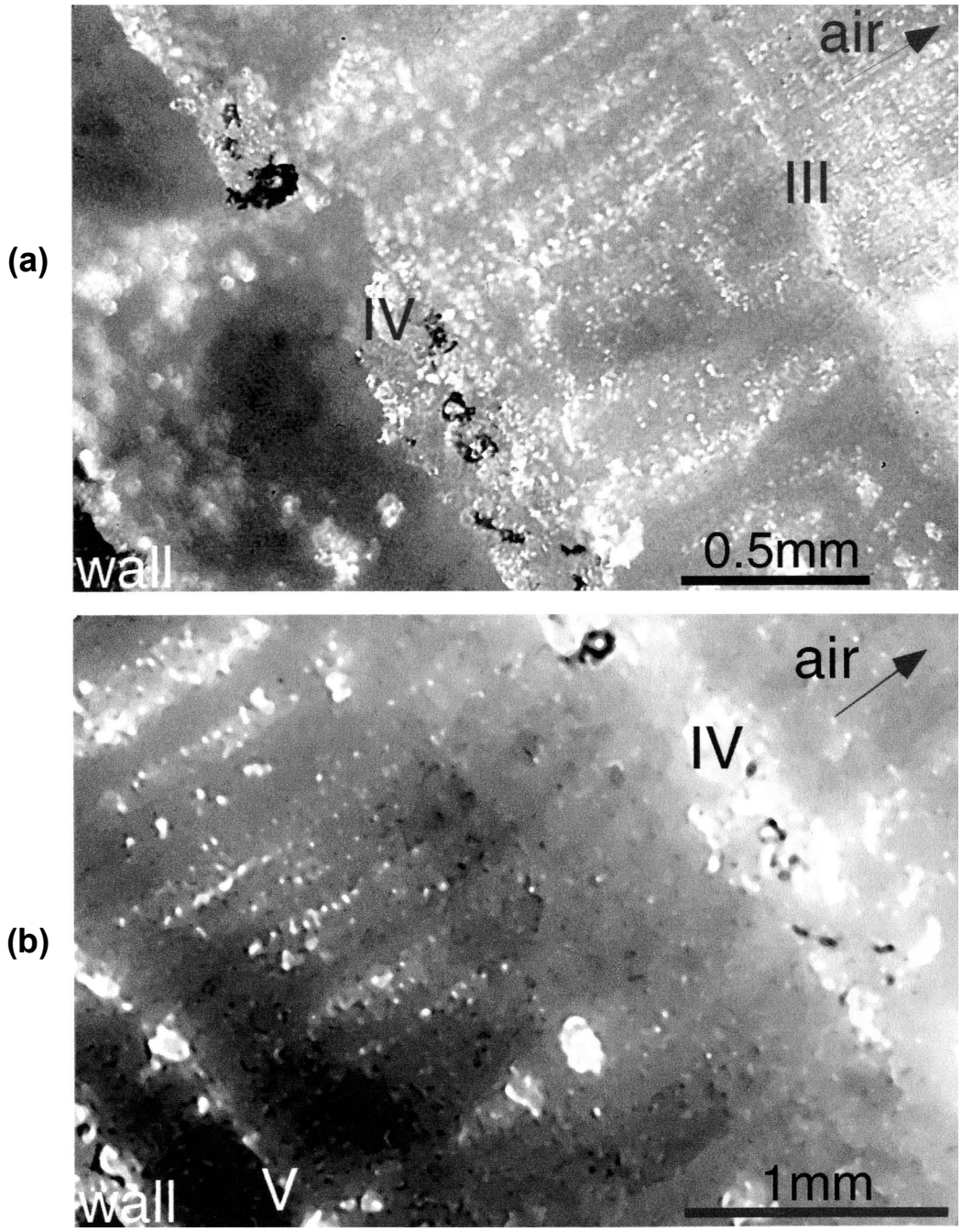

Fig. 2.16 Details of the formation of transverse discontinuity **IV** in Fig. 2.14. Two of the discontinuities in Fig. 2.14 are shown in (a), of which the younger one (**IV**, marked by a seam of granular crystals together with some pieces of wax (black spots) broken off the wax-coated ceramic wall during growth) is still in its period of formation with complete termination of fiber growth and temporary loss of cohesion at the fiber-wall contact. Seen near the wall is a void filled with some granular growth. Photo taken at time 64 hours (see Fig. 2.15). (b) shows the same discontinuity as seen 64 hours later, when fiber growth has renewed and more fibers have grown which have displaced this feature away from the wall, flattened any void and granular material close to it, and finally preserved it as a thick ridge-like feature in the sample. Also seen in (a) is another older dicontinuity (**III**) and in (b) a new discontinuity (**V**), both also marked by interruption in the continuity of fibers and concentration of granular crystals.

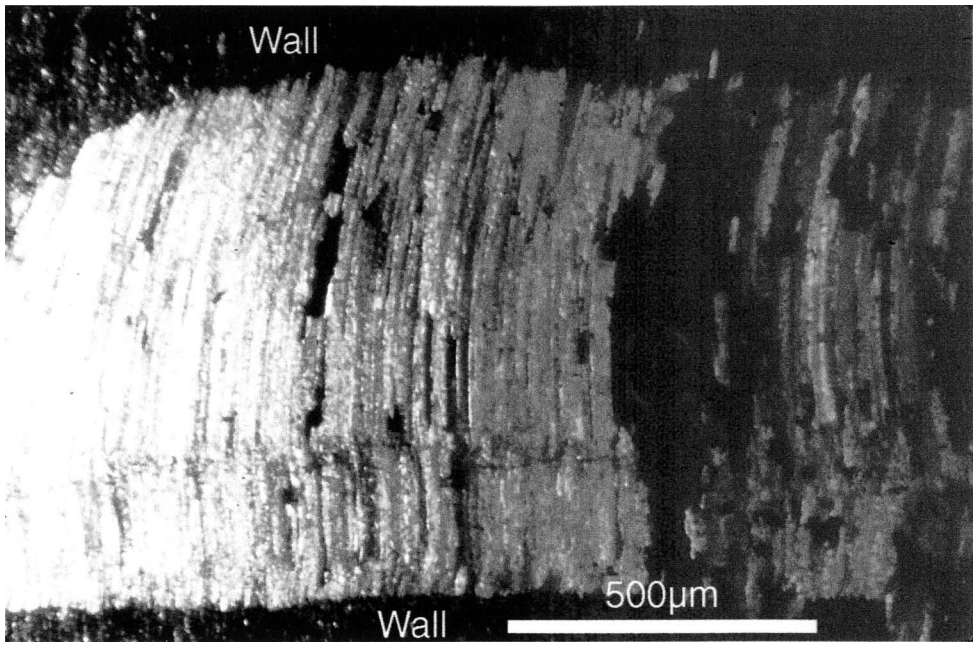

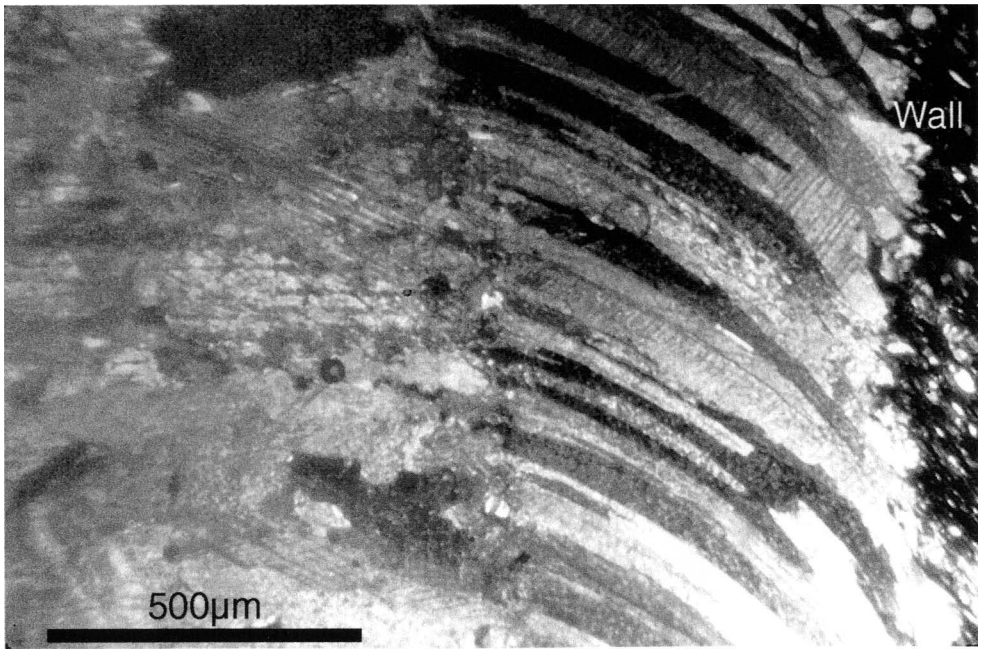

Fig. 2.17 Natural fibrous veins with Type I transverse discontinuities. (**a**) Micrograph of an asymmetric vein of calcite fibers in a slate from the Taconic belt, New York. A Type I transverse discontinuity is visible, which can either be a median line or simply a discontinuity in one side of the vein. (**b**) Micrograph of another vein of calcite fibers from the same locality, showing a Type I transverse discontinuity separating younger curved fibers from the older poorly fibrous crystals (left). Both photos taken in crossed nicols.

(c)

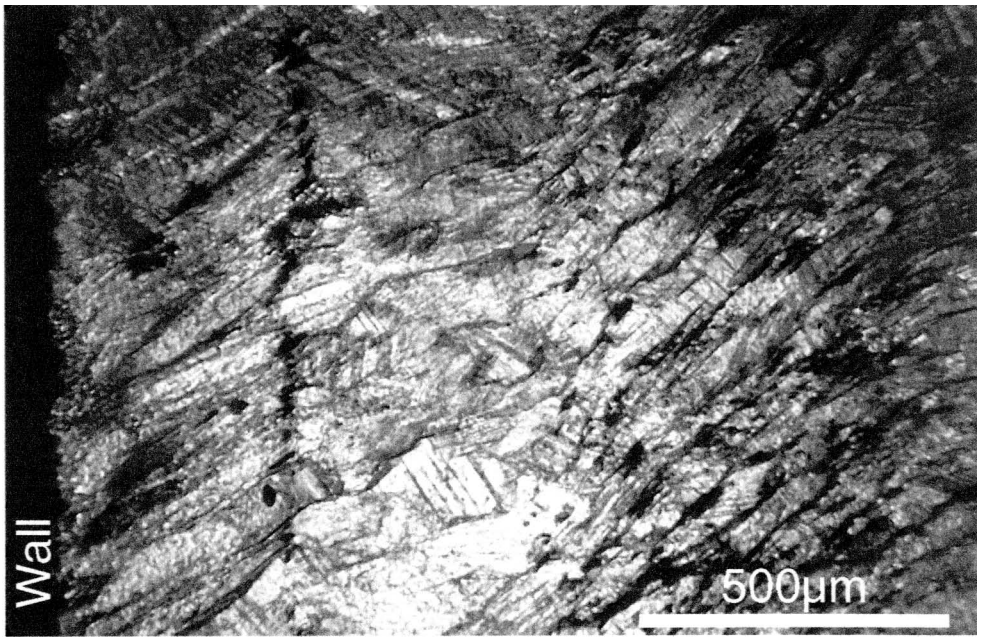

(d)

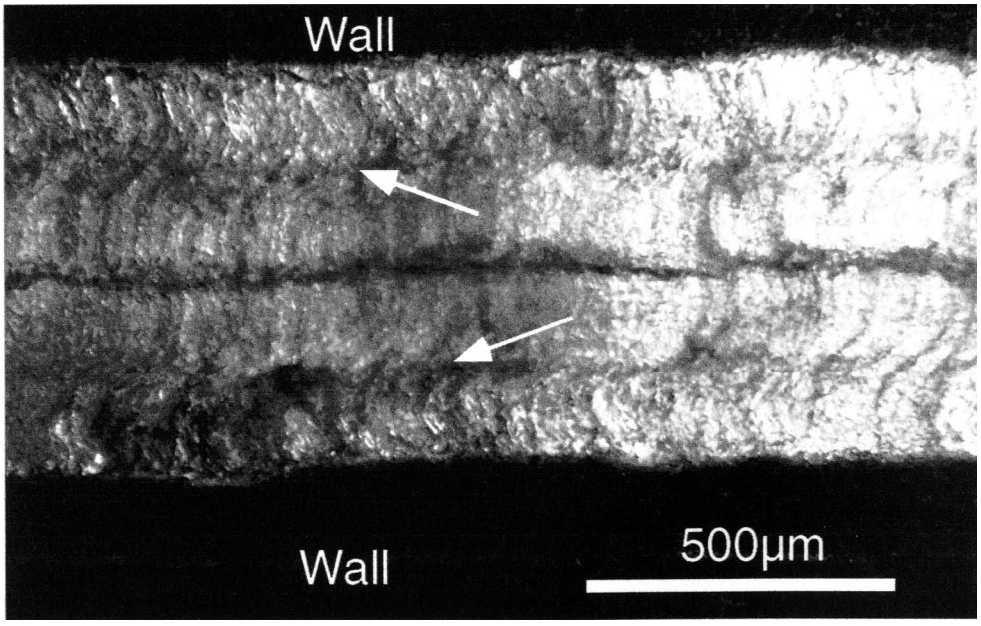

Fig. 2.17 (continued) (**c**) Micrograph of a vein of calcite fibers in a slate from the Taconic belt, New York. A Type I transverse discontinuity is visible, (**d**) Micrograph of a symmetrical vein of calcite fibers from the same locality, showing both a median suture (Ramsay 1980) and a less conspicuous Type I transverse discontinuity on both sides of the vein (arrow). Both photos taken in crossed nicols.

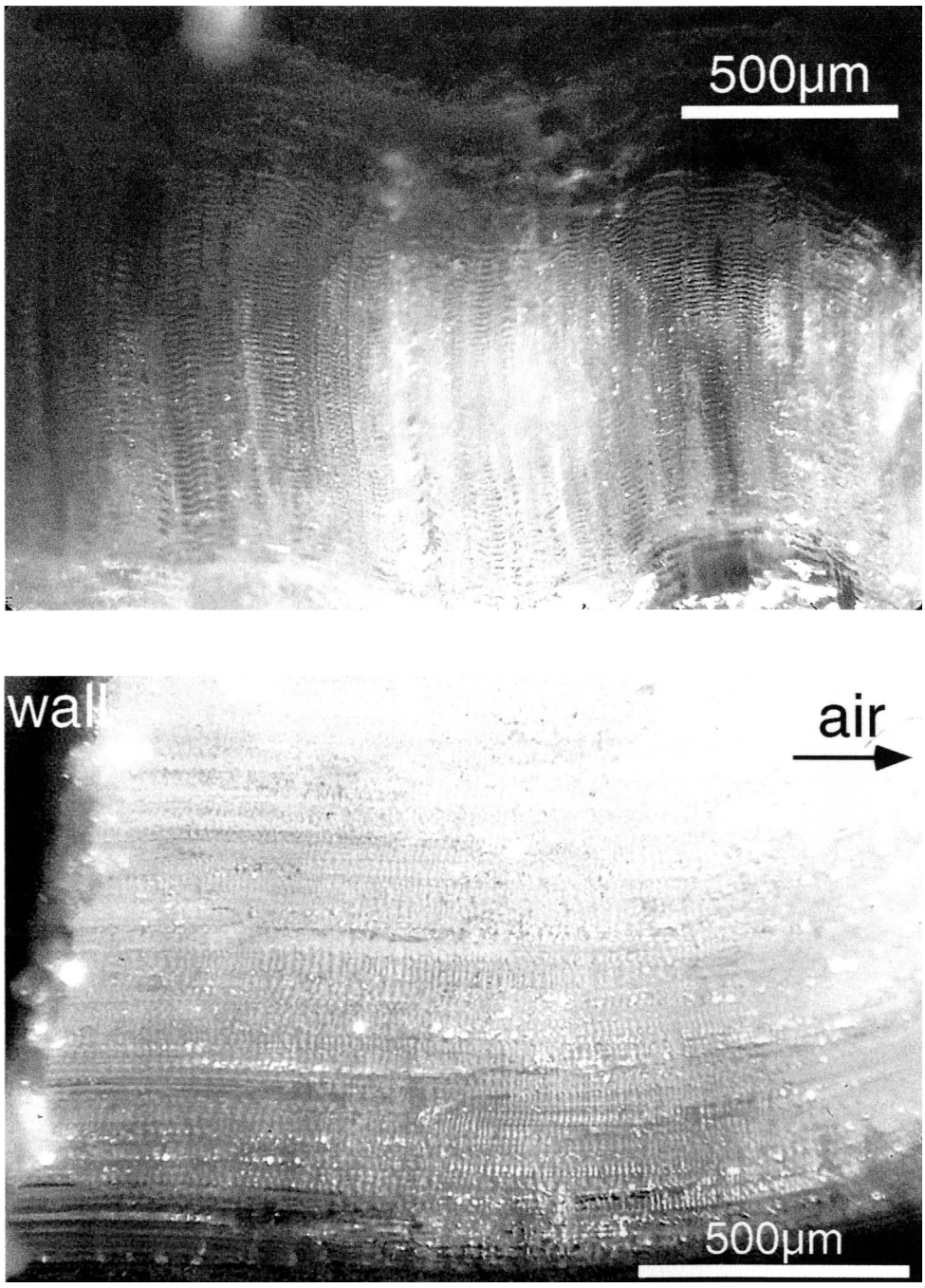

Fig. 2.18 Experimental fibers of NH_4SCN with Type II transverse features. (**a**) Fibers from single-block experiment *NFB-10a* showing numerous Type II bands with a wavy or undulated form parallel to the wall (to the bottom out of picture) and extending across the axes of fibers (vertical). The spacing is about 12-17μm. Photo taken in reflected light. (**b**) Type II fibers grown in another single-block experiment (*TB-05b*) over a period of two days, with an average growth rate of about 35μm/hr. The spacing of Type II bands ranges between 5~9μm. Photo taken in reflected light.

(c)

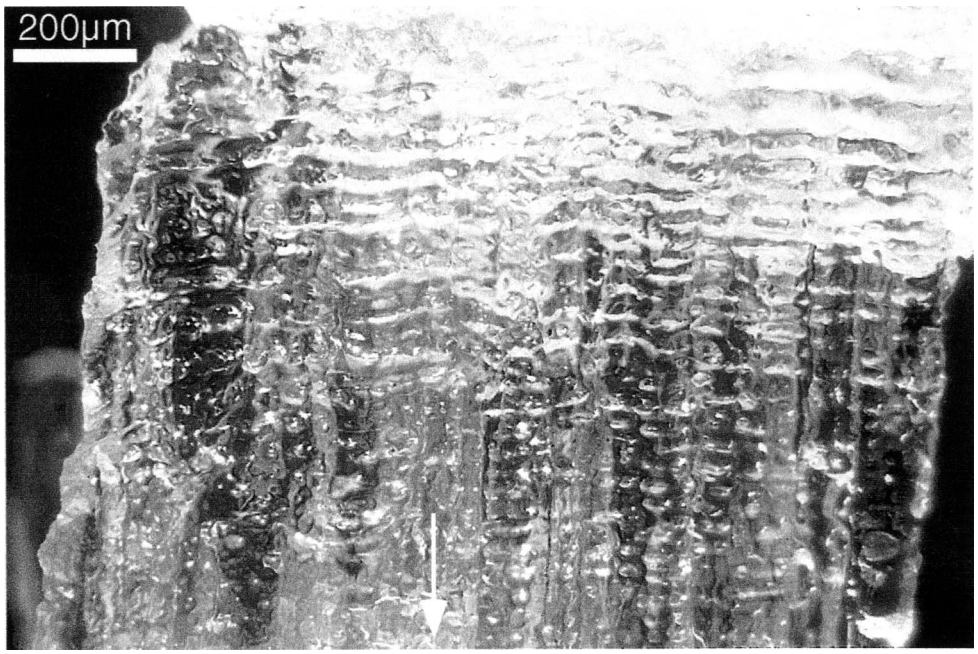

(d)

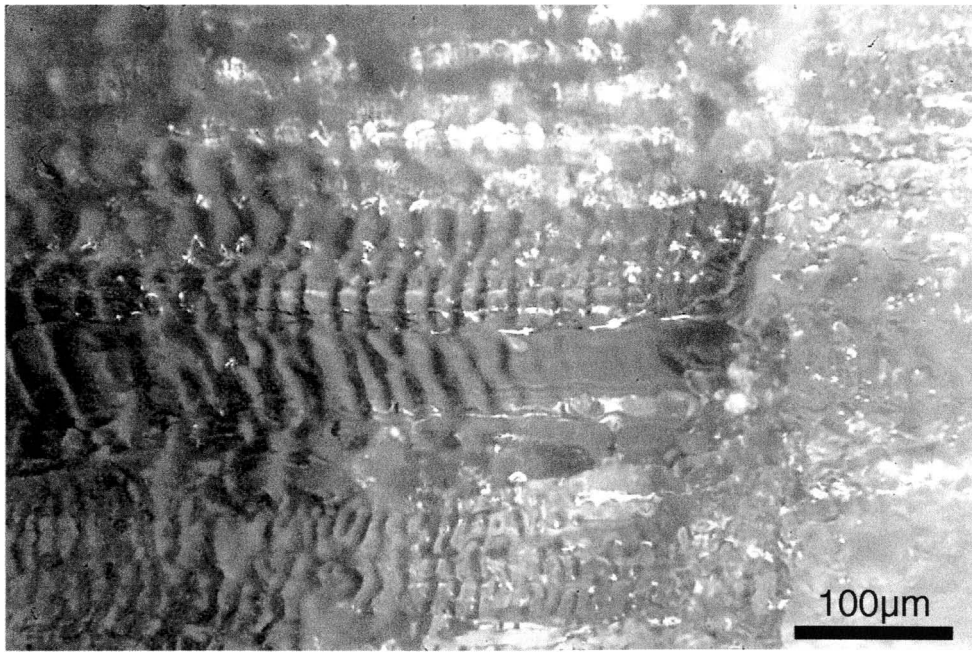

Fig. 2.18 (continued) (**c**) Micrograph of a piece of fiber aggregate from single-block experiment *NFB-09a* showing alternating irregular layers of cloudy (light-colored) and clear (dark-colored) material of Type II bands (of spacings of 30-50 µm) extending roughly perpendicular to the long axes of fibers (vertical). Arrow shows the orientation and direction of younging of fibers. Sample immersed in oil and photo taken in reflected light. (**d**) Micrograph of fibers grown in another single-block experiment (*NFB-31*) showing wavy and alternating dark and grey layers of Type II bands (of spacings of about 17~23µm). Photo taken in reflected light.

(e)

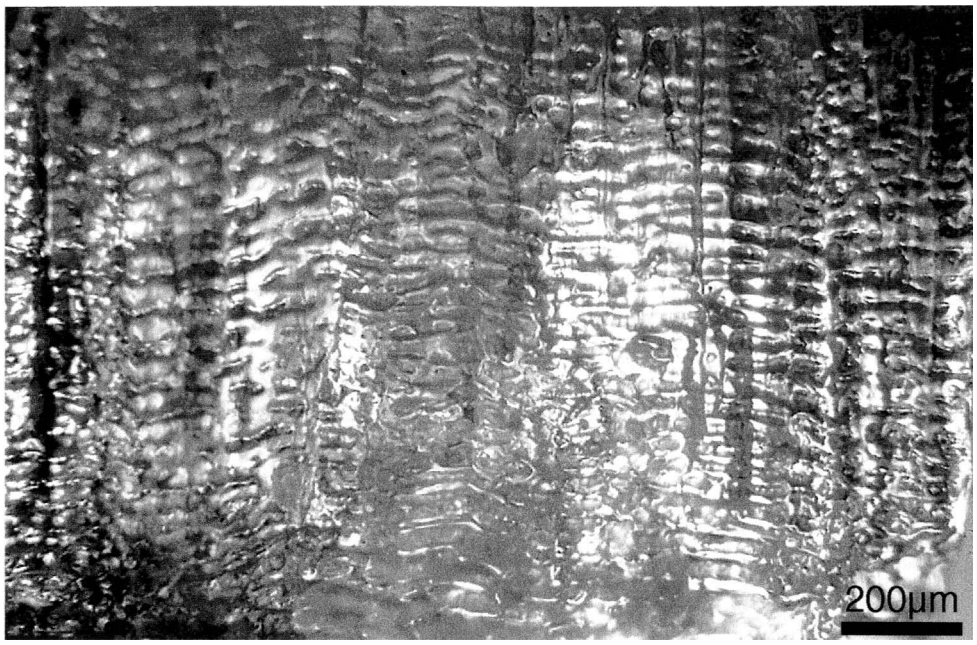

(f)

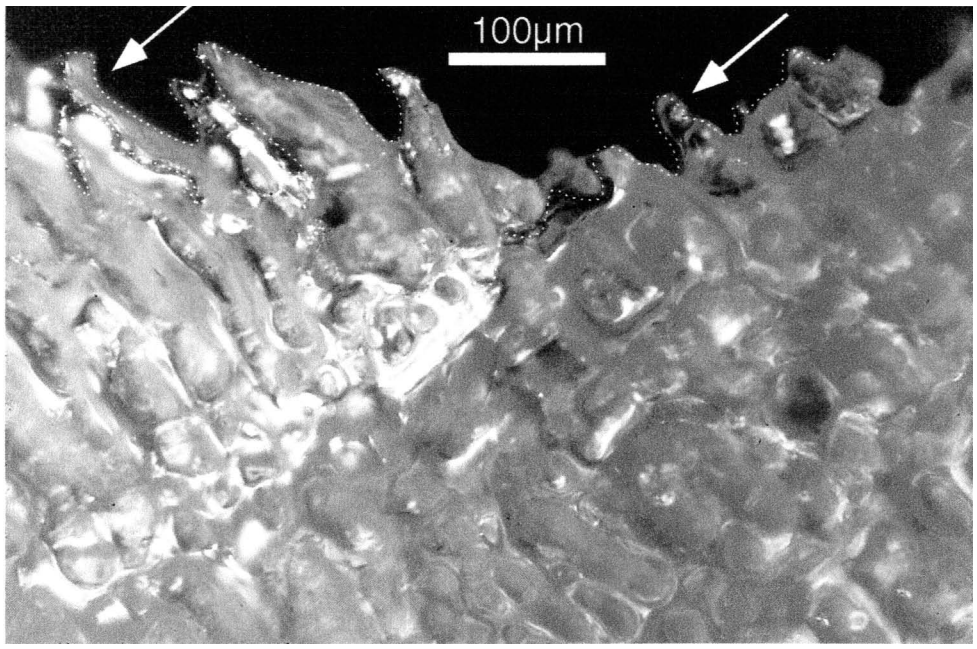

Fig. 2.18 (continued) (**e**) Micrograph of another piece of fiber aggregate from single-block experiment *NFB-09a* showing numerous Type II bands clearly marked by discontinuous, irregular 'ridges' or seams of cloudy material (of a spacing of about 30~40 μm) cutting across the long axes of fibers (vertical). Photo taken in reflected light. (**f**) Micrograph of Type II fibers from the same experiment showing details of individual bands and their resemblance of the 'crack-seal veinlets' in Ramay (1980, Fig. 1d) (see also Fig. 2.19). Also note the irregular or 'sawtooth' boundaries of fibers (dashed lines) due to the intersection of Type II bands with fiber axes (whose direction is shown by arrows), similar features also described in Ramsay (1980) (see Fig. 2.19). Photo taken in both transmitted and reflected light.

(g)

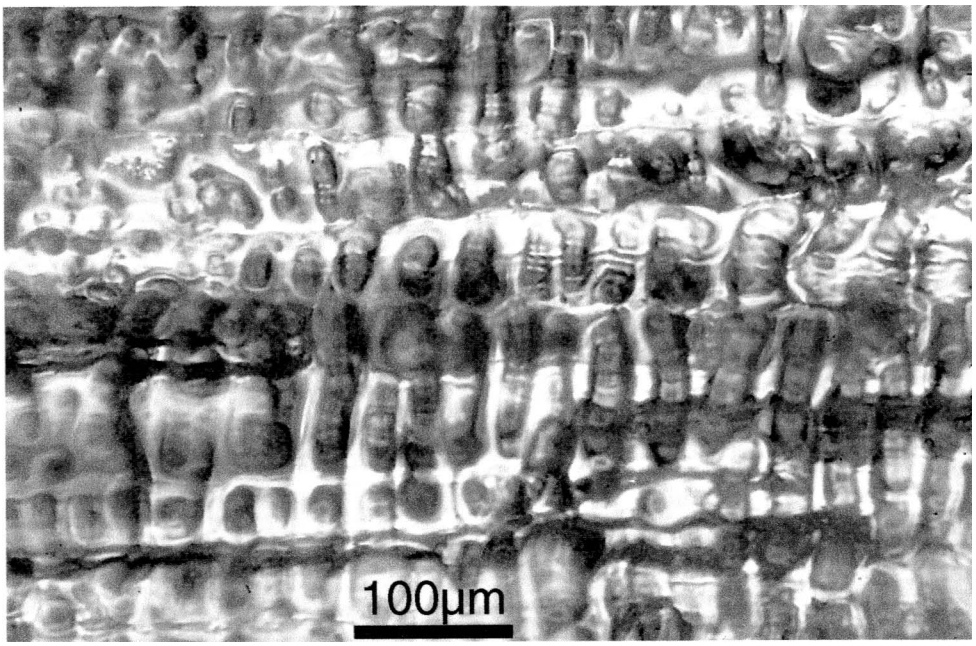

(h)

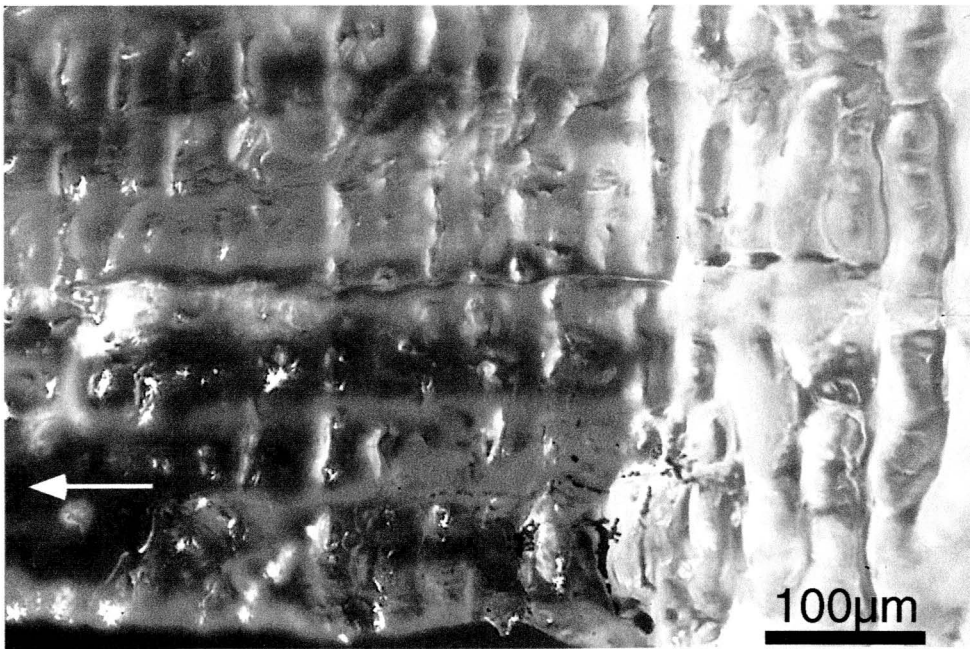

Fig. 2.18 (continued) (**g**) Enlarged view of (e) showing a characteristic honeycomb-like pattern formed by irregular ridge-like Type II features (vertical) extending discontinuously and cutting across fiber axes (horizontal). Photo taken in reflected light. (**h**) Enlarged view of (c) showing strongly-banded fibers (or 'veinlets') on the right passing into weekly-banded fibers on the left (or 'inclusion bands') as the thickness of seams of cloudy material (pale-colored) decreases over time. Arrow shows the orientation and direction of younging of fibers. Sample immersed in oil and photo taken in reflected light.

(a)

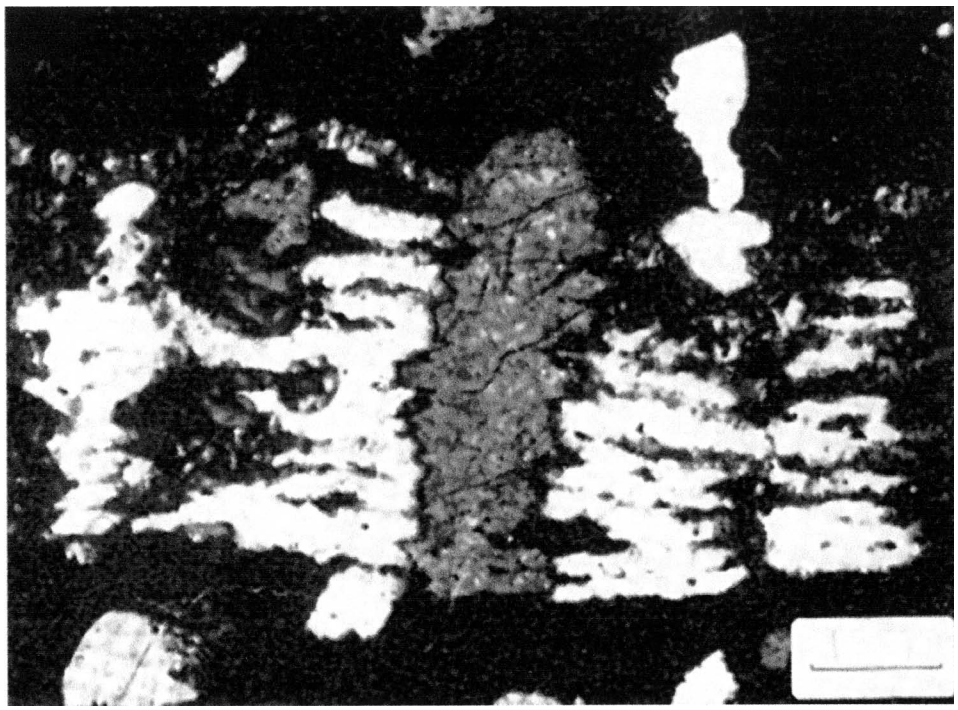

(b)

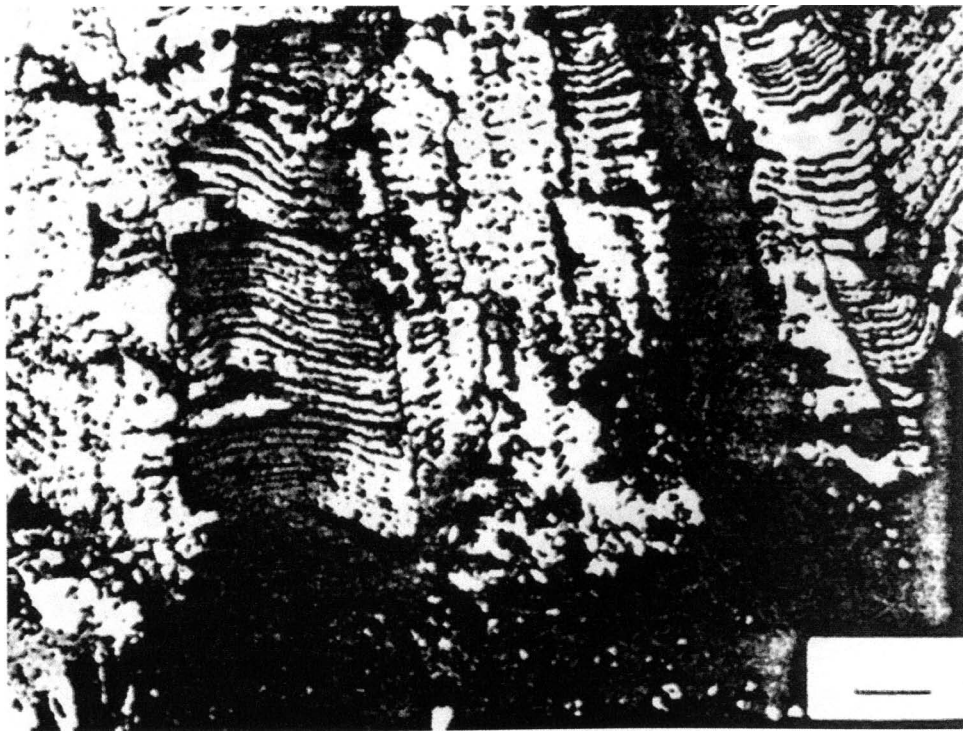

Fig. 2.19 Classical examples of natural fibers with Type II features from Ramsay (1980). **(a)** Reproduction of Ramsay's Fig. 1d. Scale bar, 100μm. **(b)** Reproduction of Ramsay's Fig. 4b. Scale bar, 100μm.

Fig. 2.20 Micrographs showing microstructures in a piece of fibrous aggregate picked from sample NFB-14. (**a**) View of the whole piece showing widely spaced, well-defined Type I features (**I**) and other closely spaced, more irregularly defined Type II transverse features (**II**). Also visible in the fibers (horizontal) are some inclusion trails (arrow) running parallel to the fiber axes. (**b**) Enlarged view of the same sample showing details of the Type I features (**I**) and inclusion trails (arrow). The spacing of inclusions in the trails is of the order of 15μm. Inclusions are also concentrated and aligned along the Type I features.

(a)

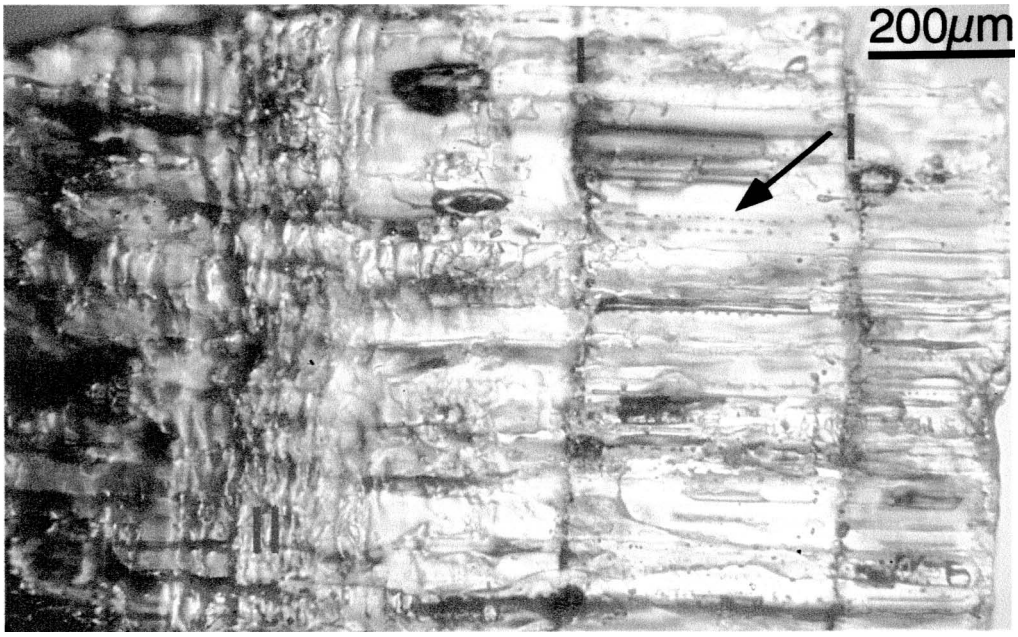

(b)

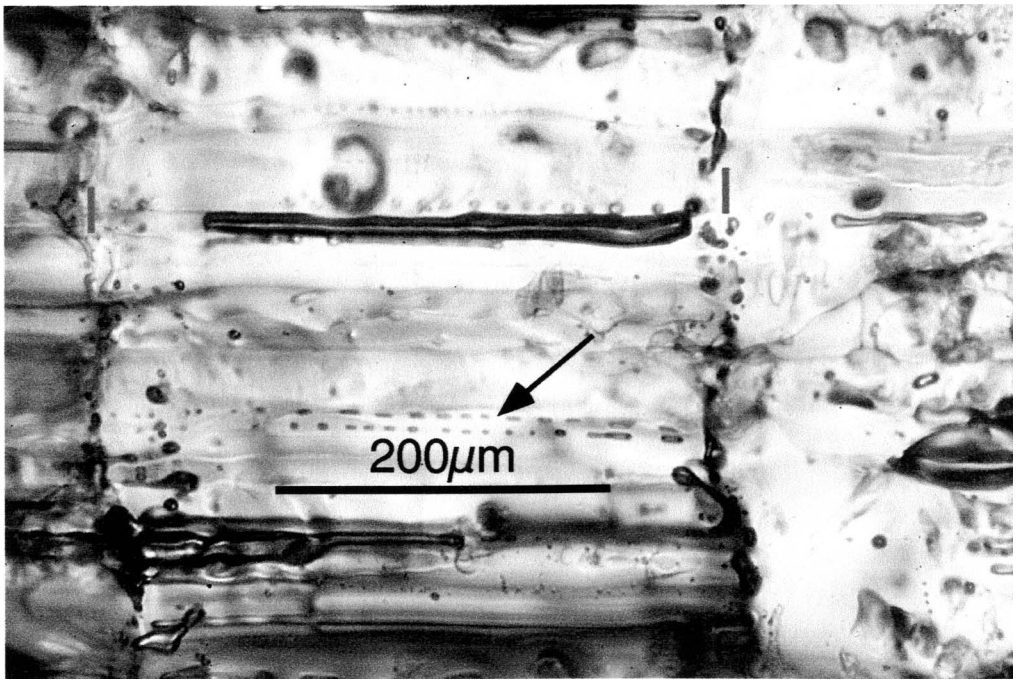

Fig. 2.21 Micrographs showing multiple fibrils and fluid inclusion trails within single fiber bundles picked from some experimental fibers. (**a**) A large thin piece of fiber bundle picked from sample NFB-22, illuminated in combined transmitted and reflected light. The grain shows alternating ridges and grooves (fibrils) as well as fluid inclusion trails along some of the fibrils. It is one grain since extinction occurs in all the fibrils at the same time (see section 2.9.3). The spacing of inclusions varies between 5 and 9.5 μm. (**b**) Micrograph of another thin piece of fiber picked from sample NFB-22, taken in combined transmitted and reflected light and in crossed nicols. The grain is in a position that all fibrils are at extinction, but some ridge-like fibrils or boundaries between them as well as fluid inclusion trails are illuminated with the reflected light. The spacing of fluid inclusions varies considerably in different trails (from 2.6 to 15 μm) and even changes abruptly along the same trails(e.g. from 2.6 to 8.2 μm in one trail in the fibril at the bottom side of the grain). (**c**) Micrograph of another fiber bundle picked from sample SM-07 grown on a cellulosic filter membrane with a nominal pore size of 0.22 μm. The fiber consists of numerous fibrils and fluid inclusions trails. Both the fibrils and inclusions show a spacing on the order of several microns (mostly between 4-9 μm). While inclusions are generally evenly spaced in most trails, it is not the case in one particular trail (arrow) in which the spacing gradually increases from about 8 up to 25μm in a direction towards the left side of the picture.

(a)

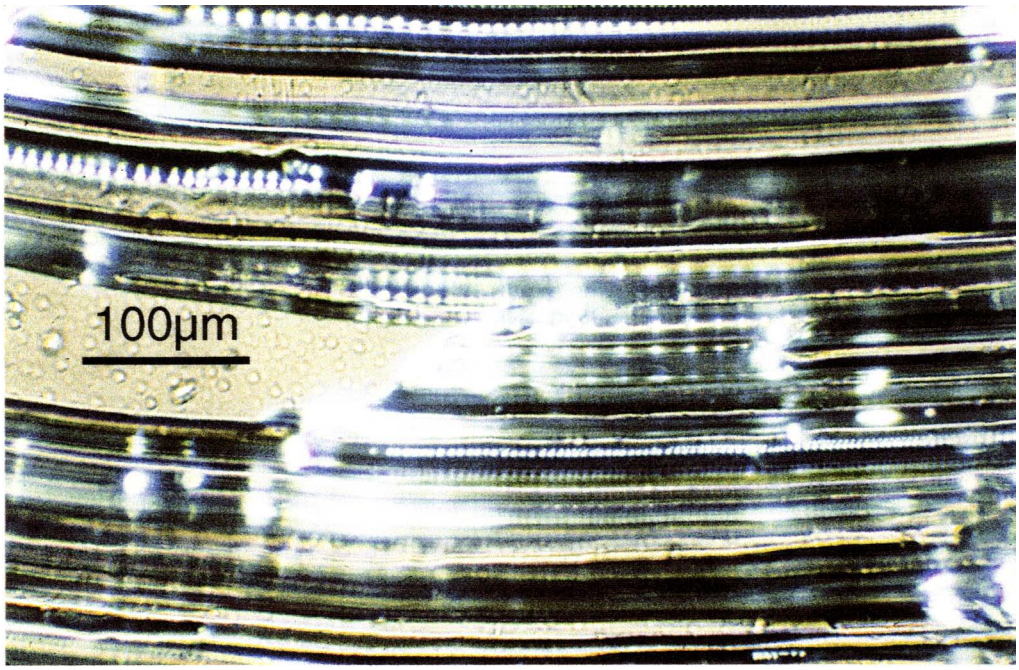

(b)

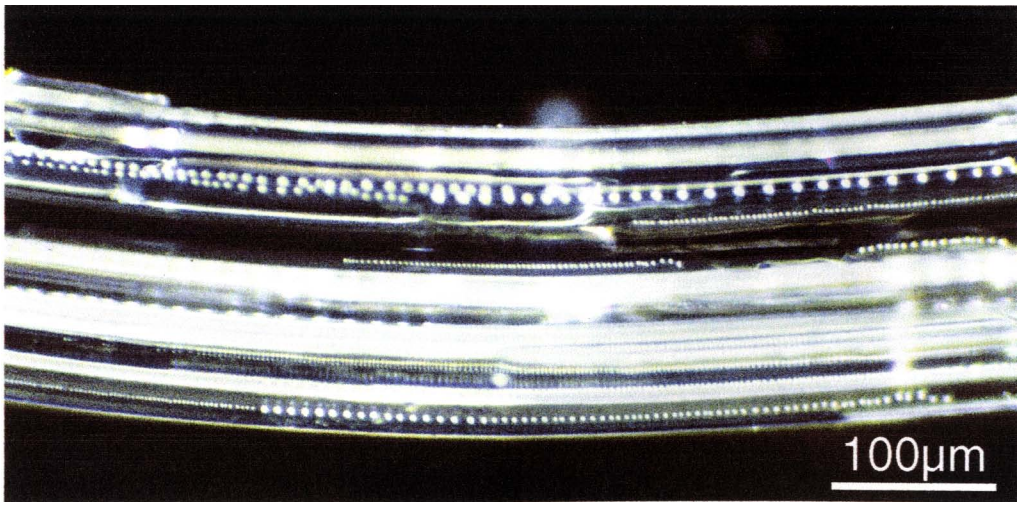

(c)

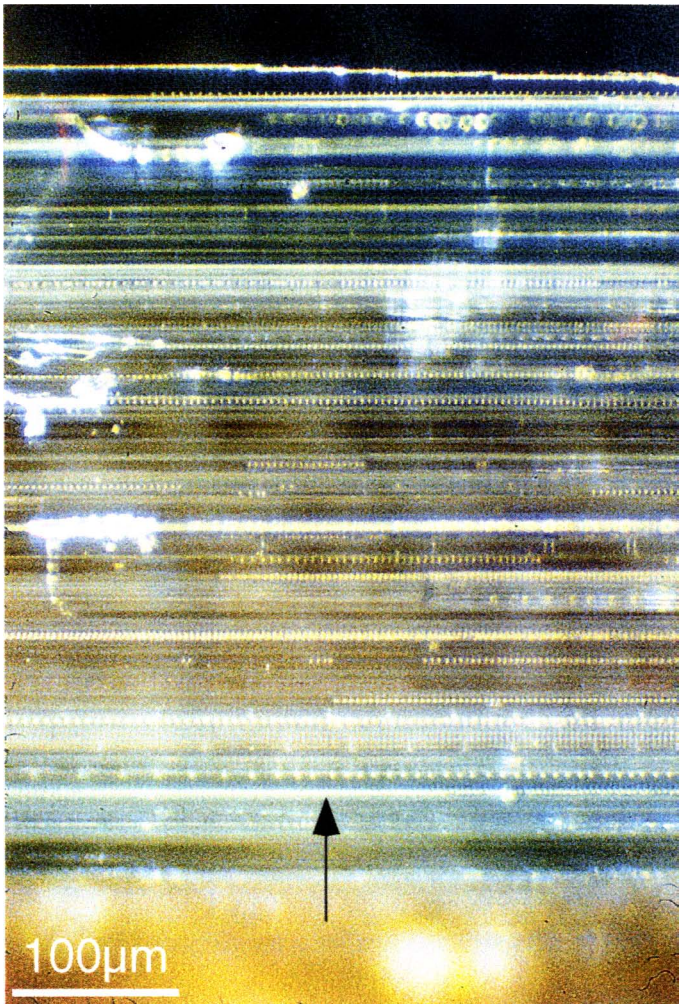

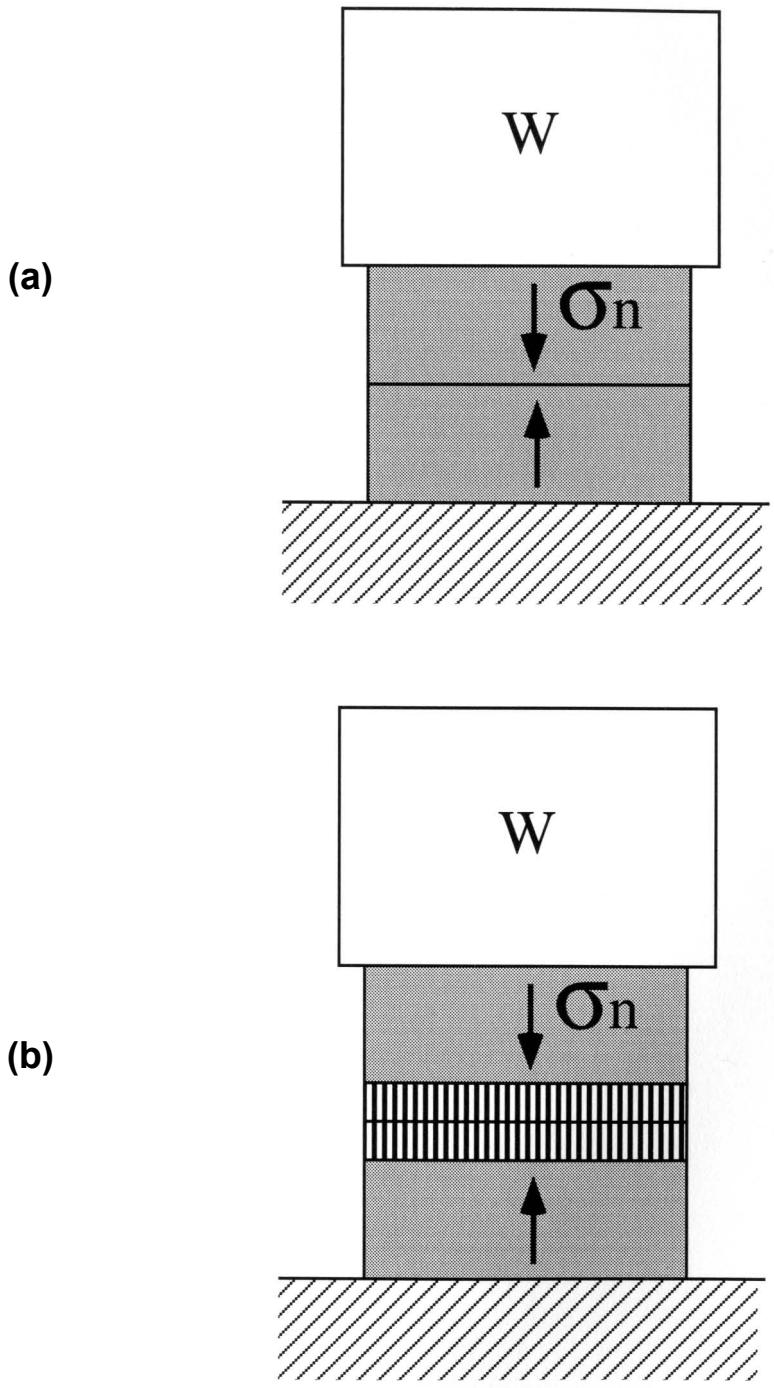

Fig. 2.22 Set-up of compressive loading two-block vein experiments. (**a**) Dead weight (**W**) is placed on top of two superposed ceramic blocks (shaded) to produce an extra pressure or normal compressive stress (σ_n) on the artificial crack between them. (**b**) Fibers grow between the pressed blocks by lifting up the upper block and the dead-weight loading.

Fig. 2.23 Growth of fibrous veins under dead-weight loading conditions (refer to the set-up in Fig. 2.22). (**a**) Initial crack between the ceramic blocks in experiment *DW-02*. The blocks were coated with epoxy except on the crack side and filled with the crystallizing fluid of NH_4SCN. Imposed on top of the blocks was a dead weight of 1160 grams (a linear pressure of 0.88 bars). The whole sample was placed in a closed desiccator with an ambient relative humidity of about 10%. (**b**) A vein of fibers grown between the blocks as seen 50 days later. Fibers grew by lifting the upper block upward from the lower block, against the extra linear pressure imposed by the dead weight. (**c**) An enlarged view of the vein. (**d**) A fibrous vein of $NaNO_3$ grown in another experiment (*DW-15*) under a dead-weight loading of about 25 kg (a linear pressure of 3.6 bars on the vein). Growth took about 9 days. Red spots in the upper-left and lower-right corners are ink markers placed on the walls to monitor opening displacements.

(a)

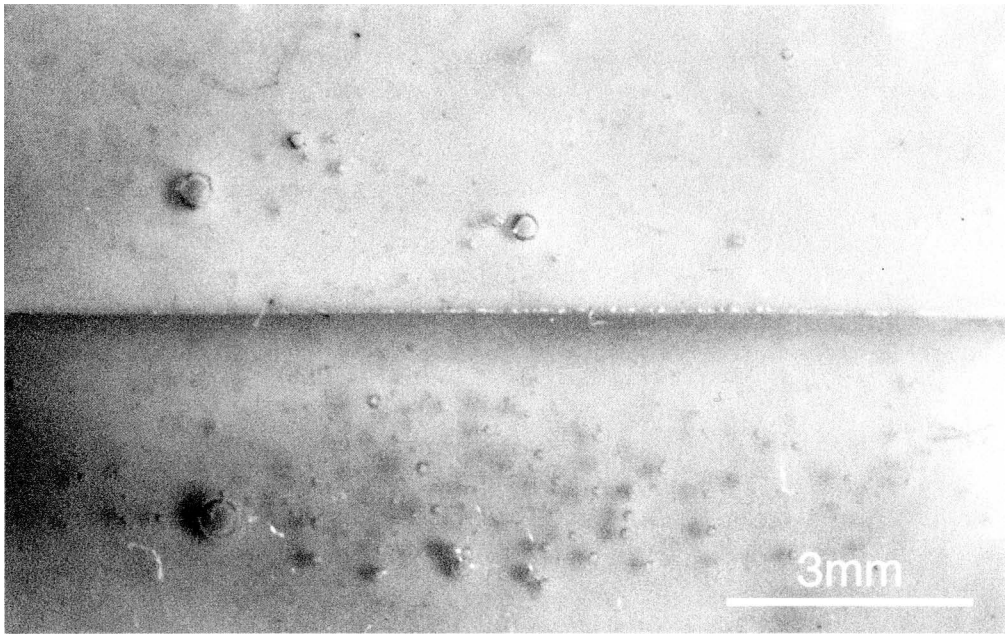

(b)

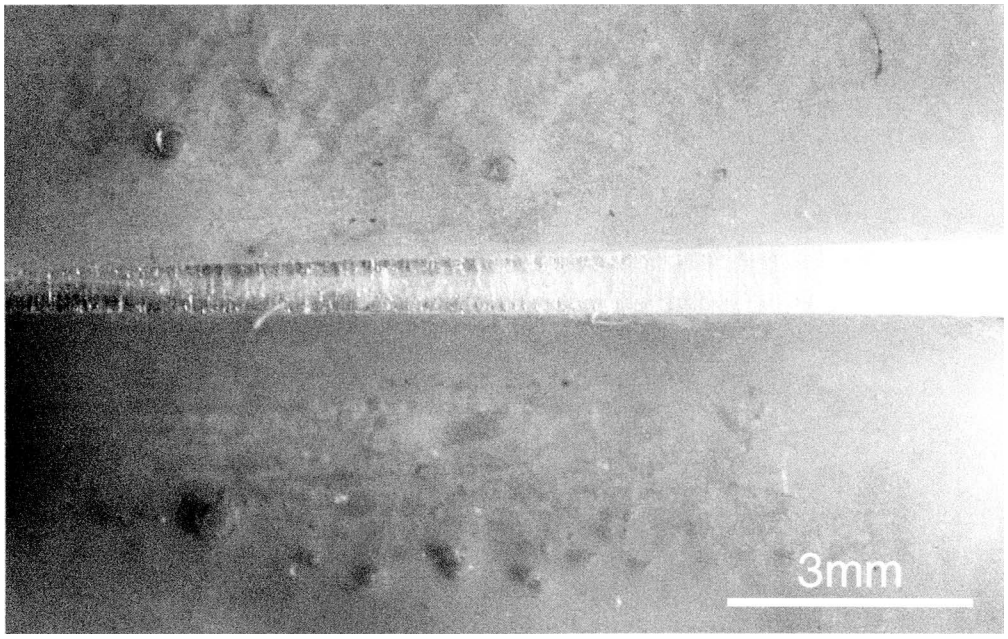

(c)

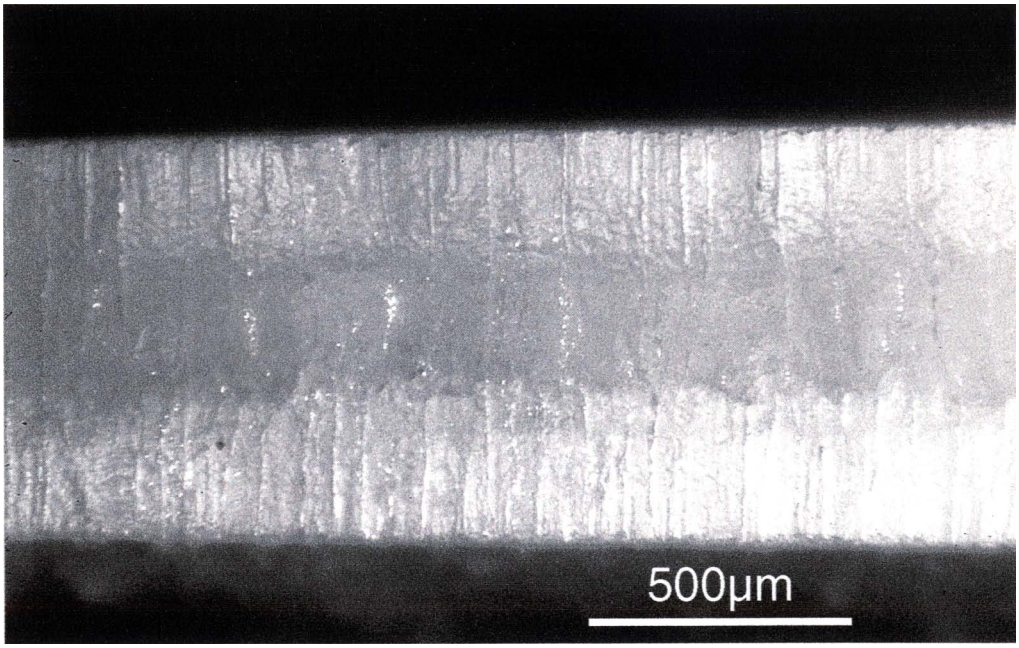

(d)

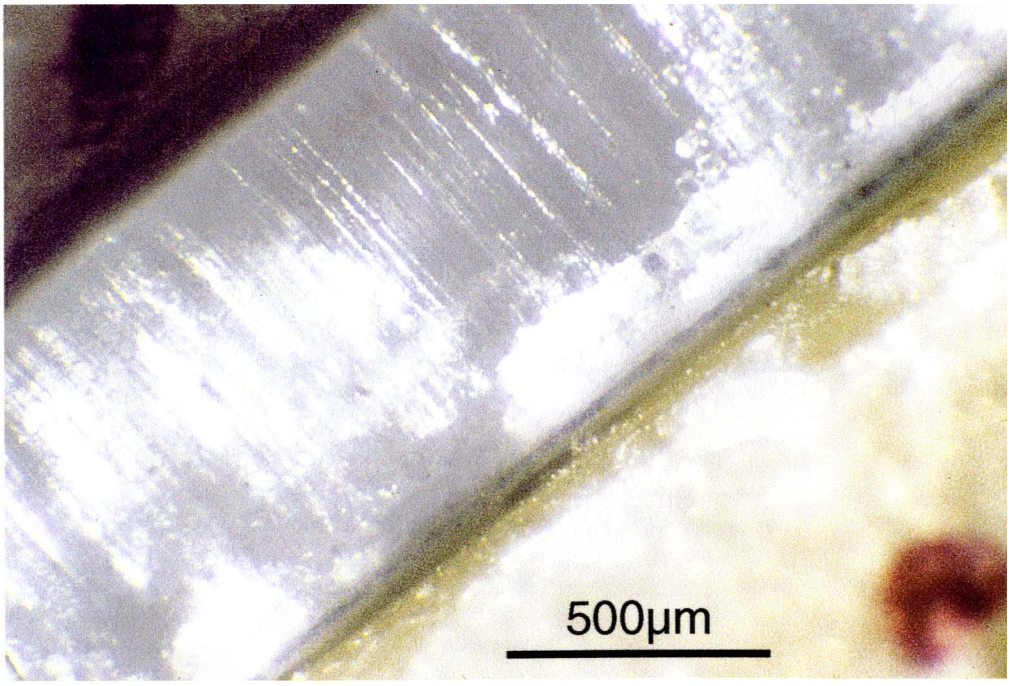

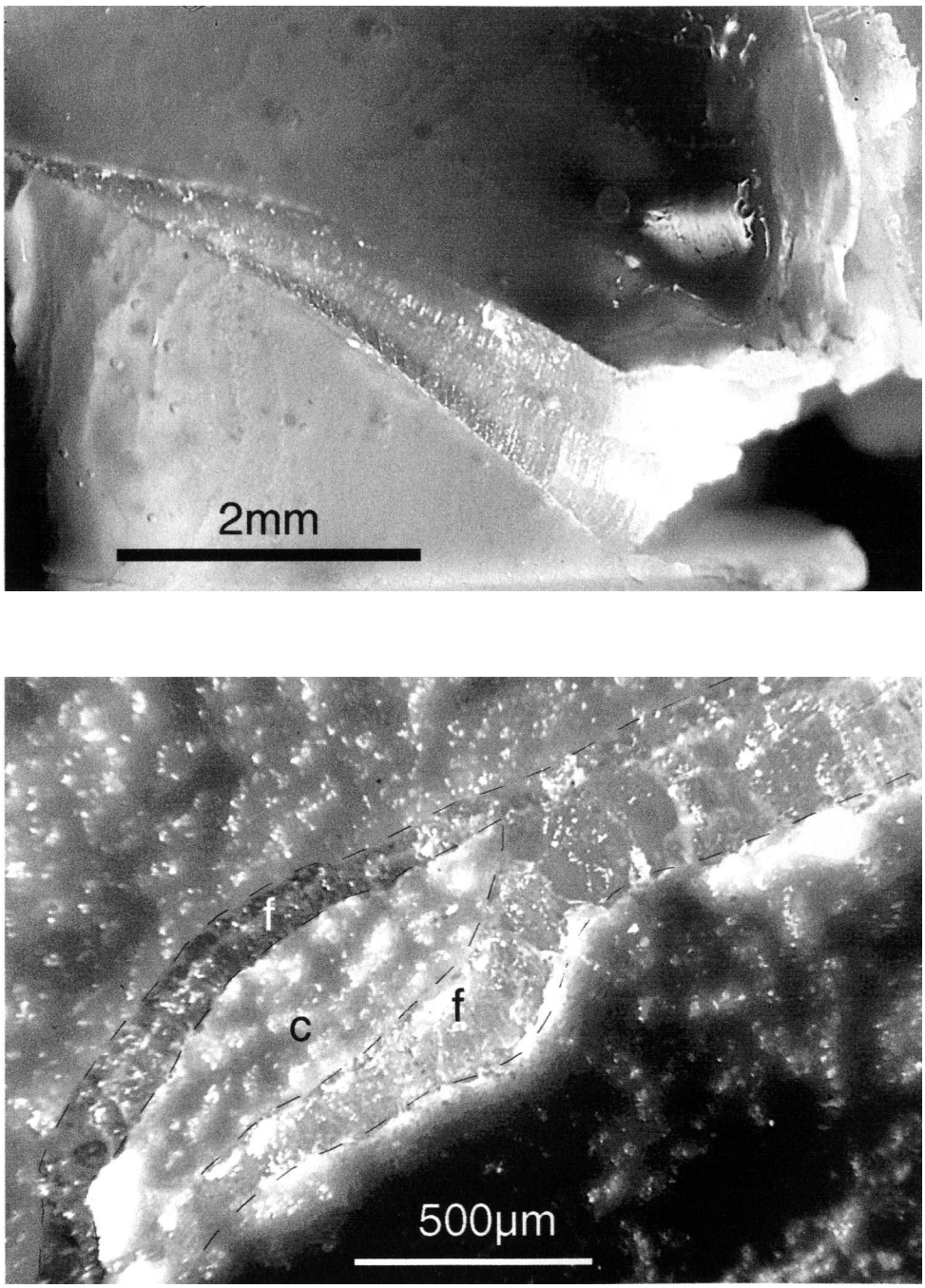

Fig. 2.24 Growth of fibrous veins in newly formed fractures in the ceramic wall under large dead-weight loading. (**a**) A vein of curved fibers of $NaNO_3$ developed in one of the epoxy-coated ceramic blocks when a dead-weight loading pressure of about 17 km/cm^2 was imposed on the contact between the blocks (*DW-13*). The curved morphology of fibers indicates that the vein must have been forced open as fibers were growing, thus forming a typical vein of synkinematic growth. (**b**) A branched vein of $NaNO_3$ fibers developed in the contact surface of one of the ceramic blocks when a dead-weight loading pressure of 5 km/cm^2 was imposed on the sample (*DW-15*). A large piece of ceramic (c) was broken from the wall and now engulfed in the sea of fibers (f), a phenomenon also found in natural fibrous veins which Taber (1918) used as evidence for vein growth by pushing apart the enclosing walls rather than in preexisting openings.

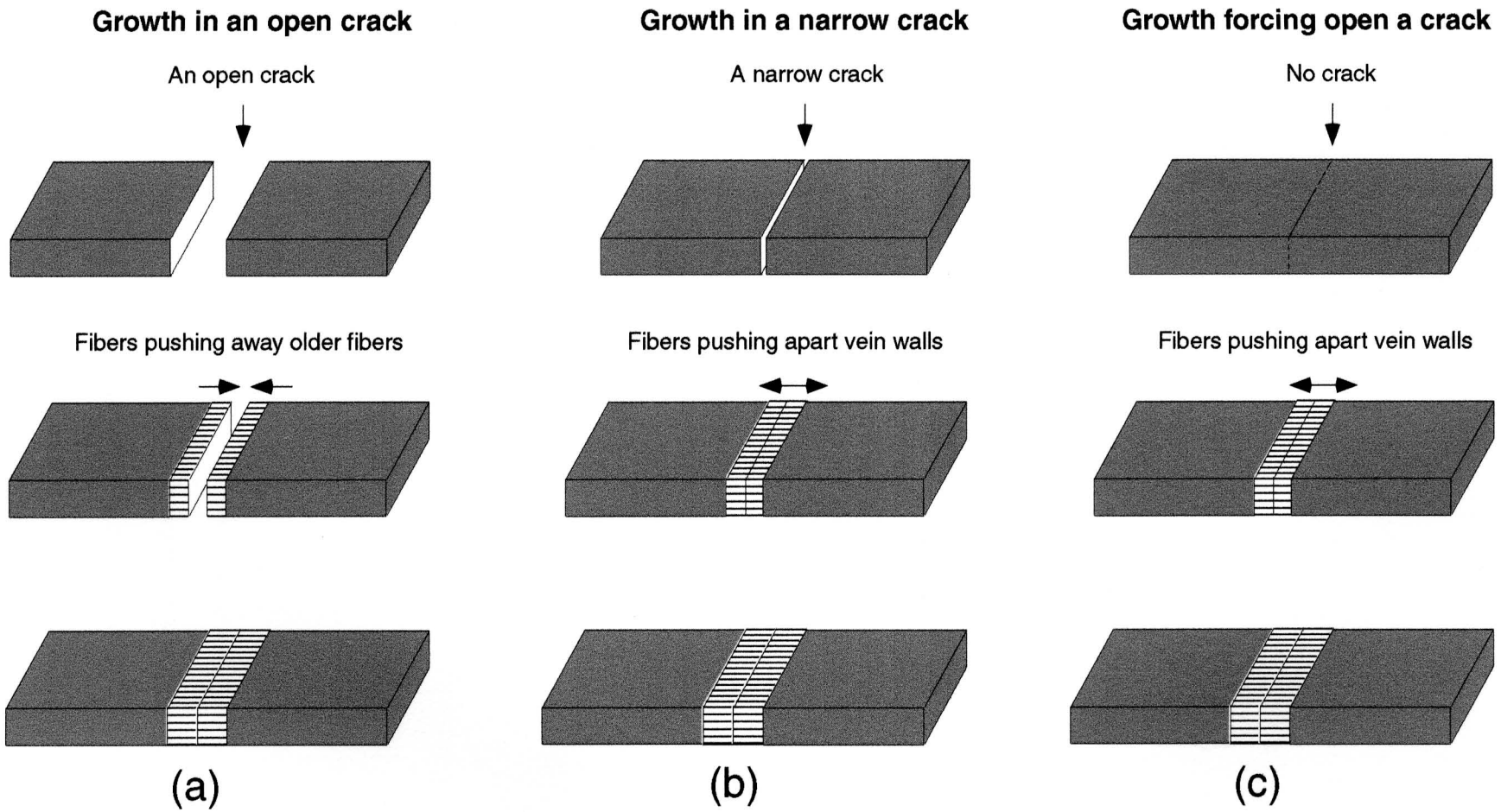

Fig. 2.25 Cartoon illustrating the basic characteristics of Taber Growth (Li & Means, 1997). (**a**) Post-kinematic growth of a fibrous vein in a pre-existing open crack. (**b**) Synkinematic growth of a fibrous vein in a narrow crack by pushing apart wall blocks. (**c**) Synkinematic growth of a fibrous vein by forcing open a crack where there is no crack present at the beginning. In (b) and (c) extra compressive loading may be imposed on wall blocks perpendicular to the veins. In all cases, growth occurs antitaxially at the cohesive fiber-wall contact and crystallizing material is fed through fine pores in vein walls.

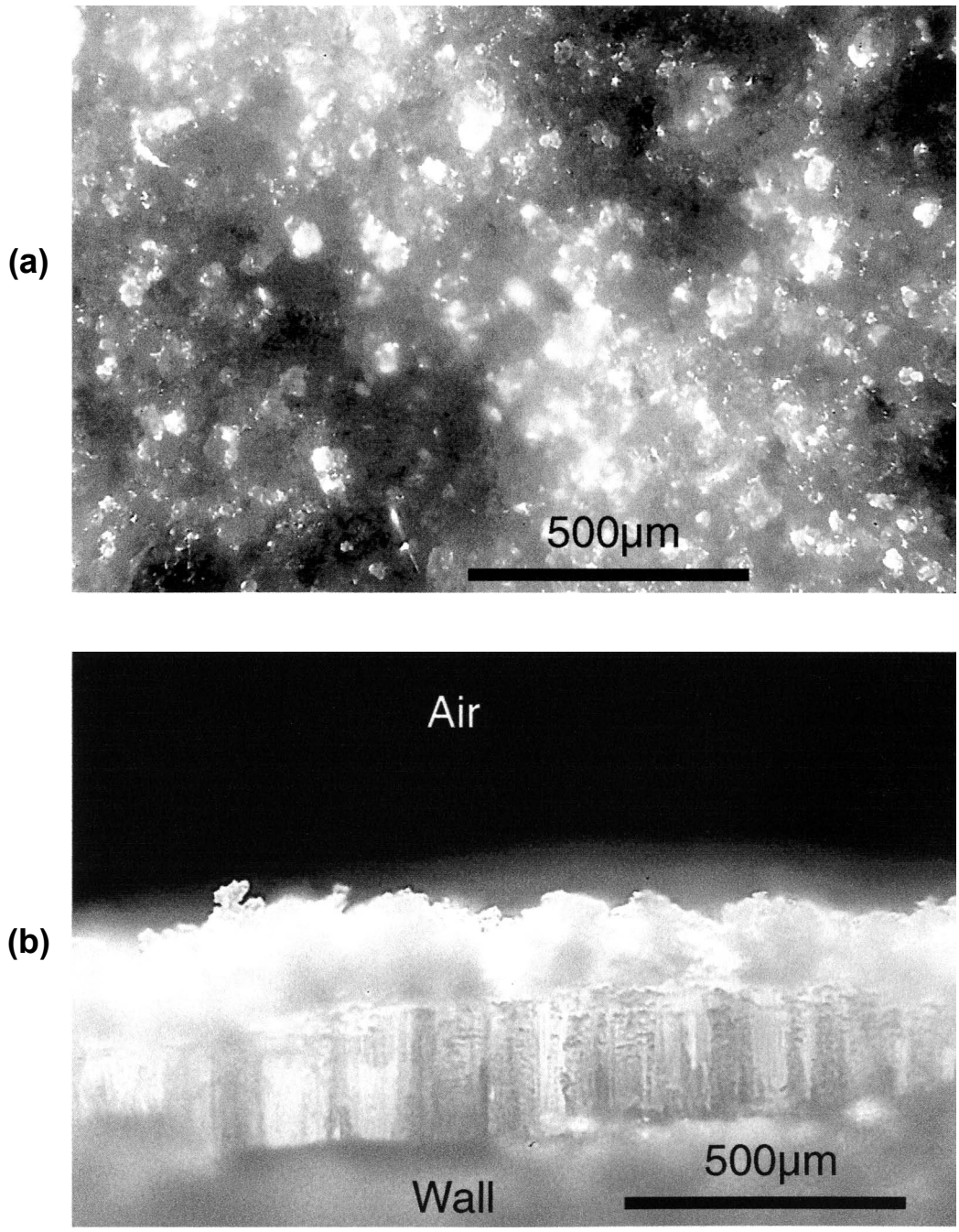

Fig. 2.26 Growth of tightly packed fibers of *NaCl* in very low humidity conditions (RH=10±5%) in a single-block experiment (*NFB-35*) with wax-coated ceramic *Big Disc*. Experiment started about 5 days before. (a) Plan view of the surface of a thick crust of granular material on the real fibers underneath. (b) Lateral view of sample showing growth of tightly packed fibers following the early granular growth.

(a)

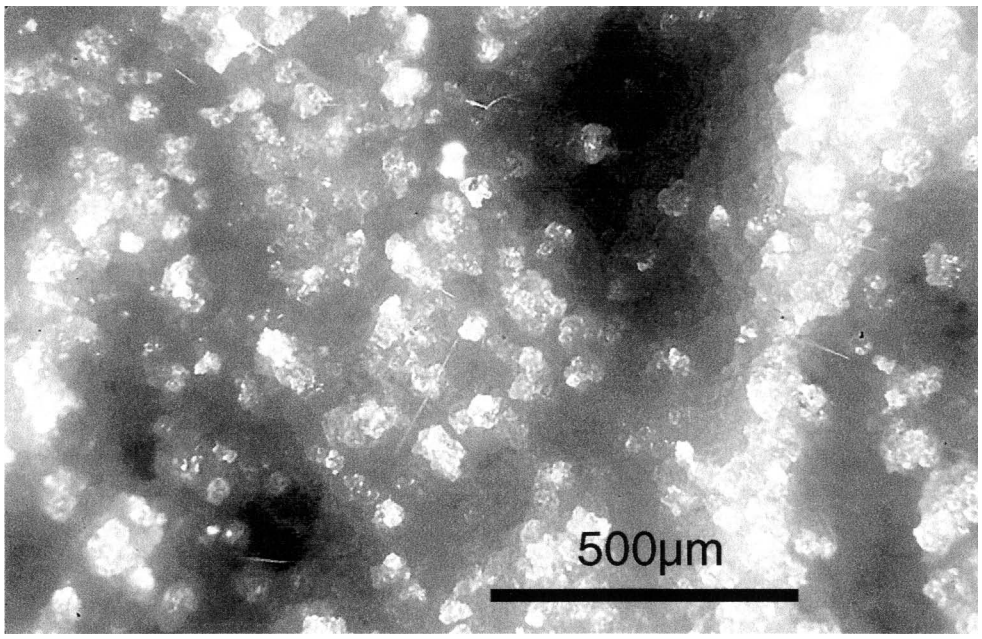

(b)

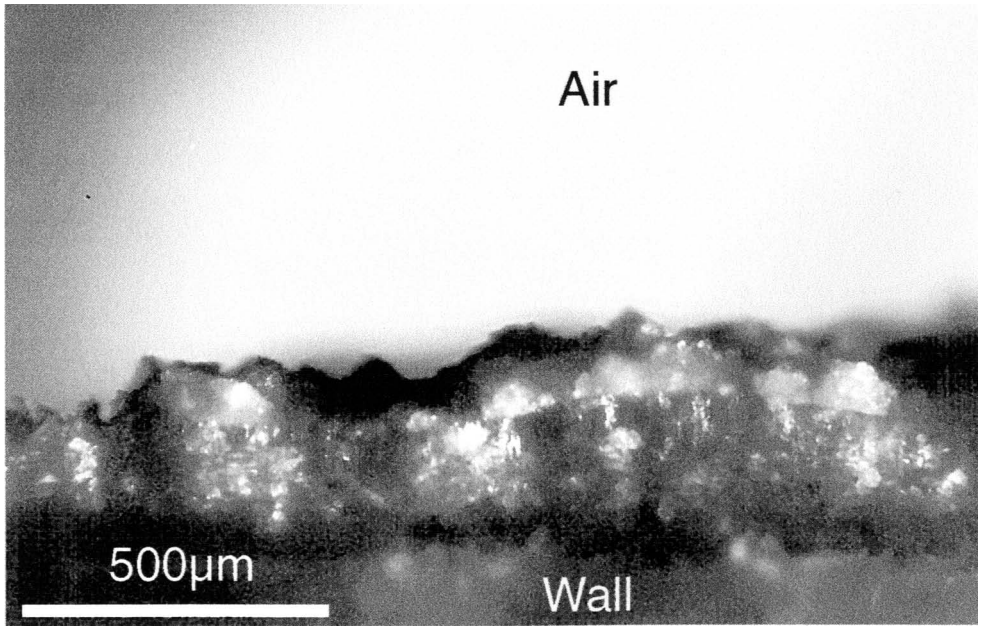

Fig. 2.27 Growth of fibers of *NaCl* in moderate humidity conditions (RH=40±5%) in a single-block experiment (*NFB-36*) with wax-coated ceramic *Big Disc*. Experiment started about 5 days before. (a) Plan view of the surface of a thin crust of granular material on the real fibers underneath. (b) Lateral view of sample showing growth of fibrous crystals following the early granular growth.

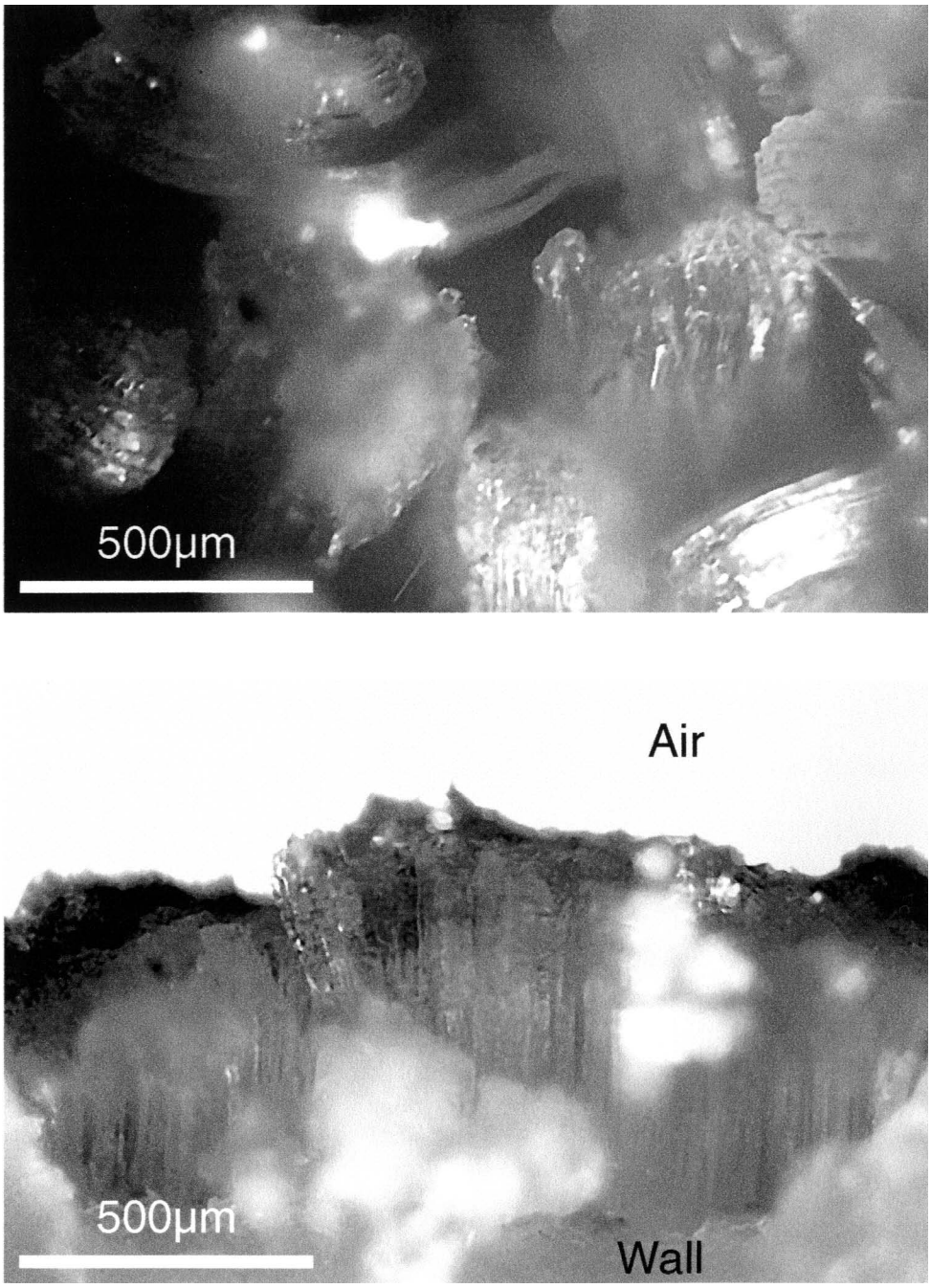

Fig. 2.28 Growth of loosely packed fibers of *NaCl* in very high relative humidity conditions (RH=68±5%) in a single-block experiment (*NFB-37*) with wax-coated ceramic *Big Disc*. Experiment started about 5 days before. (a) Plan view of the growth on the uncoated surface of sample showing direct growth of loose fiber bundles with no crust of granular material on top. (b) Lateral view of sample showing loosely packed character of fibers as well as absence of a crust of granular material at the top.

Fig. 2.29 Comparison of growth of fibers of different character in single-block experiments *TB-6b* & *TB-7b* under different humidity conditions. The two ceramic samples (*P-3-C*) were both painted black and coated with epoxy except on the growth side and were immersed in the saturated solution of NH_4SCN for 30 minutes. However, one of the samples (*TB-6b*) was placed in a closed desiccator with a RH of 15±5%, while the other (*TB-7b*) was in a desiccator with a RH of 35±5%. (**a**) Good, tightly packed fibers grown from *TB-6b*, grown over a period of 89 hours (with an average growth rate of 22-26 μm/hr). A black spot (**A**) on the fibers is an ink marker placed across the fiber/wall interface two days before but now seen to have been rifted away from the wall by antitaxial growth of younger fiber segments. (**b**) Poor, loosely packed fibers grown from *TB-7b*, photographed at the same time as *TB-6b*. The aggregate contains granular material, voids as well as a crust of granular crystals and it looks as if it has been disrupted by younger fiber growth. (**c**) Enlarged view of the fibers on *TB-6b*, close to the marker in (a) (also labeled "**A**" in here), showing good quality of fibrous structure and some faint Type I discontinuities, one of which (**I**) is better defined than others. (**d**) Micrograph of the same view in reflecting light of a different angle, bringing out numerous closely spaced Type I features while the fibrous structure becomes almost invisible.

(a)

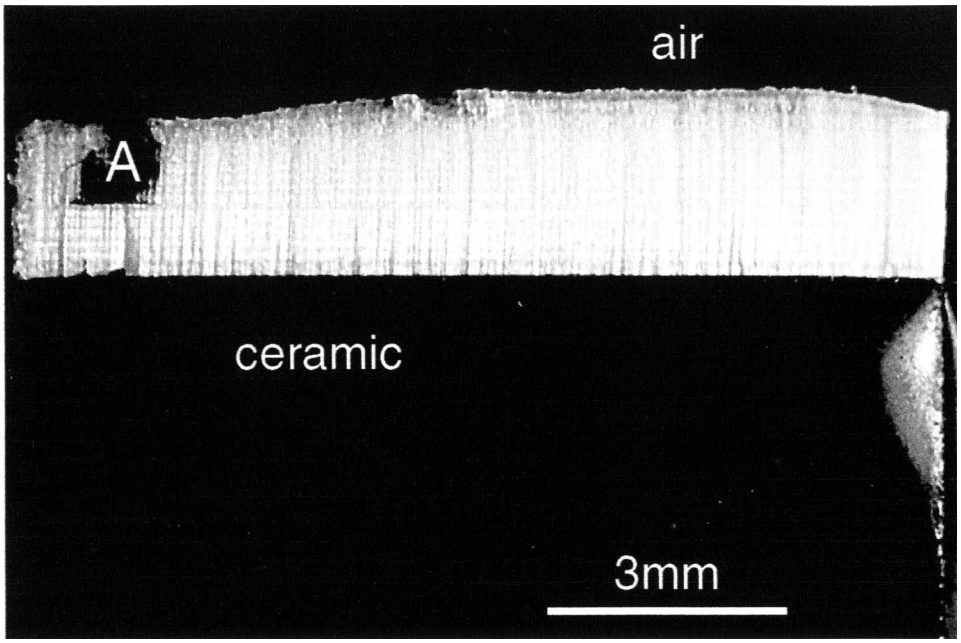

(b)

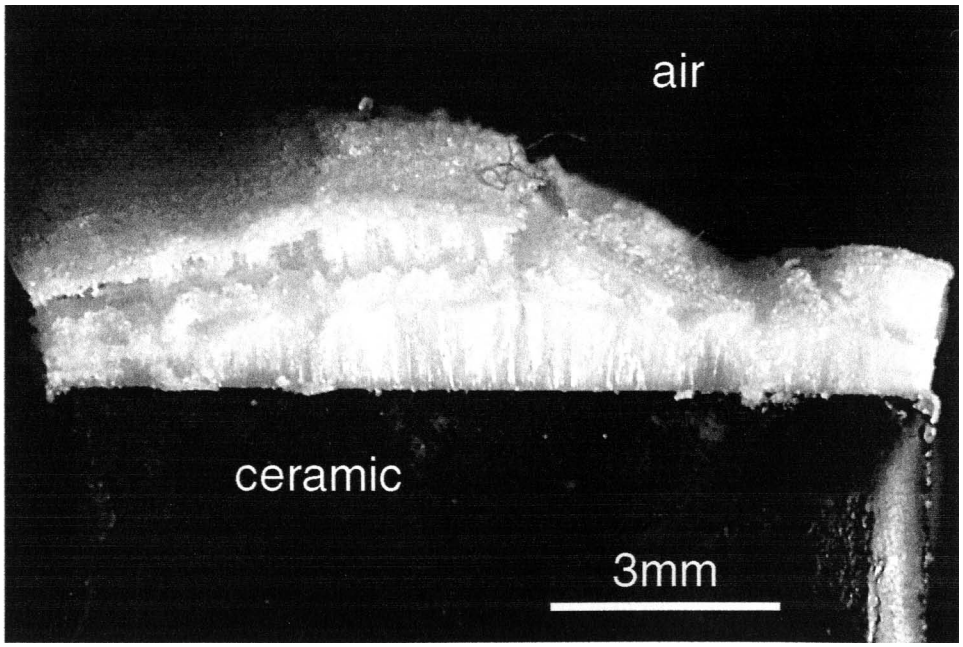

(c)

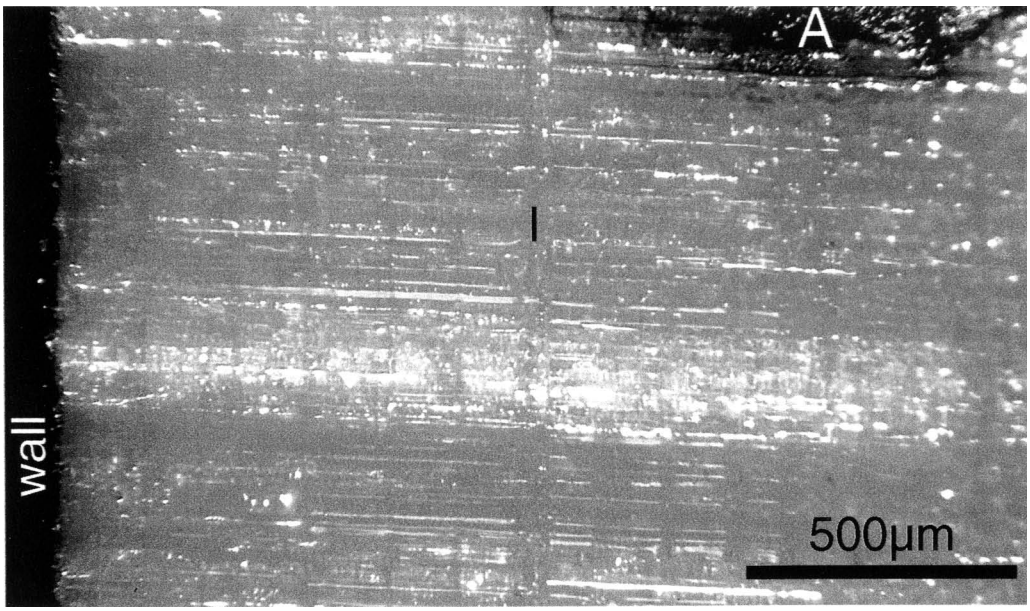

(d)

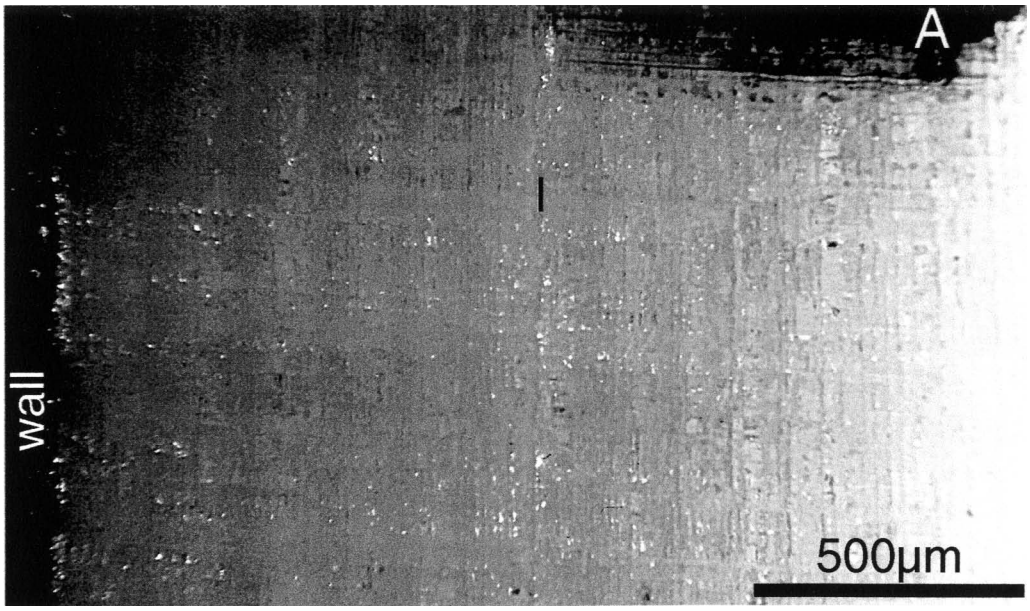

Fig. 2.30 Comparison of growth of fibers of different character in single-block experiments *TB-10a* & *TB-10b* under different humidity conditions. The two ceramic samples (*P-3-C*) were both painted black and coated with epoxy except on the growth side and were immersed in the saturated solution of NH_4SCN for 30 minutes. However, one of the samples (*TB-10a*) was placed in a closed desiccator with a RH of 20±5%, while the other (*TB-10b*) was in a desiccator with a RH of 40±5%. (**a**) Good, tightly packed fibers grown from *TB-10a*, grown over a period of 47.5 hours (with an average growth rate of 23μm/hr). (**b**) Poor, loosely packed fibers grown from *TB-10b*, photographed at the same time as *TB-10a*. Good fiber growth is preceded by a thick crust of granular crystals which appears to have been broken or pierced by younger fiber growth. The whole loose aggregate is much thicker than the growth on *TB-10a*, giving an average linear growth rate of about 100μm/hr. (**c**) Enlarged view of the fibers on *TB-10a* showing good quality of fibrous structure and ridge-and-groove features on the surface of the aggregate. (**d**) Micrograph of the same fibers at a still larger power showing abundant transverse features across the fibers.

(a)

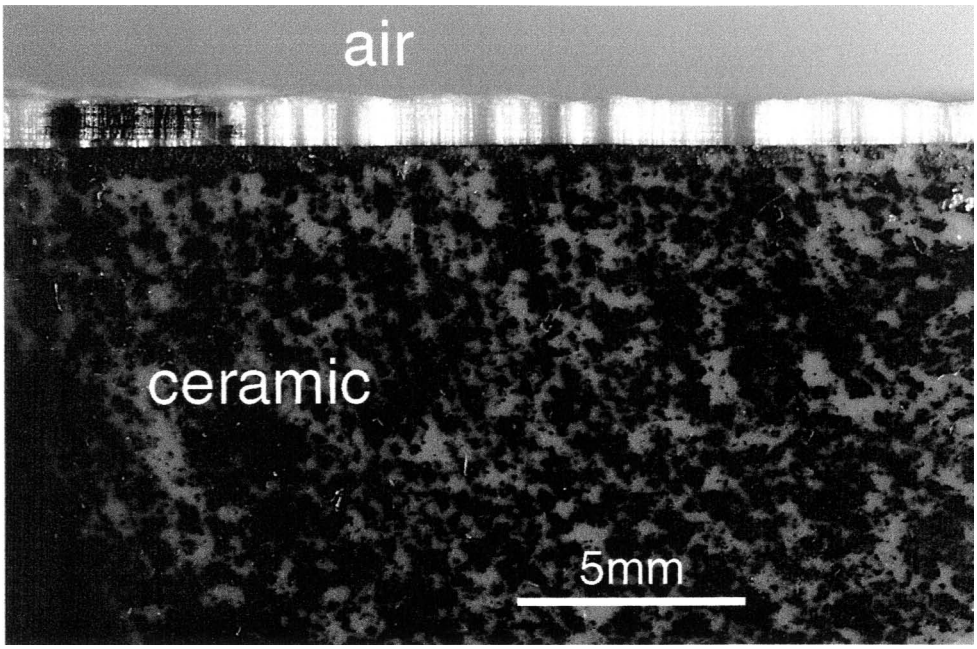

(b)

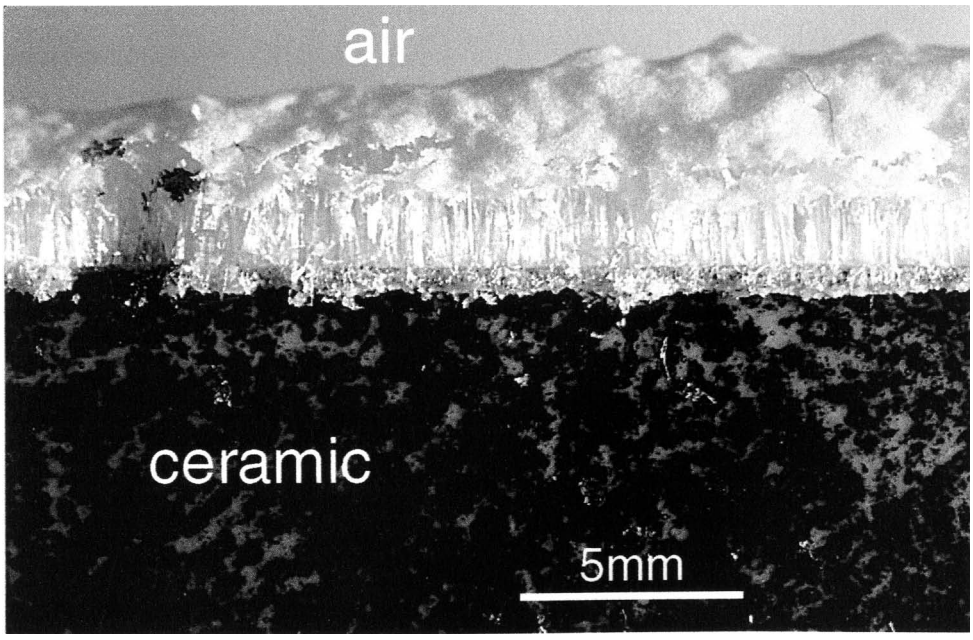

(c)

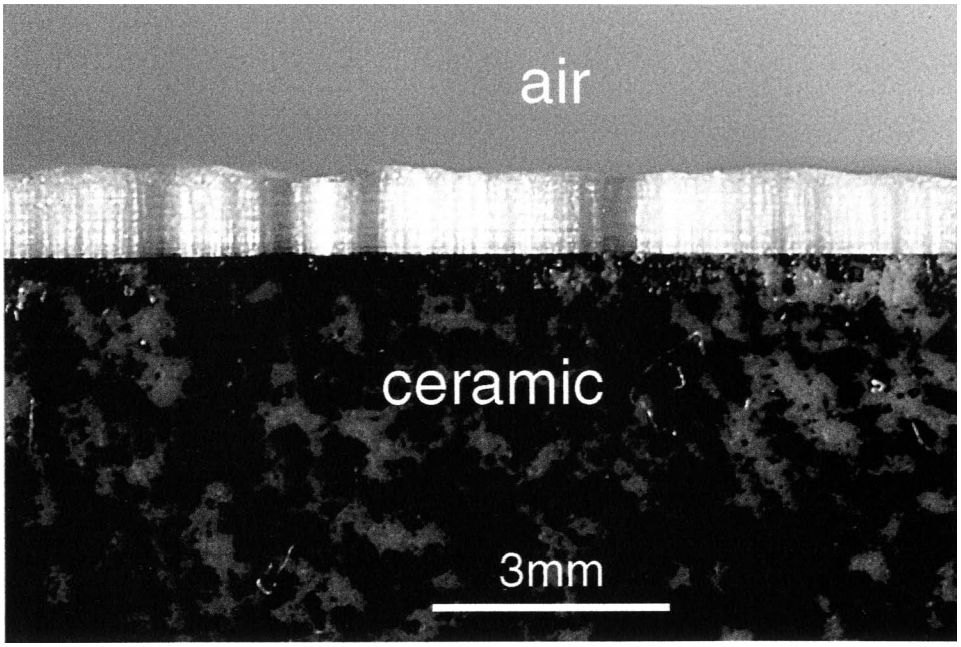

(d)

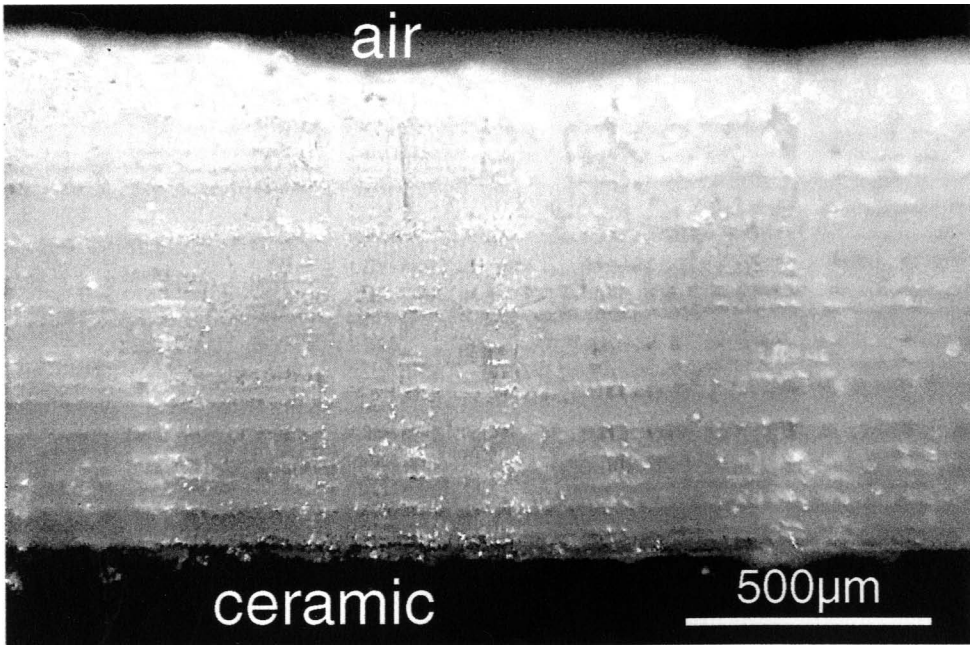

Fig. 2.31 Comparison of growth of fibers of different character in single-block experiments *TB-4a* & *TB-4b* under different humidity conditions. The two ceramic samples (*P-3-C*) were both painted black and coated with epoxy except on the growth side and were immersed in the saturated solution of NH_4SCN for 30 minutes. However, one of the samples (*TB-4a*) was placed in a closed desiccator with a RH of 10±5%, while the other (*TB-4b*) was in a desiccator with a RH of 40±5%. (**a**) Tightly packed fibers grown from *TB-4a*, grown over a period of 80 hours (with an average growth rate of 15.3μm/hr). The fibrous character of the growth is deteriorated by the presence of closely spaced Type I features. (**b**) Micrograph of the same view as in (a) but in reflected light of another angle, bringing out varying degrees of concentration of granular material along different Type I features. "**T**" indicates the position of the thickest Type I feature as also marked in (a). (**c**) Poor, loosely packed fibers grown from *TB-4b*, grown over a period of 24 hours (with an average growth rate of about 50μm/hr). The growth is loose and messy and contains Type II transverse features (**II**). (**d**) Slightly different looking poor fibers grown in the same experiment as in (c) but on the cleaned growth surface over the next 16.5 hours (with an average growth rate of about 56μm/hr). The growth again is very porous and contains numerous Type II features, destroying the fibrous structure of the aggregate and giving rise to cell-like forms or voids forming a characteristic honeycomb-like structure.

(a)

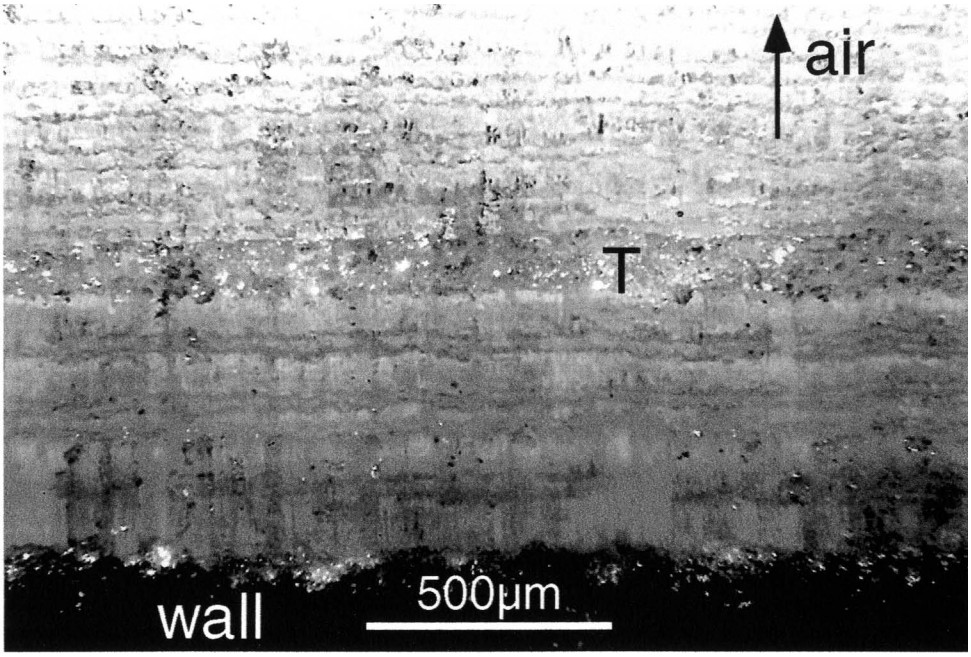

(b)

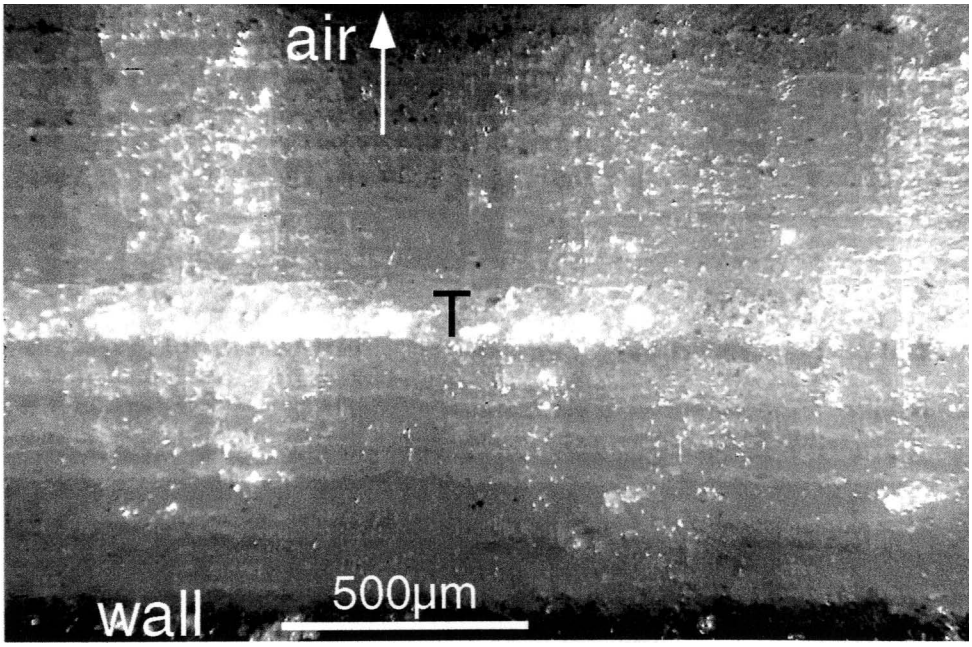

(c)

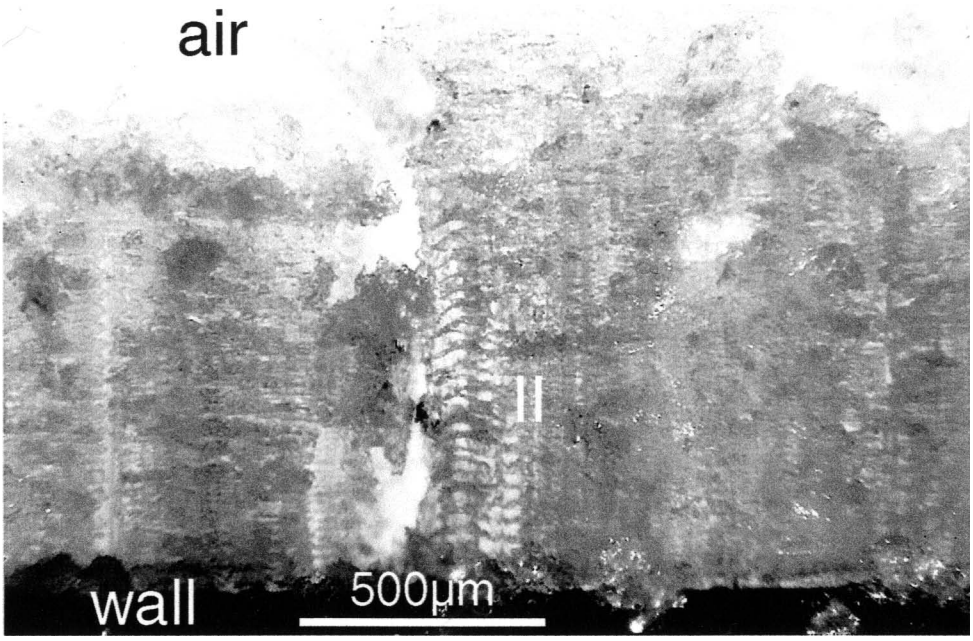

(d)

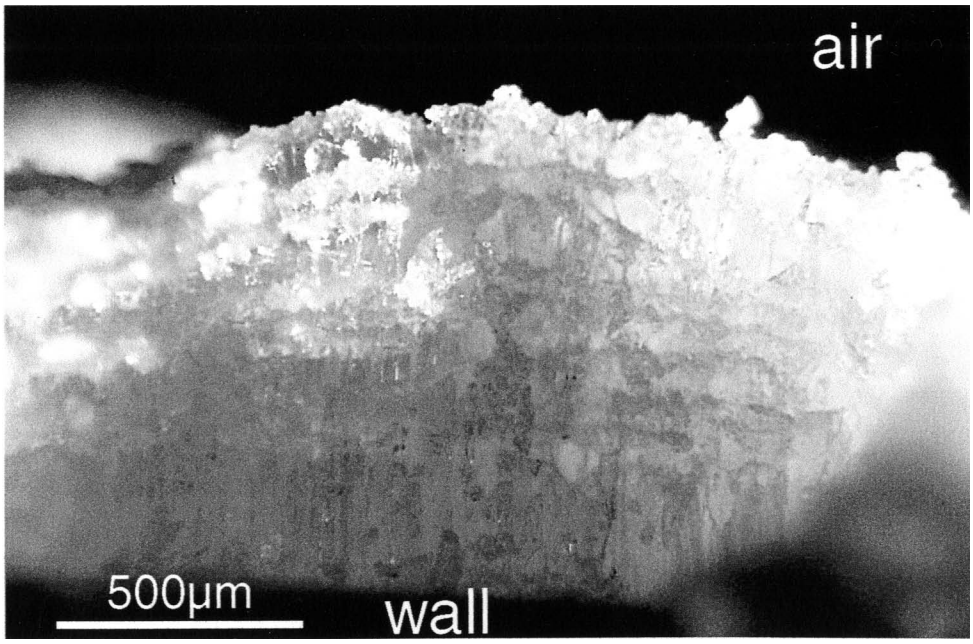

Fig. 2.32 Comparison of growth of fibers of different character in single-block experiments *TB-5a* & *TB-5b* under different humidity conditions. The two ceramic samples (*Square*) were both painted black and coated with epoxy except on the growth side and were immersed in the saturated solution of NH_4SCN for 30 minutes. However, one of the samples (*TB-5a*) was placed in a closed desiccator with a RH of 15±5%, while the other (*TB-5b*) was in a desiccator with a RH of 45±5%. (**a**) Tightly packed fibers grown from *TB-5a*, grown over a period of 48 hours (with an average growth rate of 20 μm/hr). The fibers are of good quality with only a few faint Type I features. (**b**) New good, tightly packed fibers grown on the cleaned substrate of *TB-5a* over the next 42.5 hours after the old fibers in (a) were removed. Average growth rate is about 18 μm/hr. (**c**) Moderately packed, fair-quality fibers grown from *TB-5b*, grown over a period of 24 hours (with an average growth rate of about 45 μm/hr). Besides numerous Type II bands, the fibers also contain some voids (V) and granular material. (**d**) Enlarged view of the type II fibers in (c) at a large power, showing at least 70 Type II bands over a fiber length of about 930 μm, giving an average spacing of about 7-10 μm.

(a)

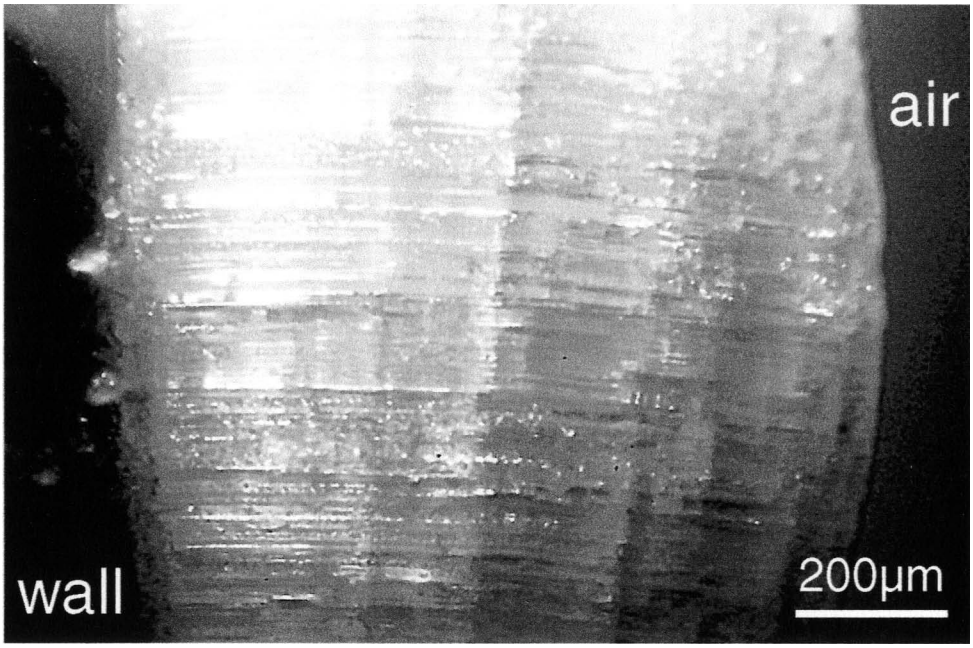

(b)

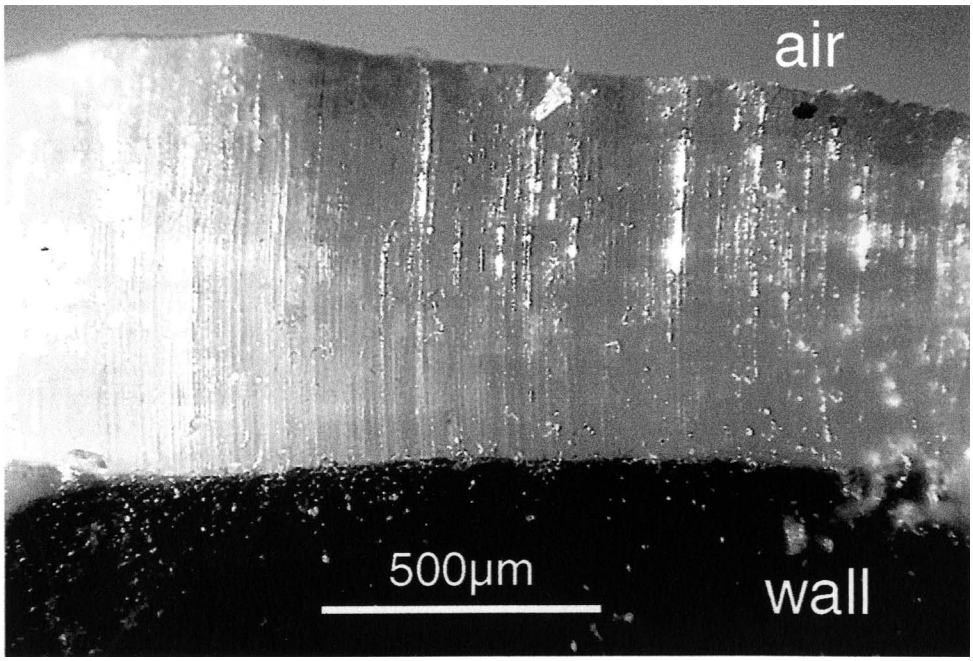

(c)

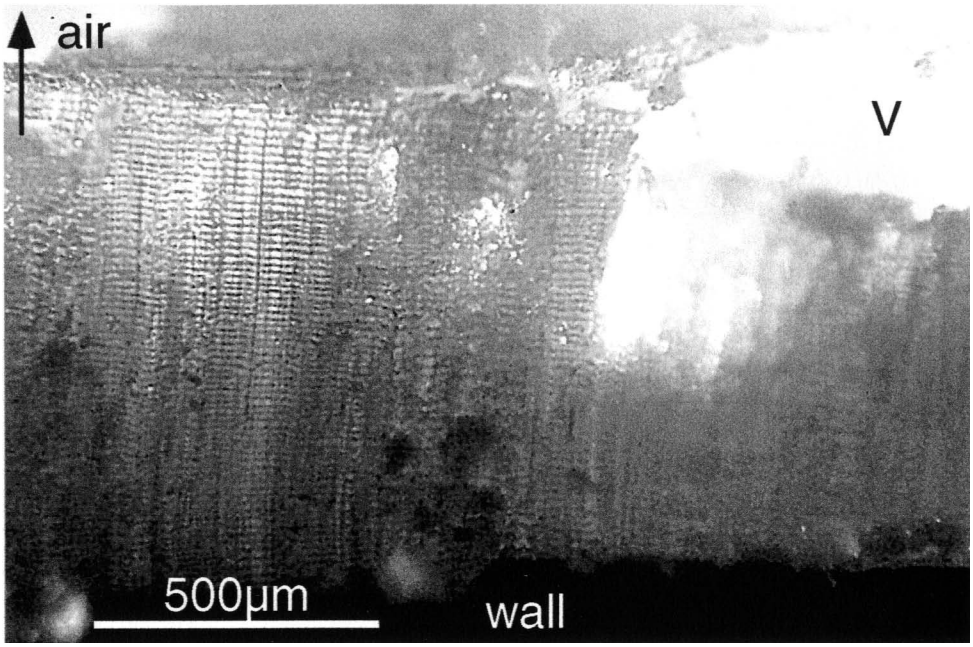

(d)

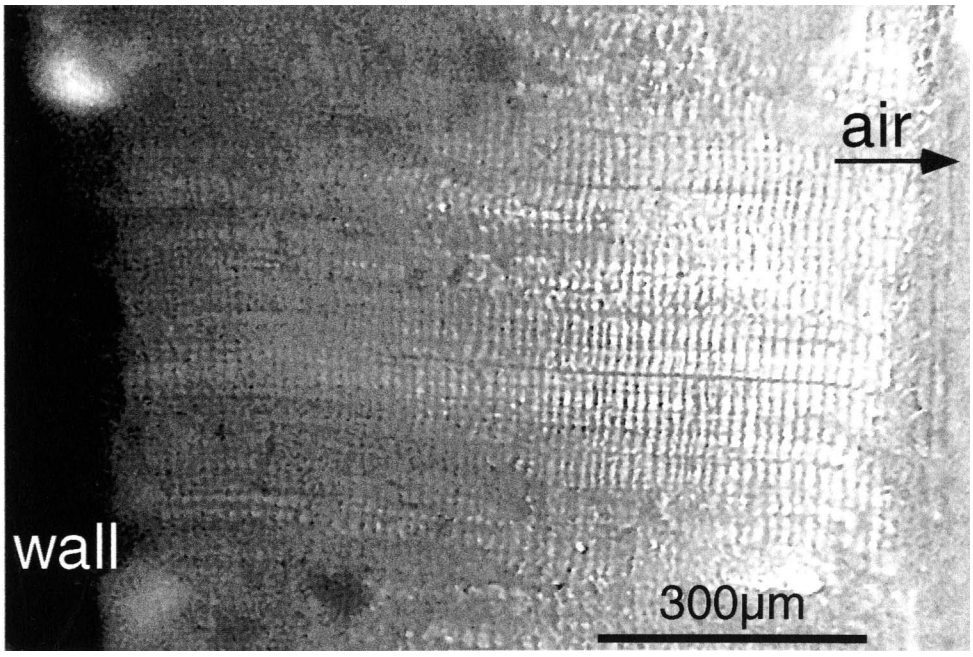

Fig. 2.33 Growth of moderately packed, fair-quality fibers of NH_4SCN in experiment *TB-09* under relatively high humidity conditions (RH=40±5%). Ceramic sample (*Square*) was painted black and coated with epoxy except on the growth side and was immersed in the saturated solution of NH_4SCN for 30 minutes. (**a**) Fast growth of good, well packed milky fibers from the sample over the first period of 74 hours (with an average growth rate of 60 μm/hr). An even faster growth rate (up to 150μm/hr) was observed during the first 20 hours. (b) A close-up view of the fibers near the wall showing numerous closely spaced Type II feature as well as a Type I discontinuity close to the wall (**T**).

(a)

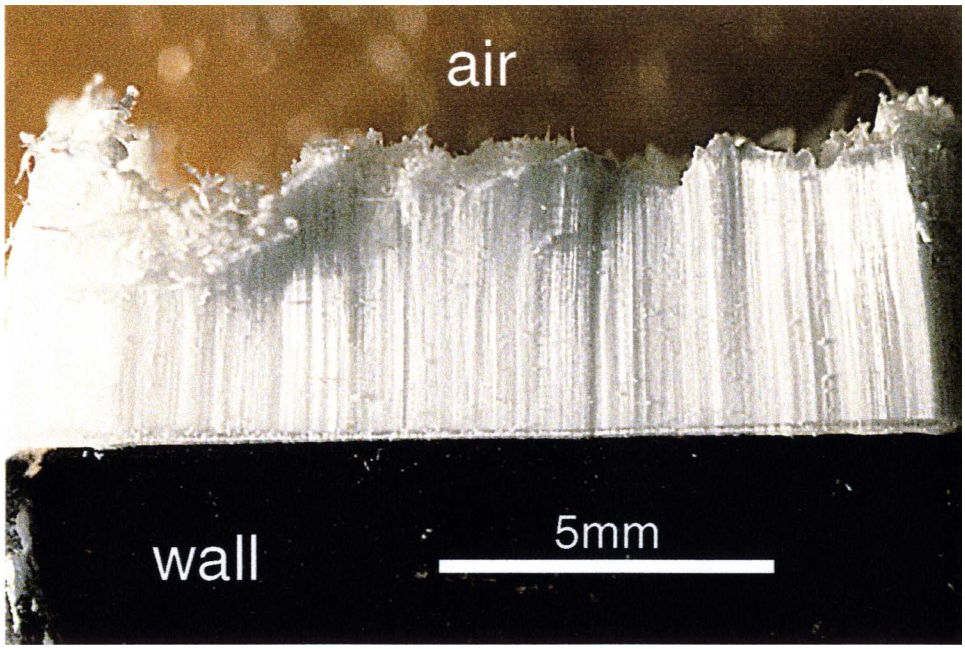

(b)

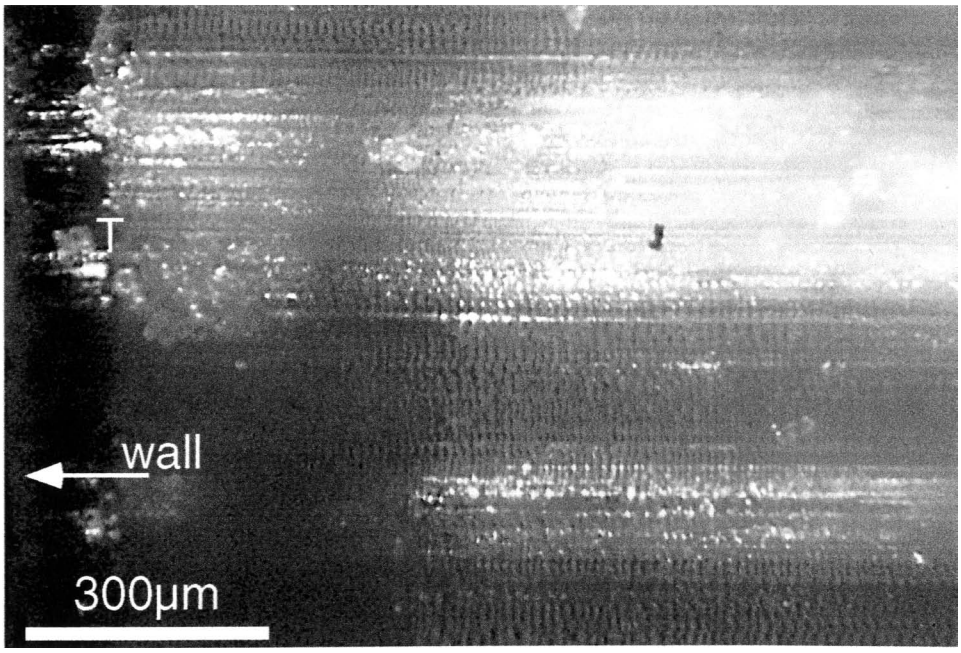

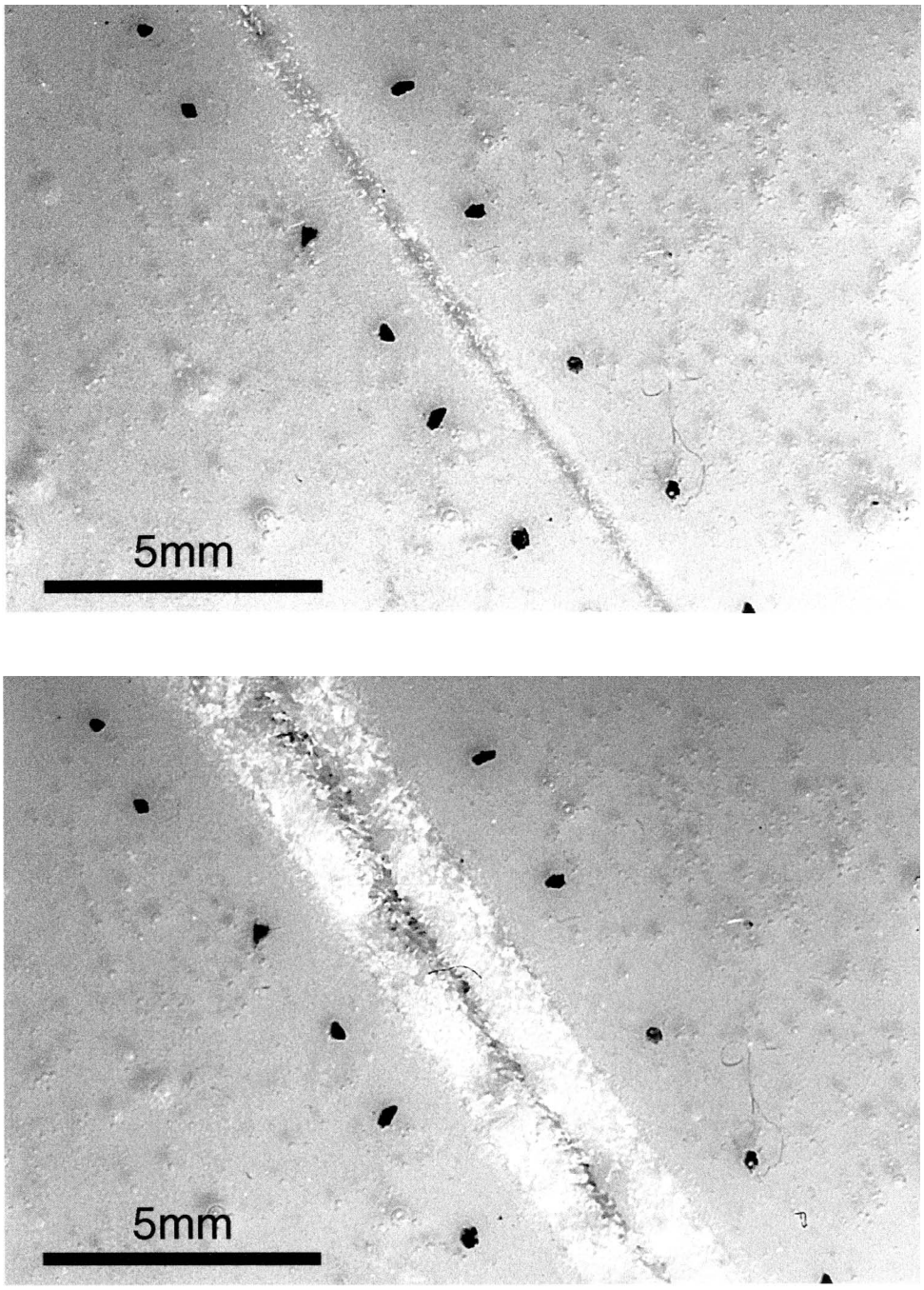

Fig. 2.34 Growth of a vein of poor fibers or non-fibers of NH_4SCN in an oblique-opening two-block experiment (*CFB-34*) (refer to Fig. 2.2b) in a closed desiccator with a RH of 30±5%. Ceramic blocks (*Big Disc*) were coated with epoxy except on the crack side and growth occurred by pushing apart the enclosing walls that were originally in contact. Black spots alongside of the vein are markers placed for the purpose of monitoring opening displacement. (**a**) Initial state of sample, with the horizontal dimension parallel to the guides. (**b**) A vein of poor fibers or non-fibers grown over a period of 79 hours (with an average opening rate of 28.5 μm/hr). Most of the growth already occurred during the first 24 hours (at a rate of 83.6 μm/hr). Notice a median line at the center of vein that contains gaps as well as fibrous crystals.

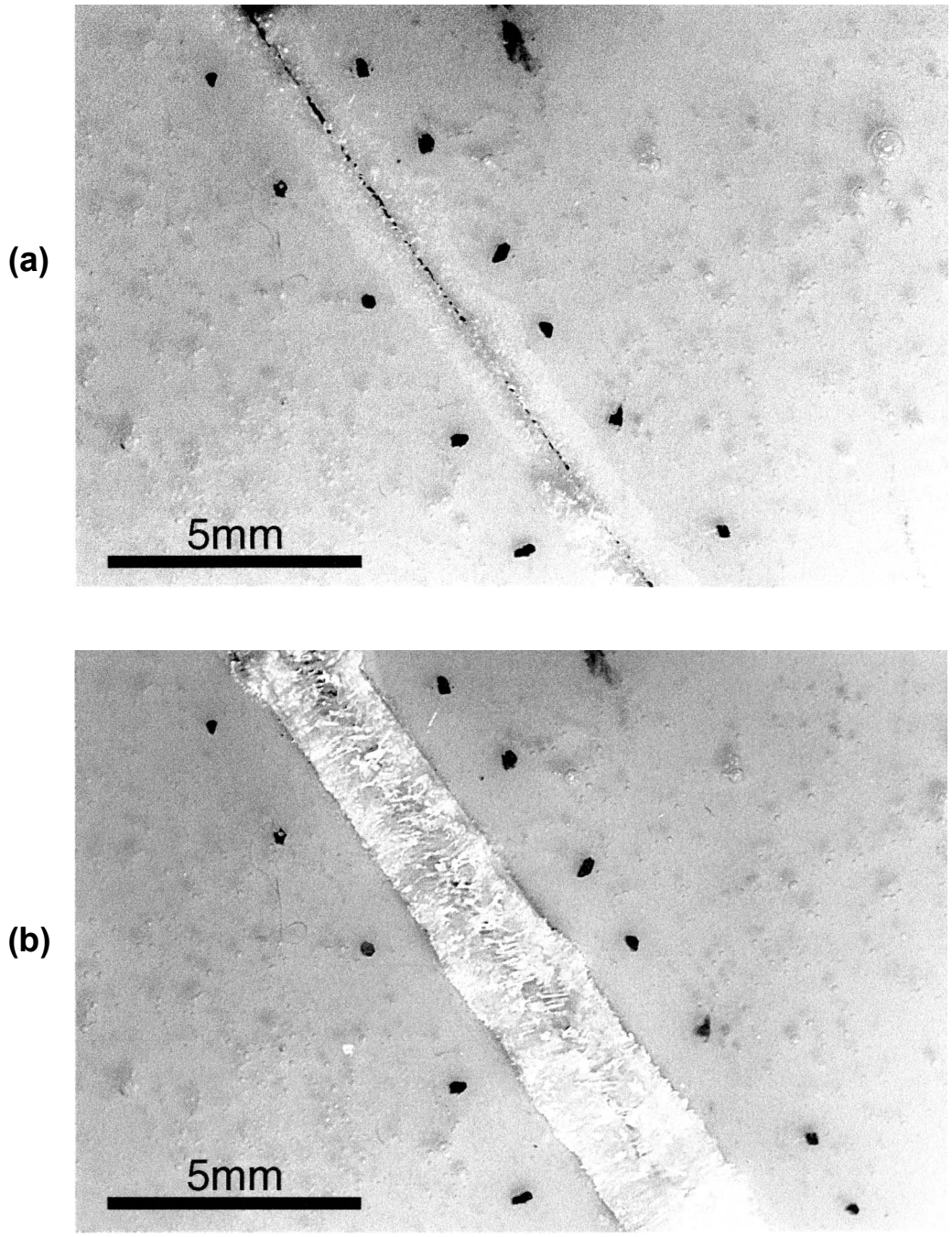

Fig. 2.35 Growth of a vein of loosely packed, poor-quality fibers of NH_4SCN in an oblique-opening two-block experiment (*CFB-36*) (refer to Fig. 2.2b) in a closed desiccator with a RH of about 40±5%. Ceramic blocks (*Big Disc*) were coated with epoxy except on the crack side and growth occurred by pushing apart the enclosing walls that were originally in contact. Black spots alongside of the vein are markers placed for the purpose of monitoring opening displacement. (**a**) Initial state of sample, with the horizontal dimension parallel to the guides. (**b**) An opened vein of poor fibers as seen 183 hours later, the left block fixed relative to the picture. Average opening rate was about 12.8 μm/hr. Fibers are loosely packed and sigmoidally curved due to the constraint of the guides.

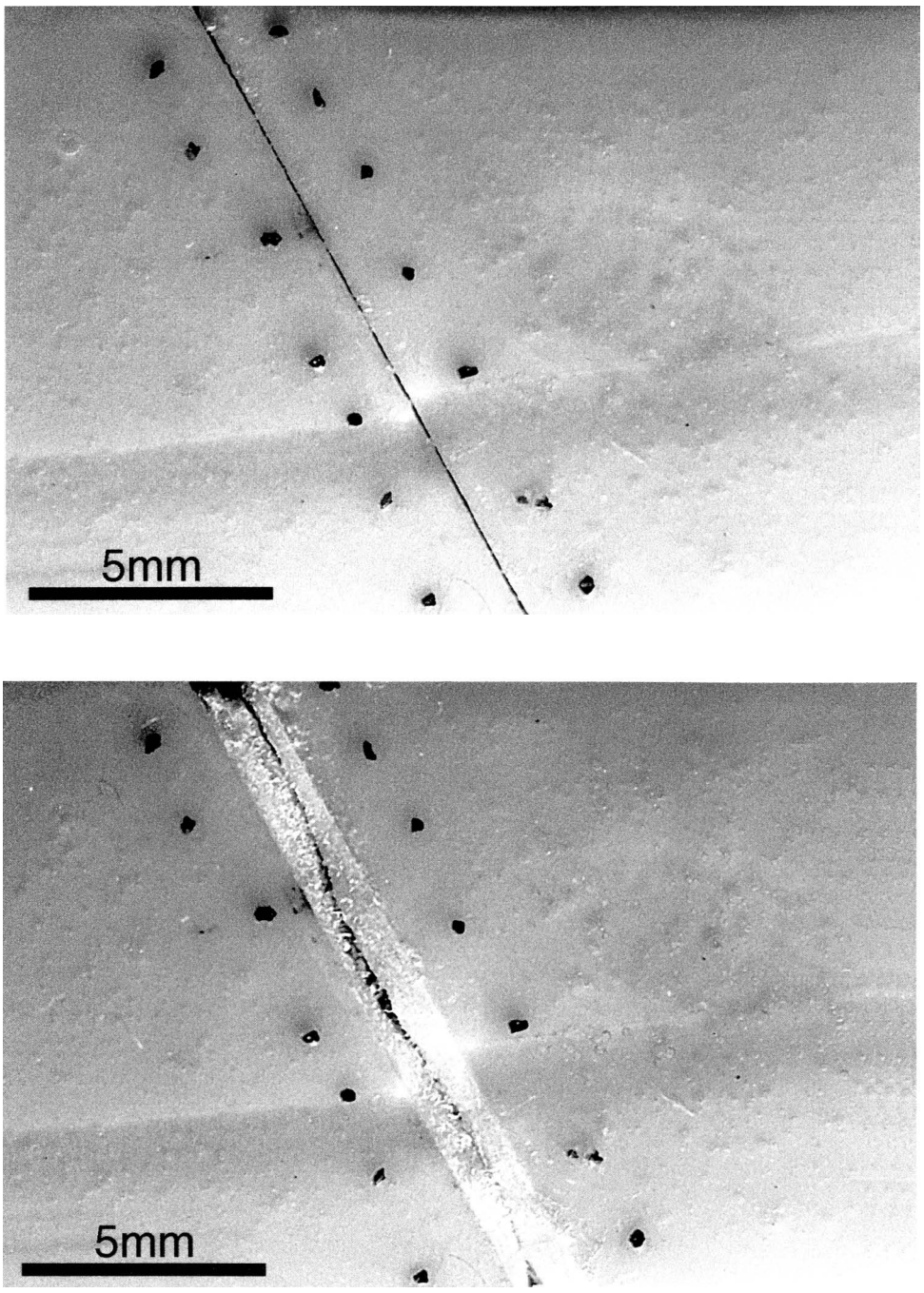

Fig. 2.36 Growth of a vein of tightly packed fibers of NH_4SCN in an oblique-opening two-block experiment (*CFB-38*) (refer to Fig. 2.2b) in a closed desiccator with a RH of about 15±5%. Ceramic blocks (*Big Disc*) were coated with epoxy except on the crack side and growth occurred by pushing apart the enclosing walls that were originally in contact. Black spots alongside of the vein are markers placed for the purpose of monitoring opening displacement. (**a**) Initial state of sample, with the horizontal dimension parallel to the guides. (**b**) Opened vein of poor fibers and/or granular material grown over the first 80 hours (with an average opening rate of 16.4 μm/hr). The growth is tightly packed although there is a line of gaps at the center of vein due to a small resistance against the opening.

(c)

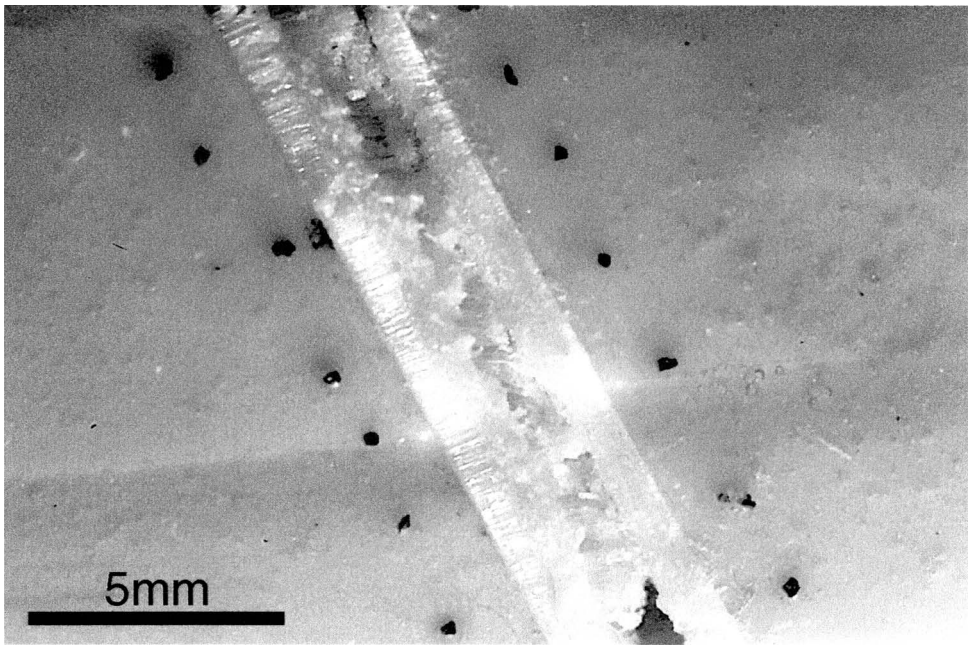

(d)

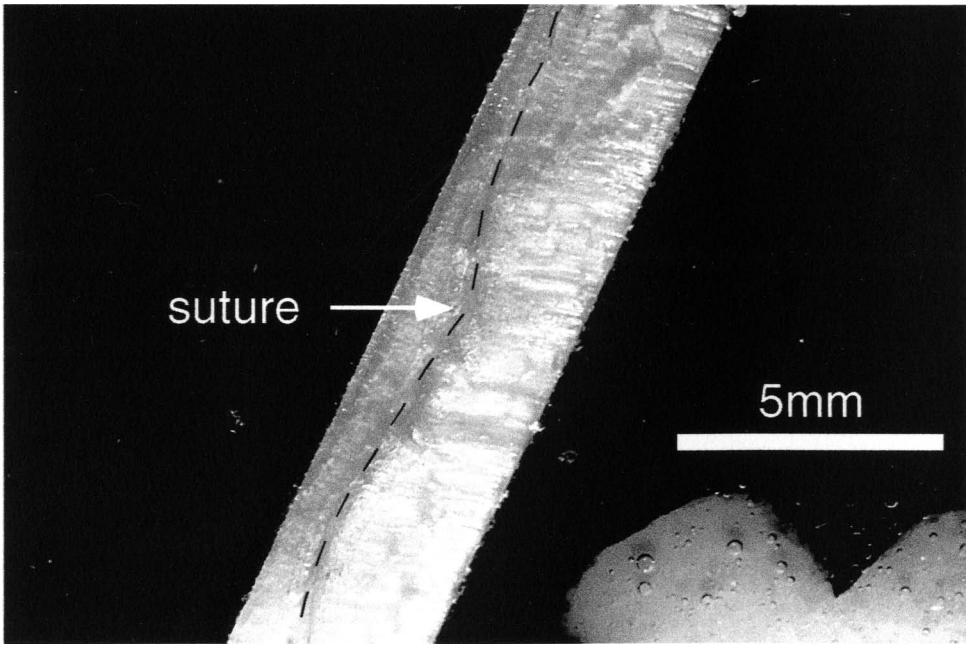

Fig. 2.36 (continued) **(c)** Further widened vein as seen another 87.5 hours later (grown with an average opening rate of 22.7 μm/hr). While the old growth near the center is of a poor quality containing voids as well as granular material, the younger growth near the walls consists of better fibers. **(d)** View of the same vein on the bottom side of sample (walls painted black and coated with epoxy), again alinged with the horizontal dimension parallel to the guides. All fibers are tightly packed on this side, with few voids present and the vein has an asymmetric geometry with the right half better developed.

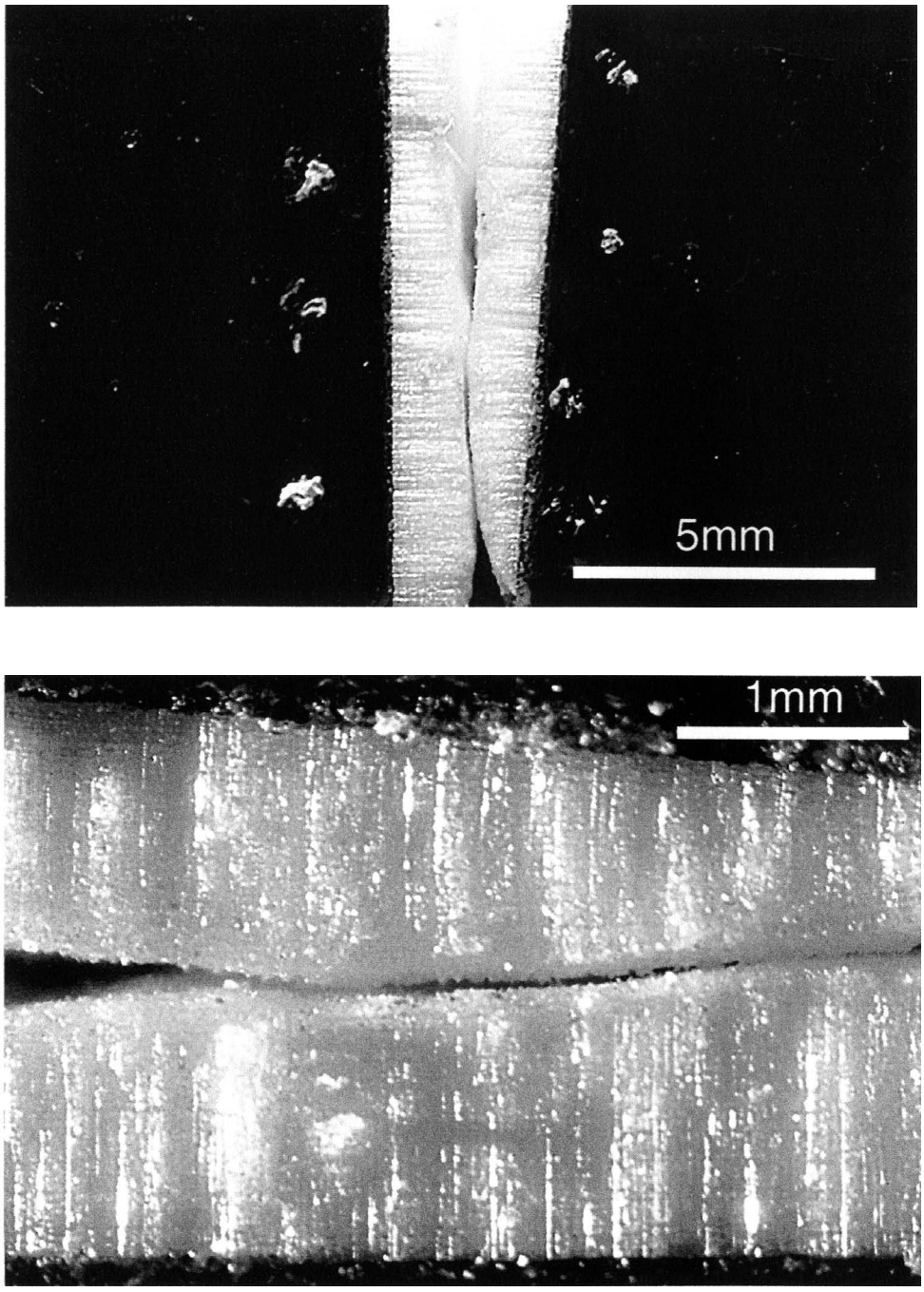

Fig. 2.37 (**a**) Tightly packed fibers grown in a two-block experiment (*TB-19b*) in a closed desiccator with an ambient RH of about 10±5%. Ceramic blocks (*P-3-C*) were painted black and coated with epoxy except on the growth side and growth occurred by pushing apart the blocks that were originally in contact. White spots alongside of the vein are markers placed for the purpose of monitoring opening displacement. The growth took about 3 days (with an average growth rate of about 30 μm/hr). (**b**) Micrograph of the same vein at a larger power, showing clear, good fibers with only some weakly developed Type I features. Gaps remain at the center of vein because of lack of large resistance against the opening.

(a)

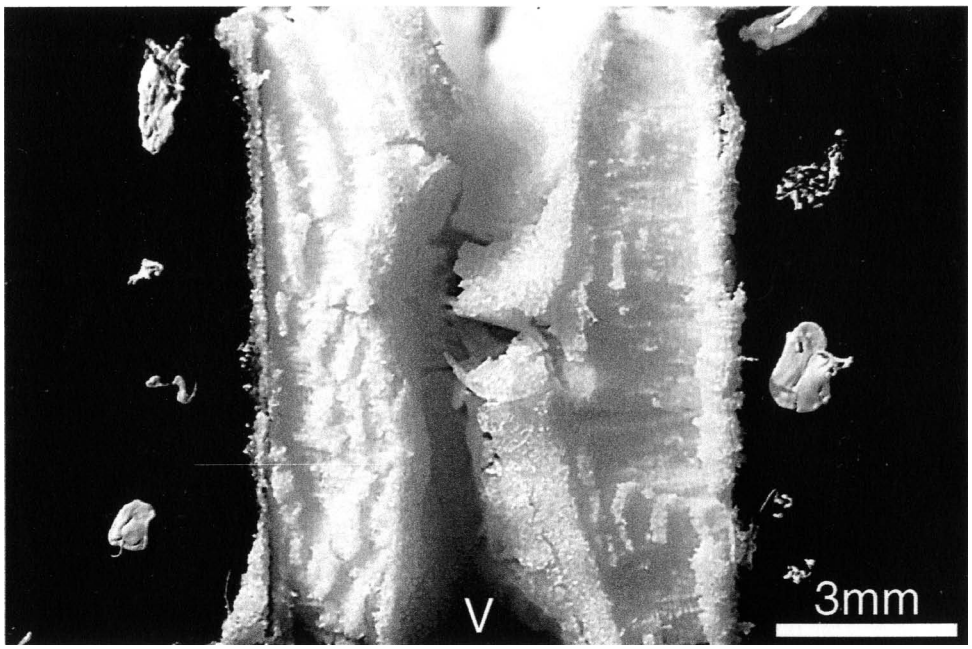

(b)

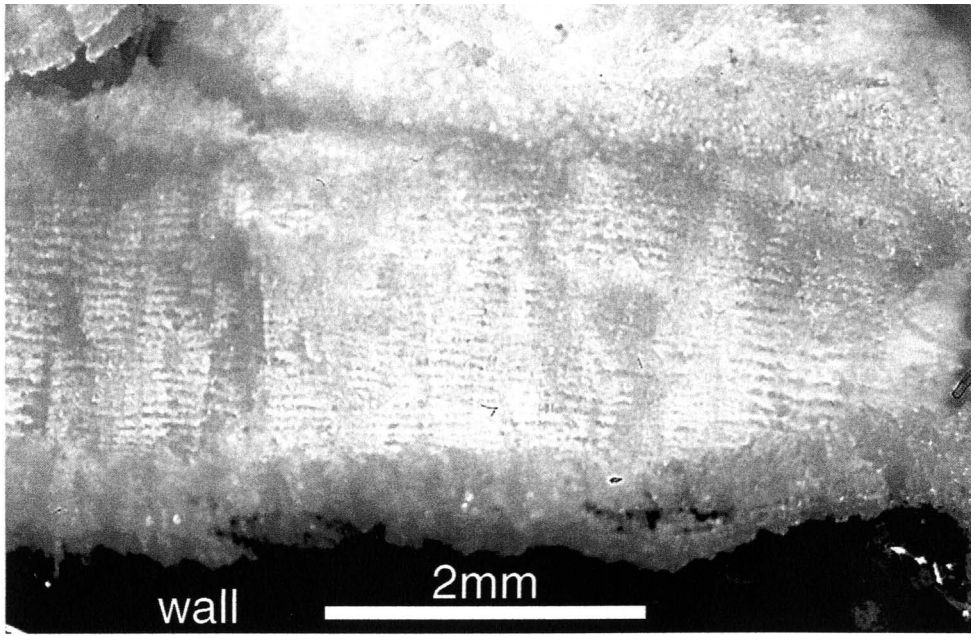

Fig. 2.38 (**a**) Poor, loosely packed fibrous crystals grown in a two-block experiment (*TB-15a*) in a closed desiccator with an ambient RH of about 35±5%. Ceramic blocks (*P-3-C*) were painted black and coated with epoxy except on the growth side and growth occurred by pushing apart the enclosing walls that were originally in contact. White spots alongside of the vein are markers placed for the purpose of monitoring opening displacement. The growth occurred for 38 hours (with an average opening rate of 195 μm). The aggregate is disrupted and contains voids near the center (**V**). (**b**) Micrograph of part of the same vein at a larger power, showing numerous Type II features across the fibers (with an average spacing of 64 μm).

(a)

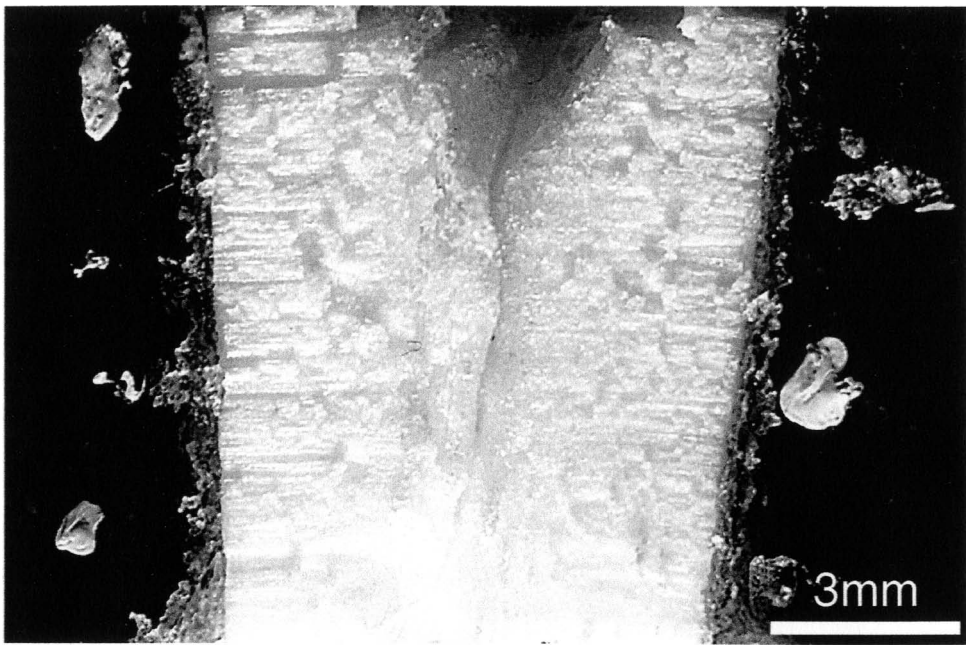

(b)

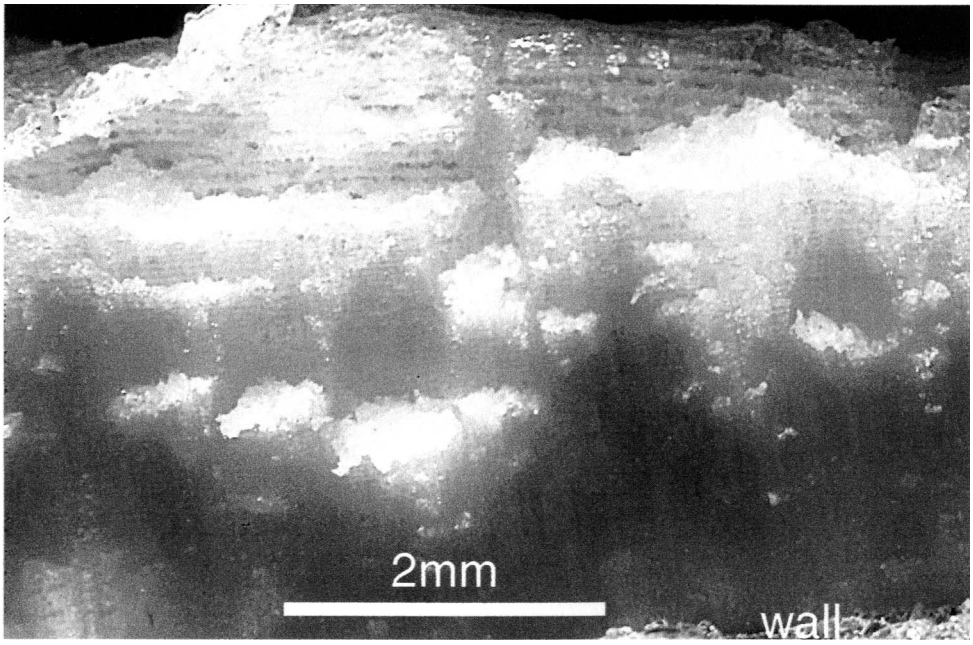

Fig. 2.39 (**a**) Moderately packed, fair-quality fibers grown in a two-block experiment (*TB-20a*) in a closed desiccator with an ambient RH of about 30±5%. Ceramic blocks (*P-3-C*) were painted black and coated with epoxy except on the growth side and growth occurred by pushing apart the enclosing walls that were originally in contact. White spots alongside of the vein are markers placed for the purpose of monitoring opening displacement. The growth occurred for about 4 days (with an average opening rate of 88 μm/hr). The fibers are rather tightly packed but are milky-looking and include blocky grains. Note also the striations-like features on the surface of the aggregate. (**b**) Micrograph of part of the same vein at a larger power, showing steps on 'striations' as well as Type II features across the fibers.

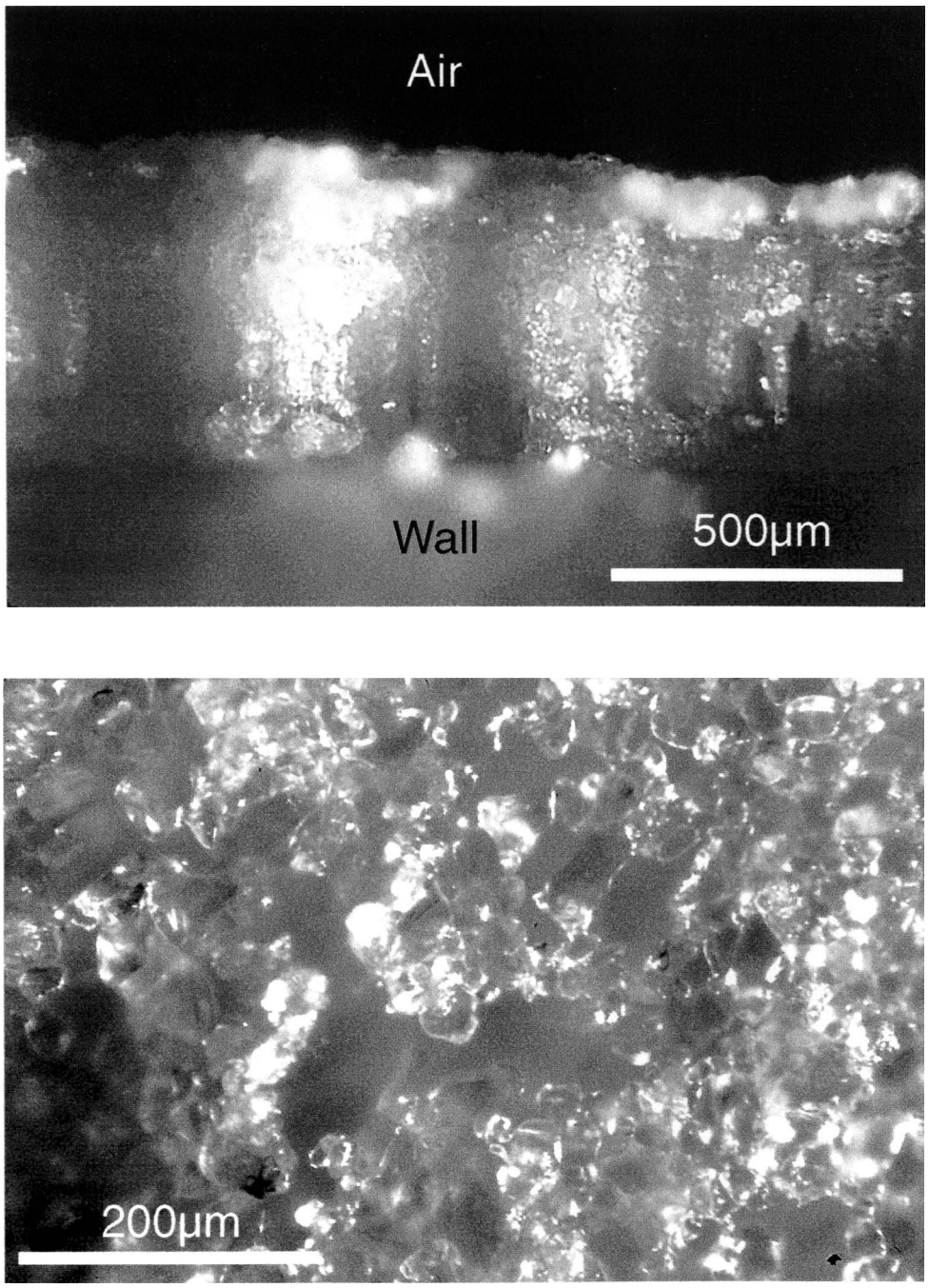

Fig. 2.40 Growth of fibers of NH_4SCN of varying character under conditions of varying relative humidities in a single-block experiment (*NFB-38*) with wax-coated ceramic *Big Disc*. (**a**) Tightly packed poor fibers grown at a relative humidity of about 10±5% during the first two days. These can be seen to be capped by a thick crust of granular material representing the earliest growth. (**b**) Micrograph of the equidimensional crystals on the free surface of the granular crust.

(c)

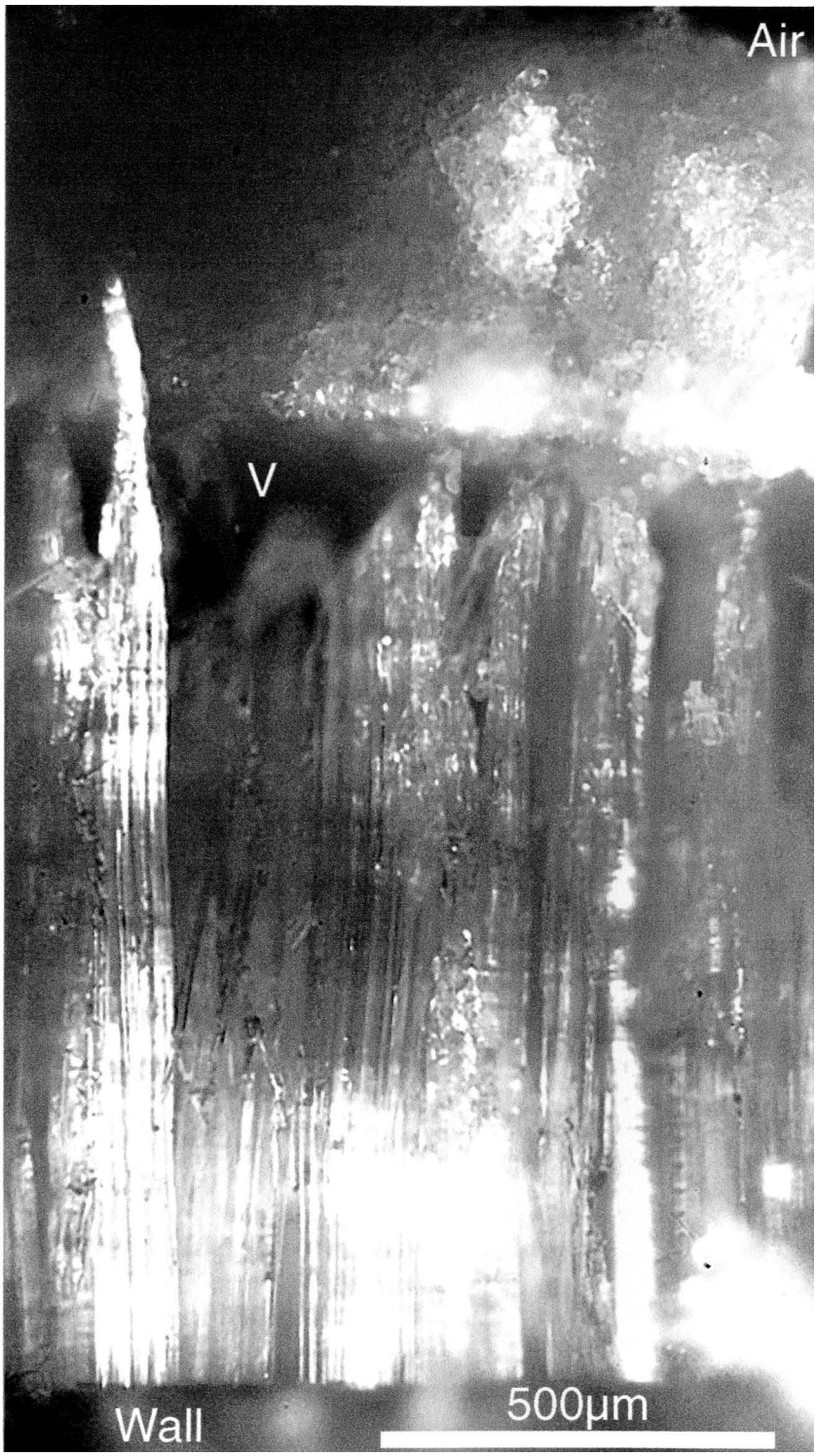

Fig. 2.40 (continued) (**c**) Fast growth of loosely packed fibers at an increased relative humidity (RH=41±5%) over a short period of about 19 hours. These can be seen to be separated from the older poor fibers or non-fibers by a pronounced Type I discontinuity as well as voids (**V**).

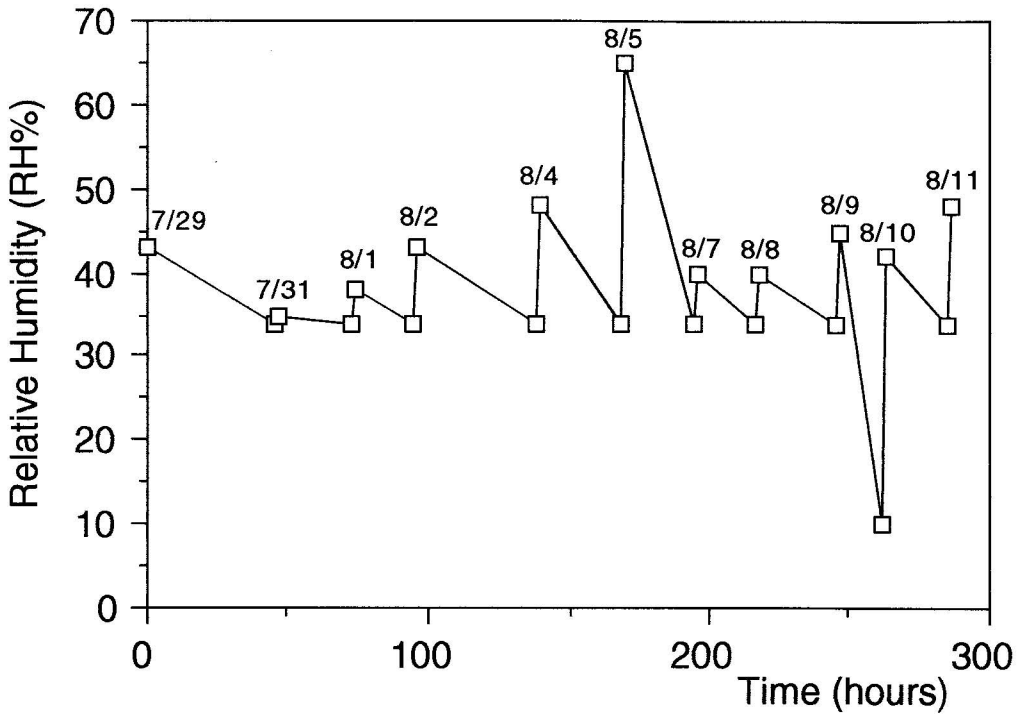

(a)

Fig. 2.41 History of variation of the ambient relative humidity during experiment *NFB-33* compared with type I features that occurred across the fibers at various stages of experiment. (**a**) Plot of room relative humidities measured intermittently over time. Numbers above each high plot point represent the date of measurement. Errors are about ±5%. (**b**) Sketches of fibers and their type I transverse features as observed at four successive times. Corresponding date of observation is shown at the top of each diagram. Type I features are numbered as I, II, ..., VI from oldest to youngest. (**c**), (**d**), (**e**) & (**f**) Photographs of the real sample at the four corresponding times, all taken in transmitted light. Besides type I discontinuities, the sketches and micrographs also show type II features (short wriggled lines in sketches).

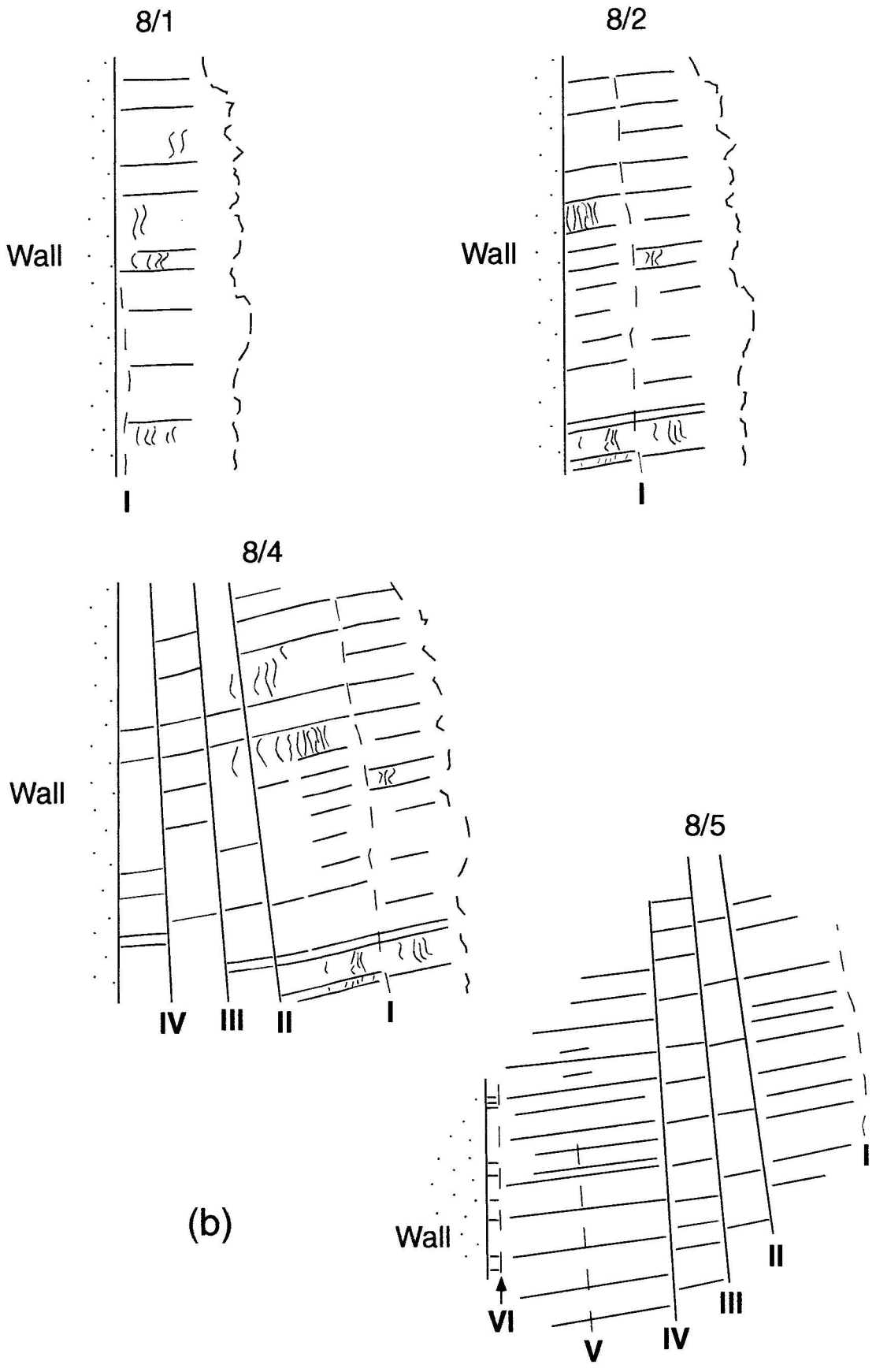
8/1
Wall
I
8/2
Wall
I
8/4
Wall
IV
III
II
I
8/5
(b)
Wall
VI
V
IV
III
II
I

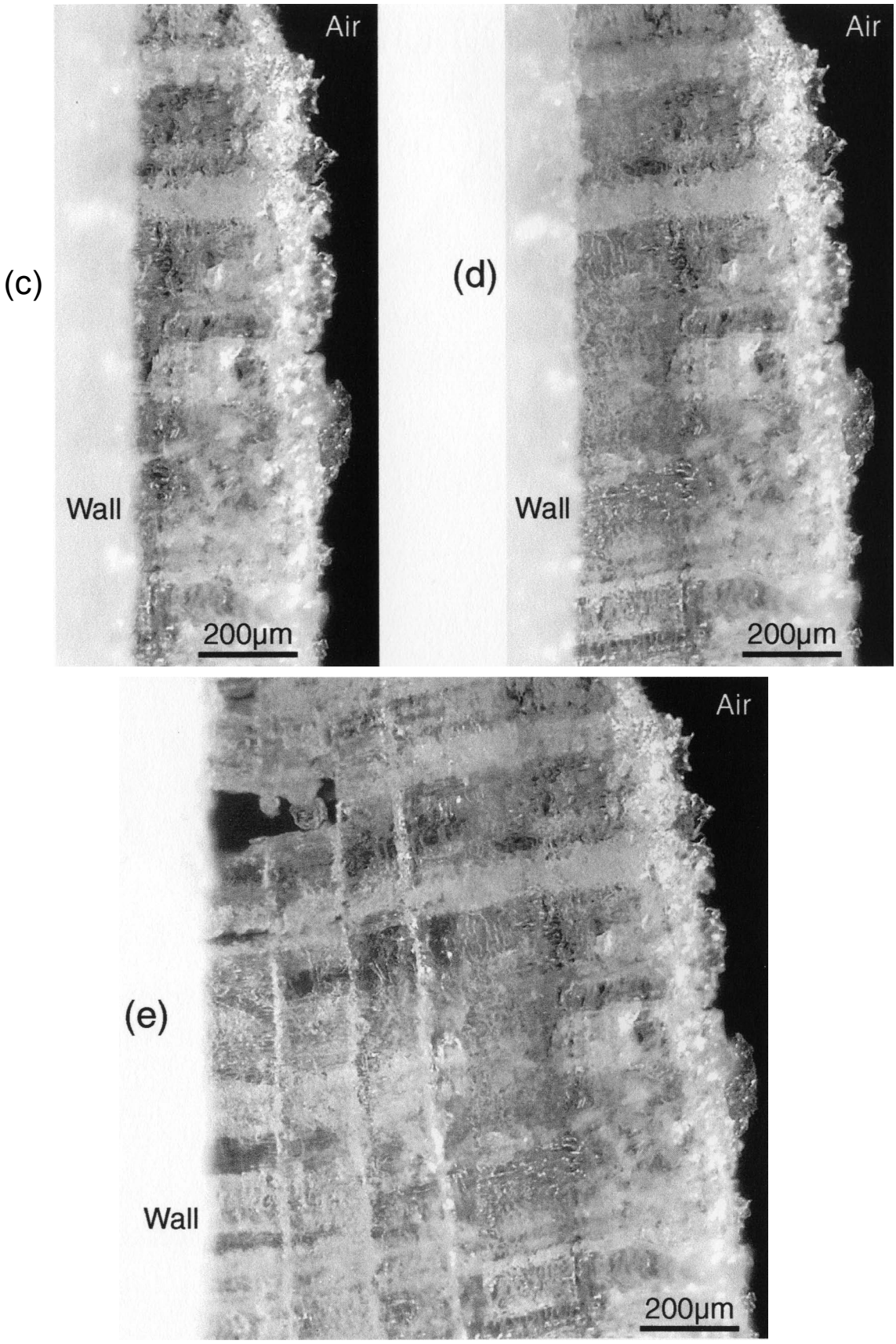
(c)
Air
Wall
200μm
(d)
Air
Wall
200μm
(e)
Air
Wall
200μm

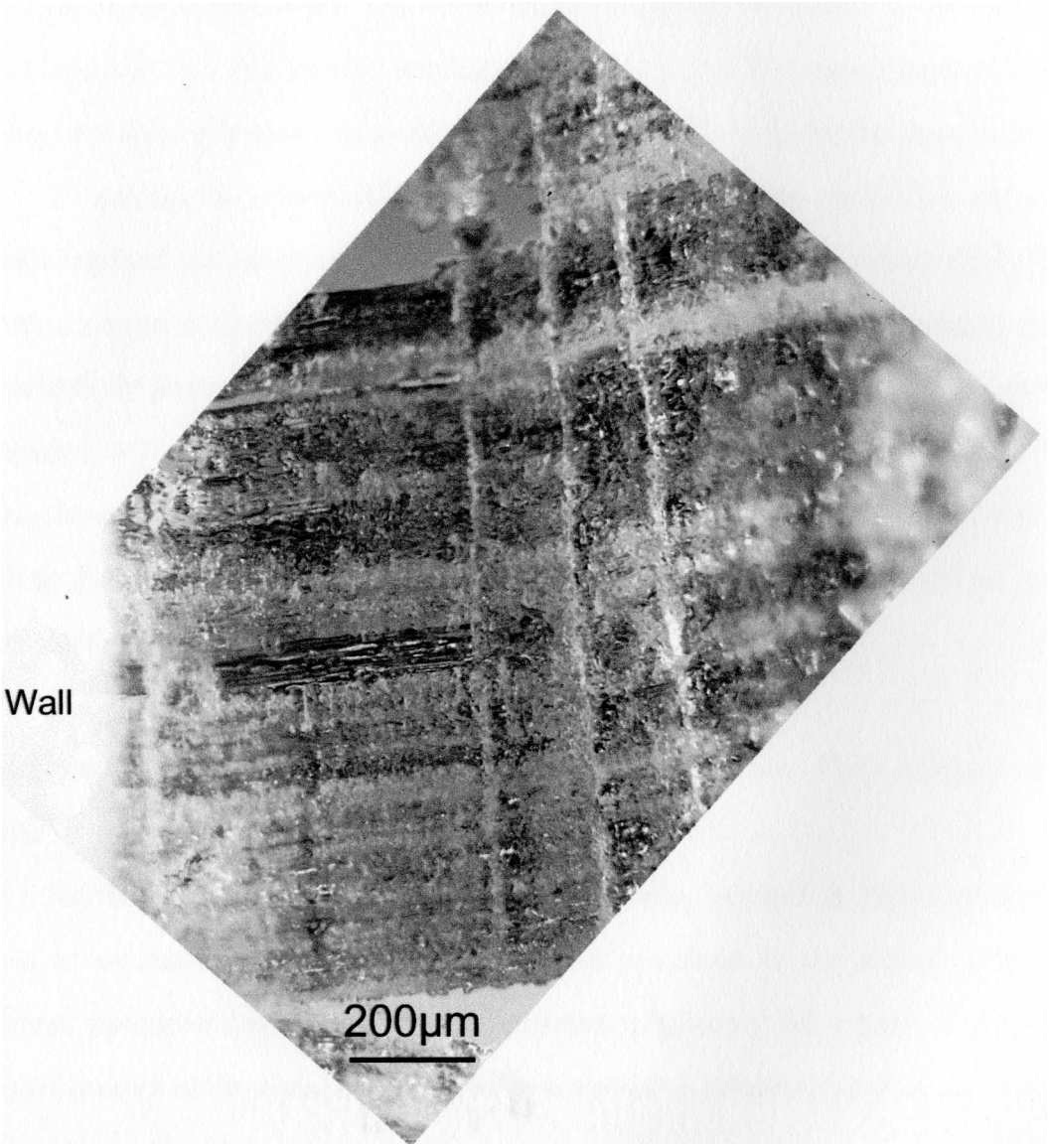

(f)

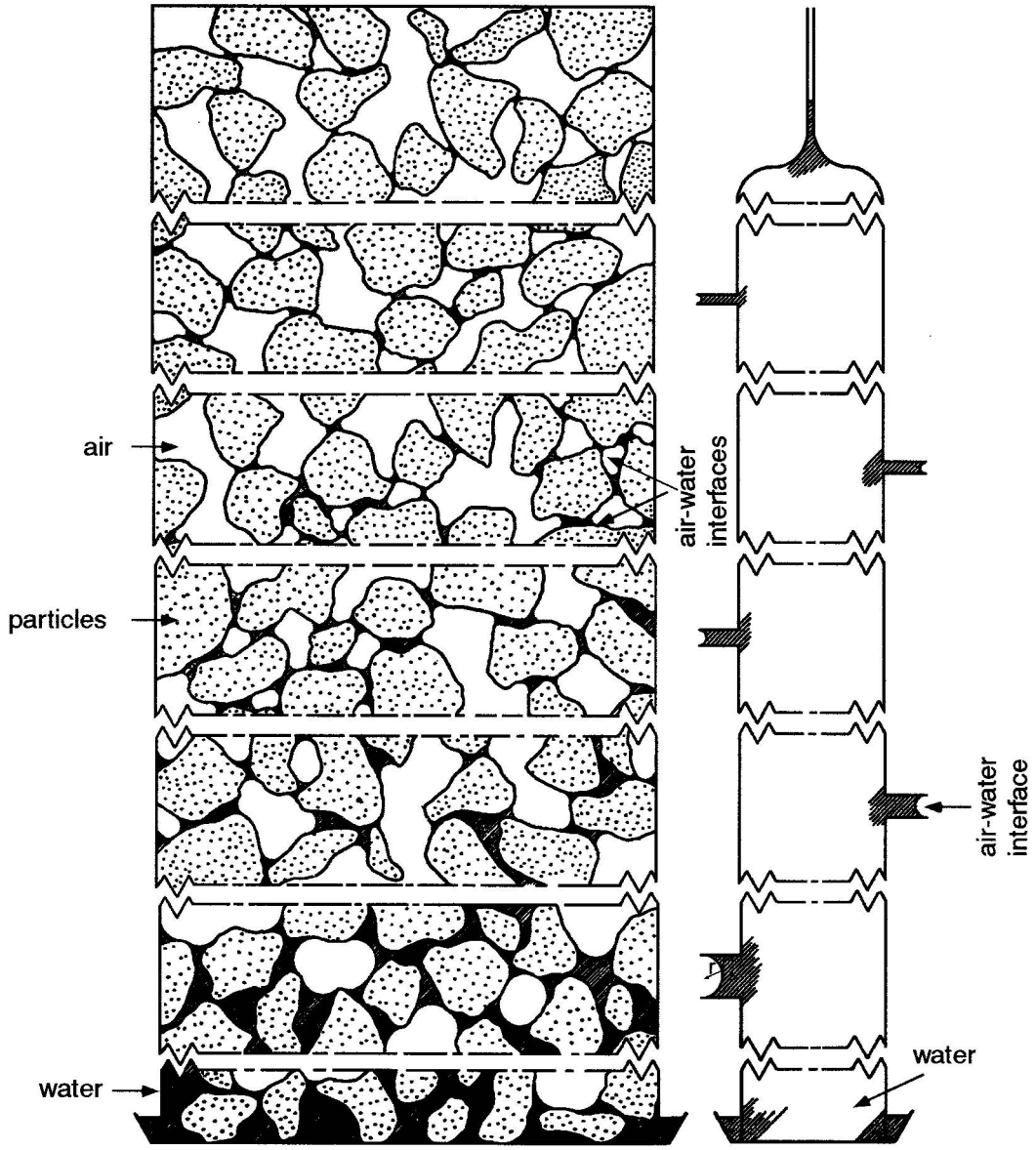

Fig. 2.42 Air-water interfaces in a porous medium with various amounts of moisture (from Kirkham & Powers 1972, p.28). At the left, the column of porous material contains progressively less moisture at progressively higher levels above a water table. At the right, a vertical tube with menisci corresponging to the curved water-air interfaces in the porous material is shown. The less moisture the porous material contains, the smaller the radius of curvature (r) at the air-water interfaces.

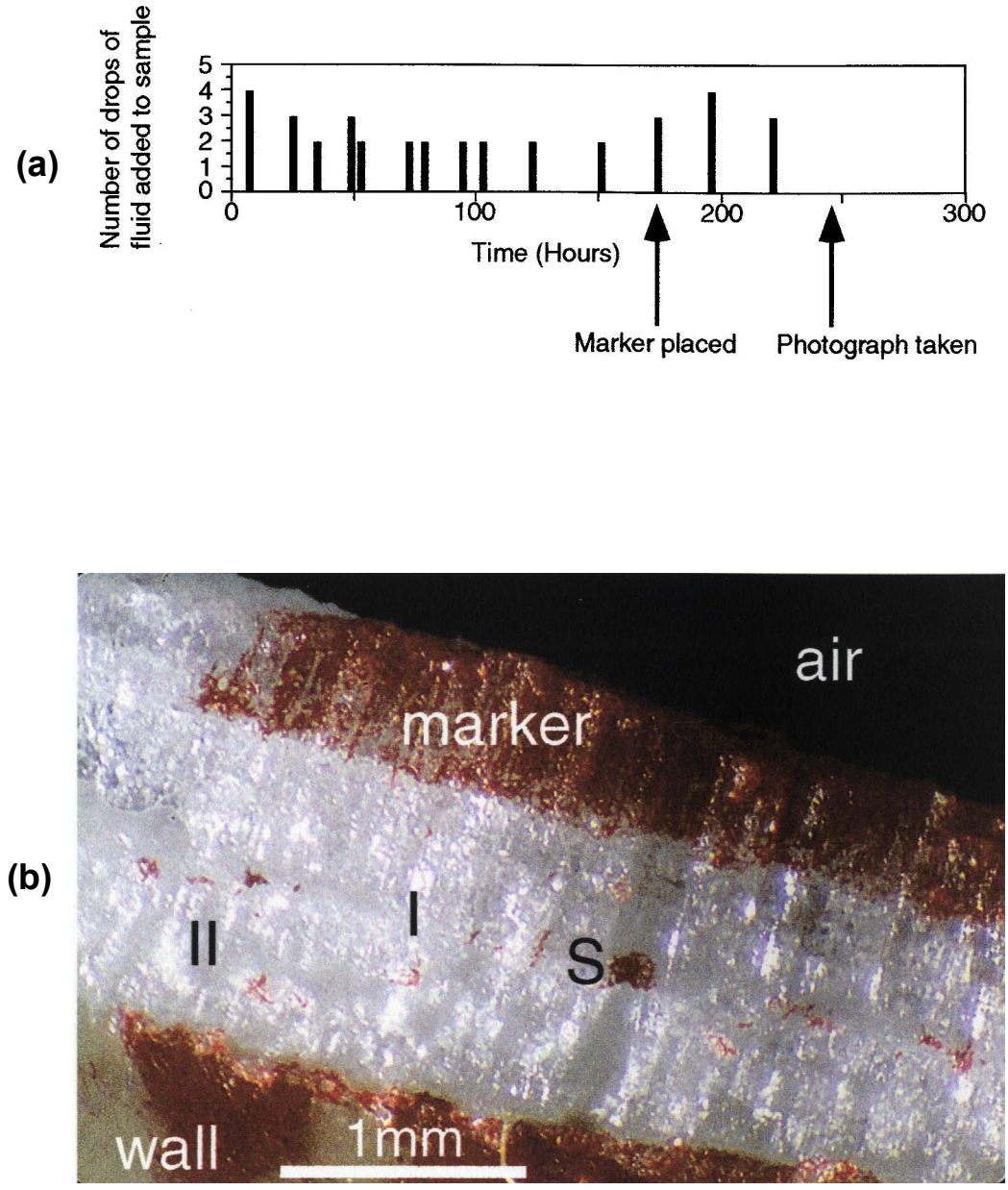

Fig. 2.43 Growth of tightly packed but poorly shaped fibers of NH_4SCN in a single-block experiment (*NFB-01*) in which more crystallizing fluid was repeatedly added to sample *during* the experiment. (**a**) Diagram showing the history of fluid addition. Arrows indicate the time when an ink marker was placed across the fiber-wall interface and the time when sample was photographed. (**b**) Photograph of sample taken at the time as shown in (a) (about 10 days after experiment was started), showing the poor quality of fibers due to presence of much granular material, wall-derived inclusions of pen ink (S) and Type I (I) and Type II features (II).

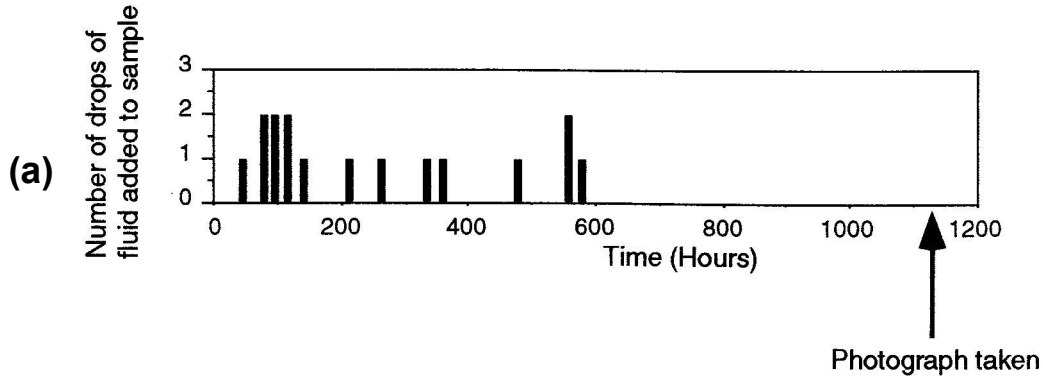

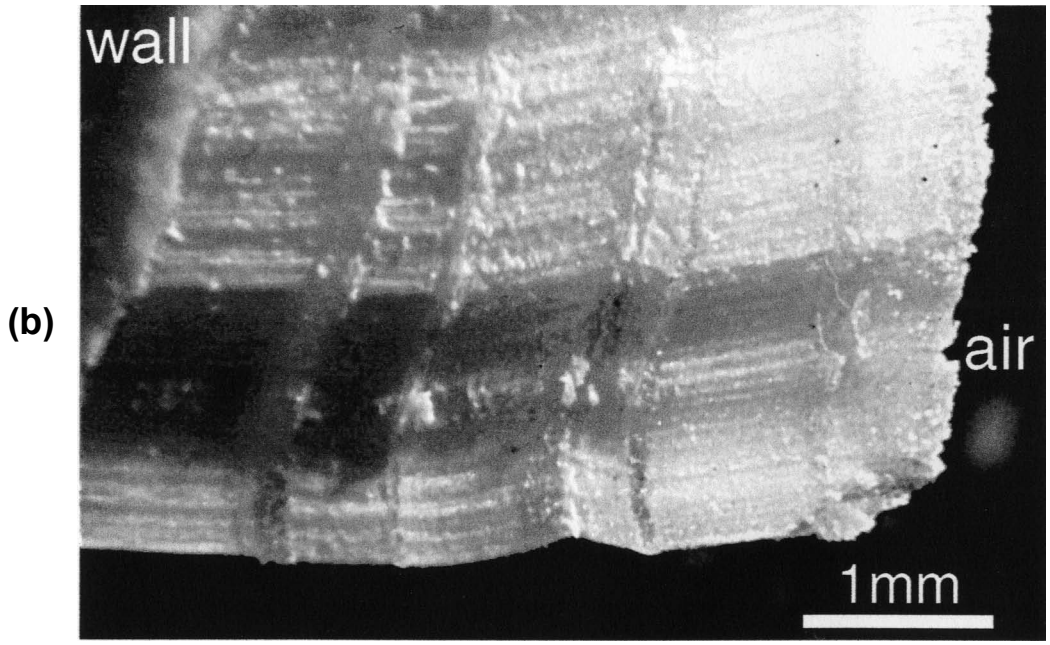

Fig. 2.44 Growth of tightly packed fibers of NH_4SCN in a single-block experiment (*NFB-10b*) in which more crystallizing fluid was repeatedly added to sample *during* the experiment. (**a**) Diagram showing the history of fluid addition. Arrow indicates the time when sample was photographed. (**b**) Photograph of sample taken at the time as shown in (a) (about 47 days after experiment was started), showing the tightly packed character of fibers and the presence of five ridge-like seams of granular material (Type I features) across the fibers. Although clearly related to the fluid additions, these features cannot be simply correlated with the individual fluid addition events in (a).

(a)

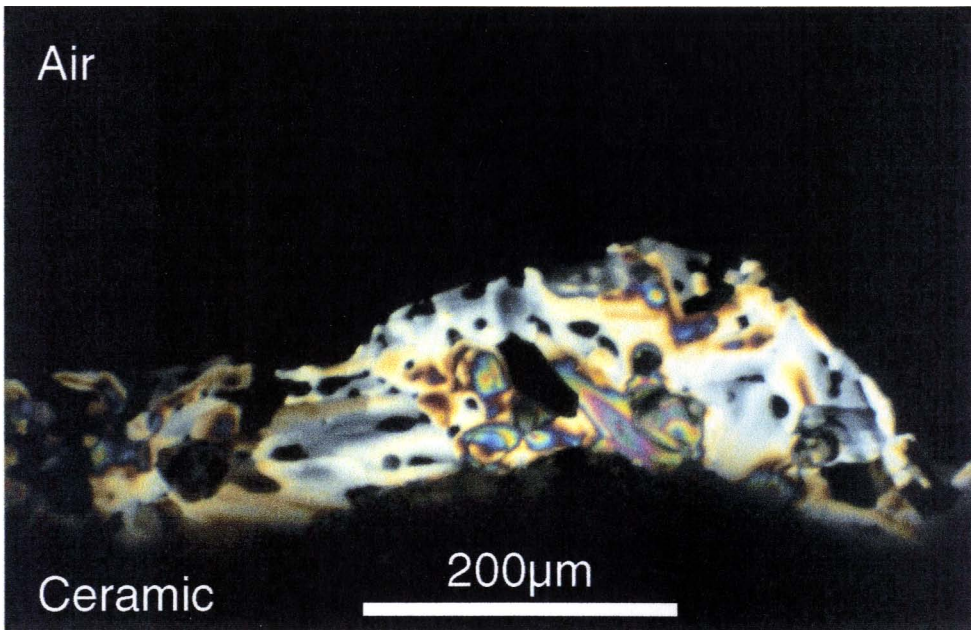

(b)

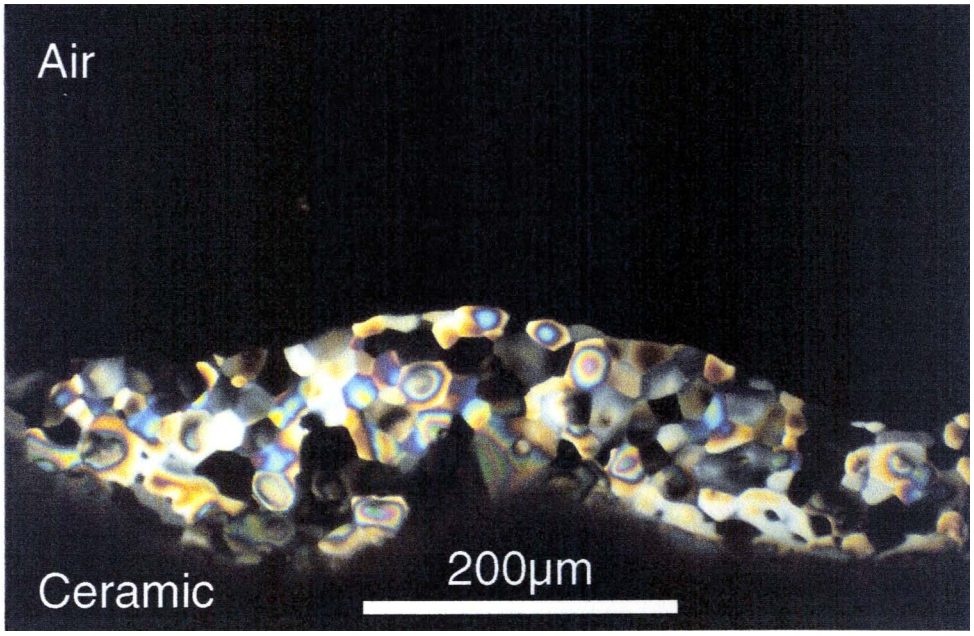

Fig. 2.45 Growth of granular NH_4SCN crystals at the edge of a thin piece of ceramic (*Big Disc*) (ca. 400μm in thickness) soaked with too much fluid at the beginning of experiment (no. *ST-03*). (a) Irregular non-fibers as seen about 2 hours after experiment started. (b) Micrograph of the same site as seen about 28 hours after the first picture was taken, showing equi-dimensional crystal grains derived from the older crystals. Both pictures were taken under crossed nicols.

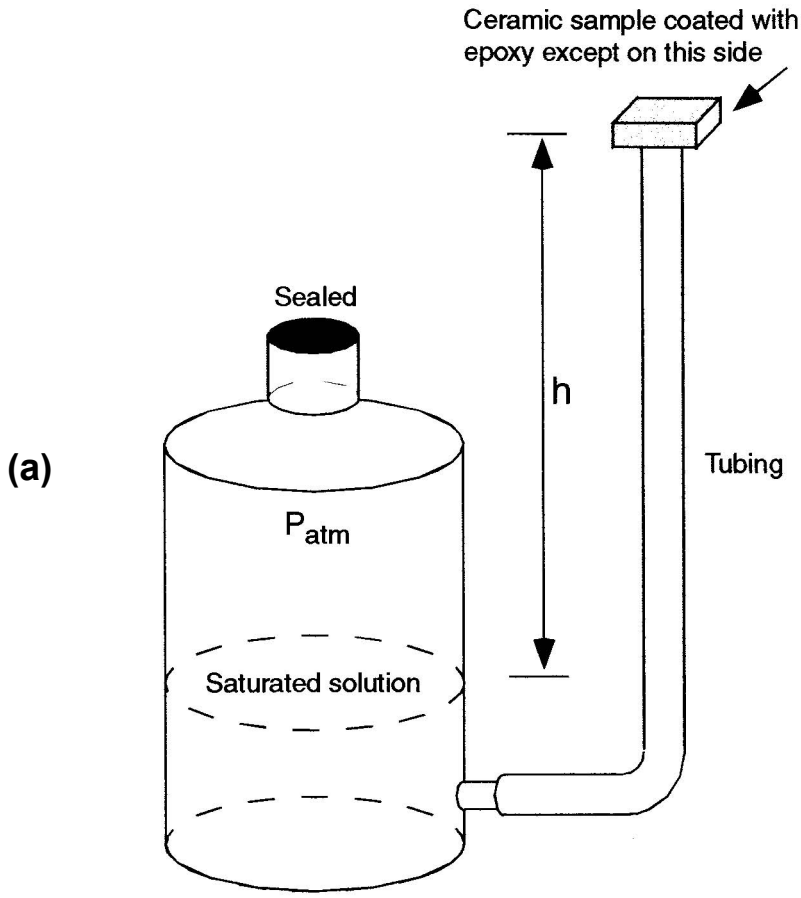

Fig. 2.46 Experimental set-ups for maintaining a constant pore fluid pressure in ceramic sample during growth of fibers. (**a**) Sample is placed at an adjustable height (h) relative to the surface of the fluid in the reservoir jar to maintain a lower pore fluid pressure in sample relative to the atmospheric pressure. (**b**) A vacuum pump is used to reduce the pressure of the ambient air over the solution in the reservoir bottle, thus controlling the magnitude of the pore fluid pressure in sample relative to the atmospheric pressure over sample in the desiccator. (**c**) Same as (b) except the sample consists of two pieces of ceramic of a two-block experiment (refer to Fig. 2.47).

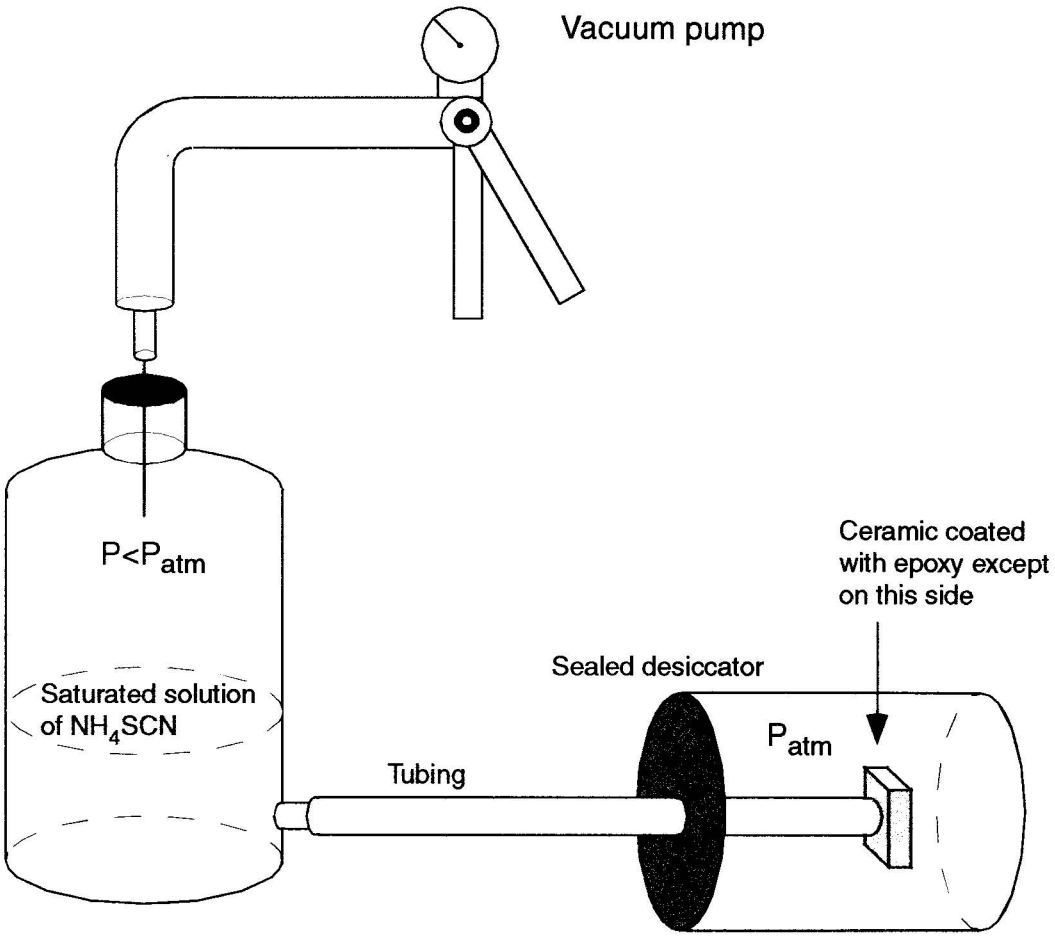
Vacuum pump
P<P$_{atm}$
Saturated solution
of NH_4SCN
Tubing
Sealed desiccator
Ceramic coated
with epoxy except
on this side
P$_{atm}$

(b)

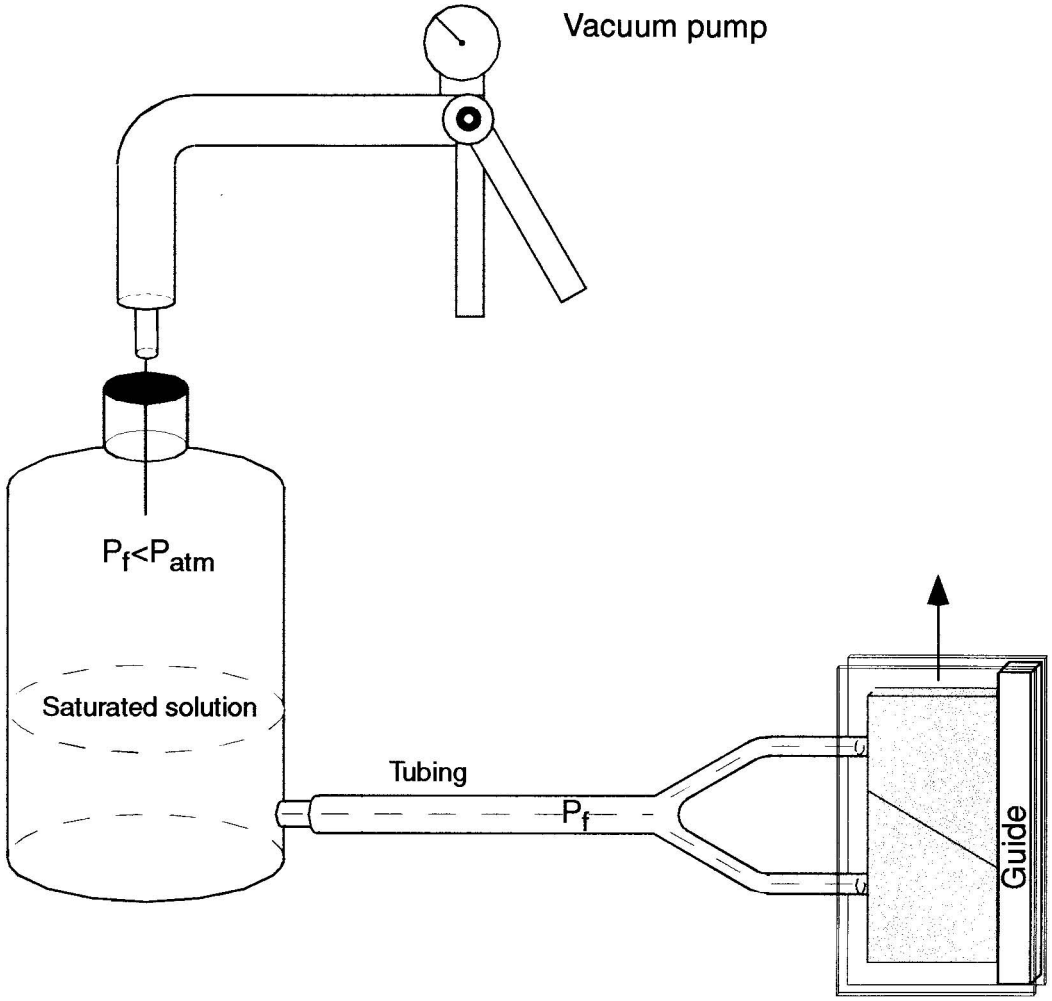

(c)

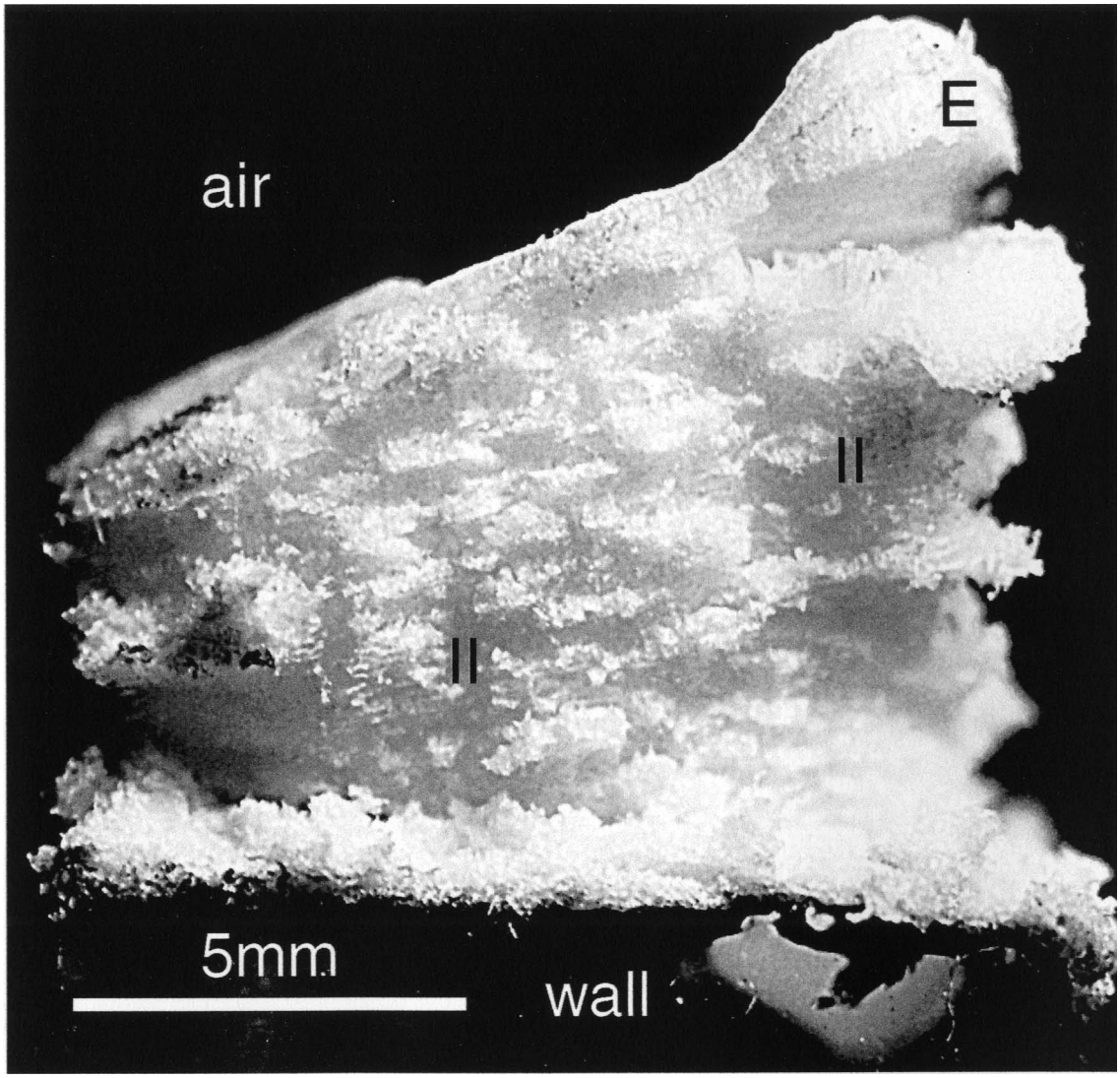

(a)

Fig. 2.47 Growth of poor fibers of NH_4SCN in a constant fluid pressure experiment (*CP-04*). Ceramic sample (*Square*, painted black and coated with epoxy except on the growth side) was connected to a small reservoir with a fluid pressure variably smaller than the atmospheric pressure and kept in a closed jar with a relative RH of about 10±5% (set-up as illustrated in Fig. 2.46b). Growth occurred over a total number of 25 days, with the fluid pressure kept at 25 in. Hg of vacuum or 1/6 P_{atm} in the first 8 days but changed to 10 in. Hg of vacuum (2/3 P_{atm}) in the later 17 days. (**a**) Photograph of the whole sample, showing overall poorly fibrous and loosely packed crystals grown upward from the ceramic block by Taber growth. Fibrous structure is hardly visible but Type II features (**II**) are present (running horizontally). The earliest growth (**E**) that occurred at a lower fluid pressure (1/6 P_{atm}) in the first 8 days is clearly better fibered and more tightly packed than the younger crystals grown at 2/3 P_{atm}.

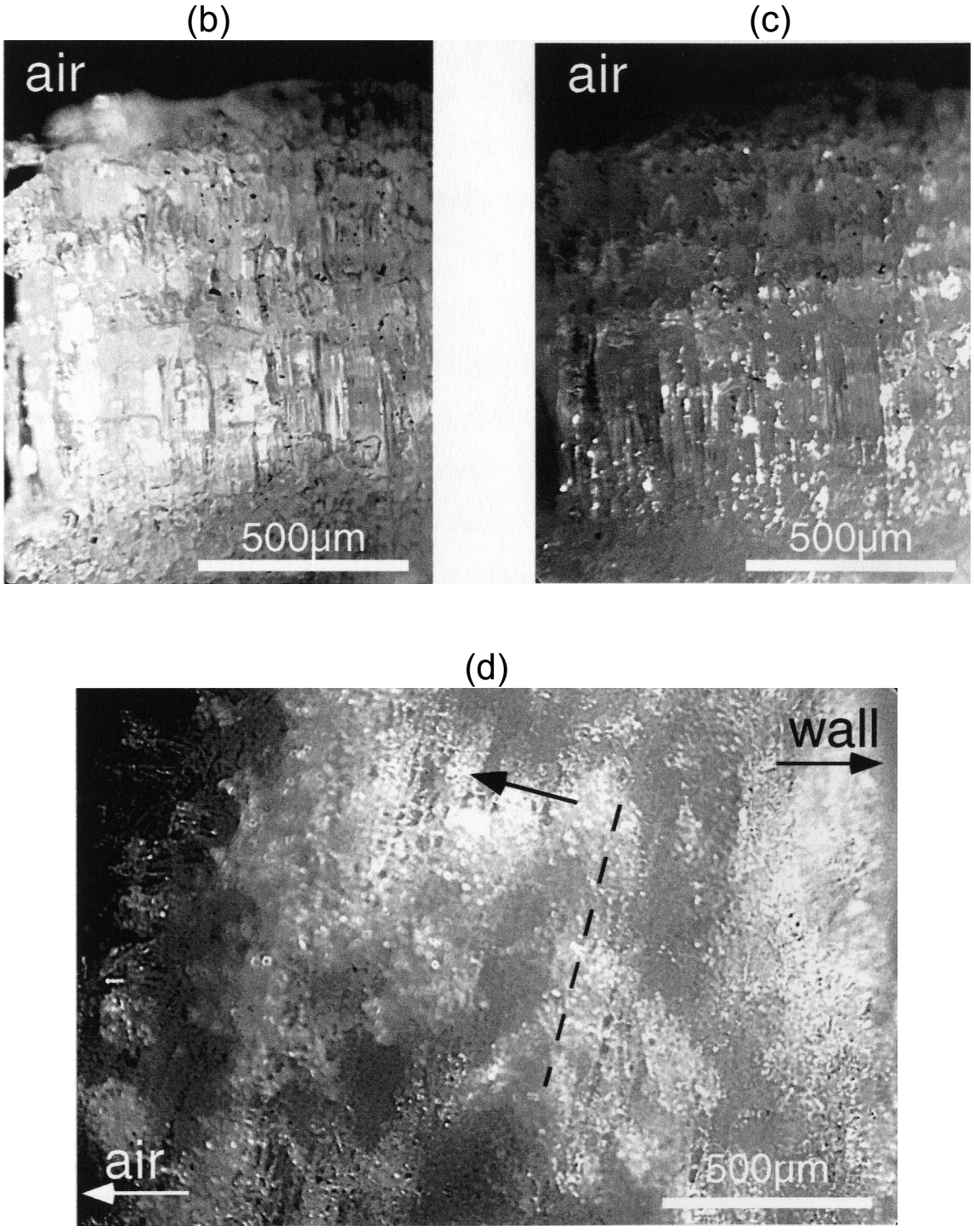

Fig. 2.47 (continued) (**b**) & (**c**) Close-up views of the oldest fibers grown at a lower fluid pressure. Fibers run roughly vertically. (**d**) Close-up view of the younger poorly fibrous crystals grown at a higher fluid pressure. Fibrous structure (fiber orientation indicated by arrow) is hardly visible, except for the presence of some Type II features in the aggregate, extending in a NNE orientation (dashed line).

(a)

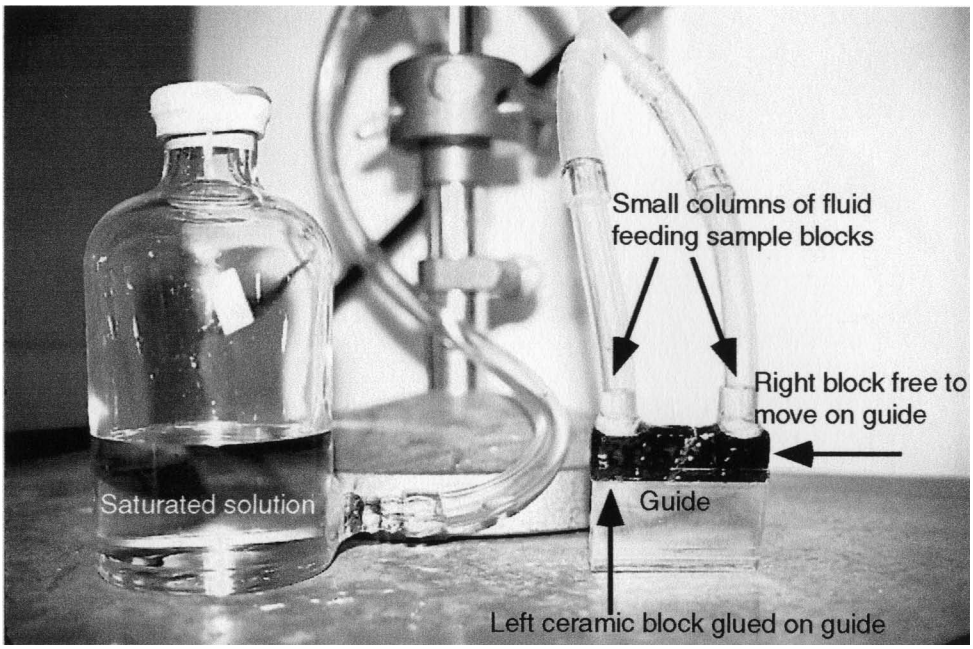

(b)

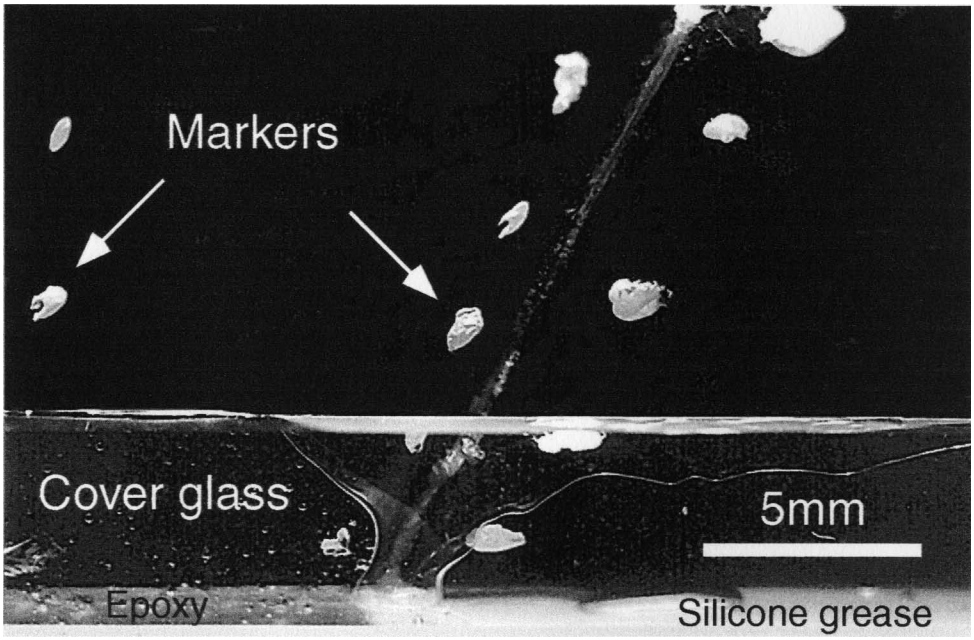

Fig. 2.48 (**a**) Photograph of the set-up for constant fluid pressure experiments (see also the cartoon in Fig. 2.46c). Fluid pressure of the reservoir is reduced by pumping air out of the bottle using a vacuum pump. In some experiments, small columns of fluid disconnected from the main reservoir are made to feed the sample blocks. (**b**) Photograph of sample *CP-08* at its initial state illustrating details of the sample in the set-up in (a). While the left ceramic block is glued on the guide with epoxy, the right block sits on the guide on silicone grease. Also glued on the guide is a cover glass on both sides of sample for holding the right movable block in place during vein opening. White patches on epoxy-coated, black-painted blocks are markers used for monitoring displacements.

(a)

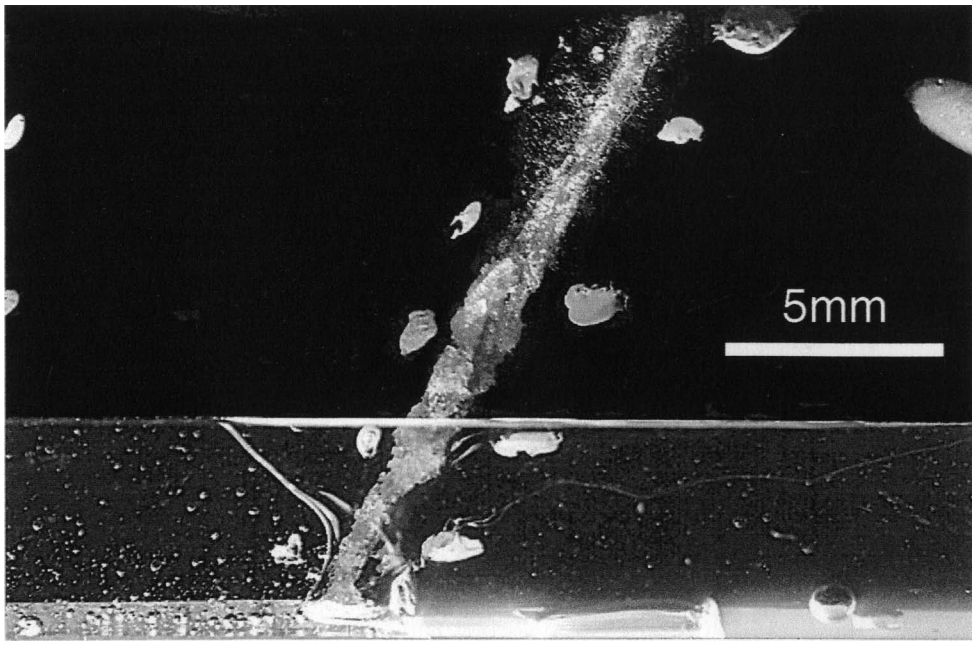

(b)

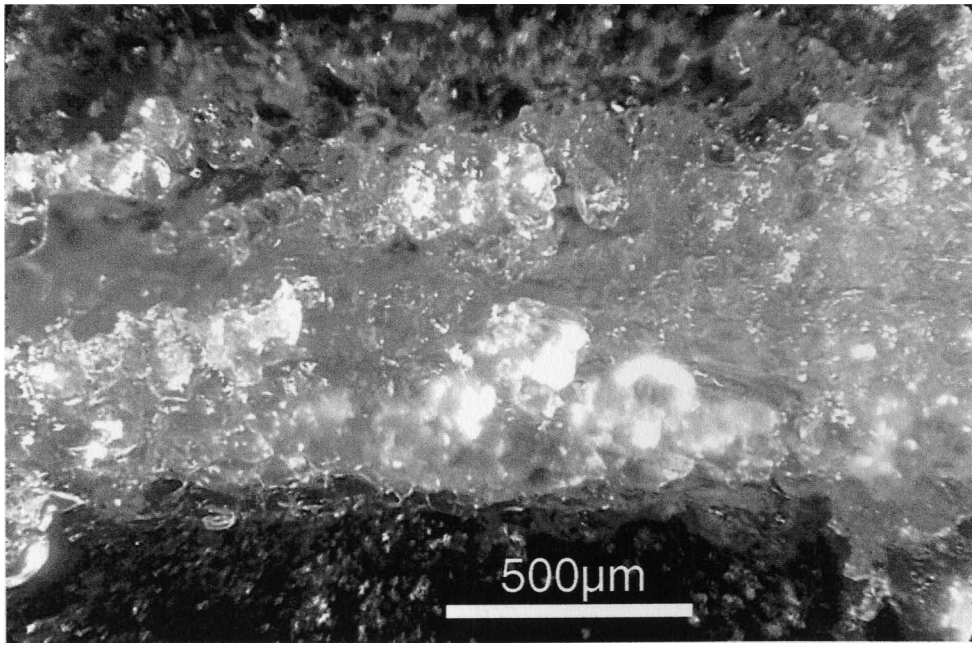

Fig. 2.49 Growth of non-fibers in constant fluid pressure experiment *CP-08* in which the fluid pressure was kept at about 5/6 of the atmospheric pressure (5 in. Hg of vacuum) and sample was exposed to the room air with relative humidities varying between 30~52%. (**a**) Photograph of sample about 12 days since Fig. 2.48b was taken, showing only granular growth along the crack and little opening as monitored by the markers. (**b**) Enlarged view of the granular growth on the crack. Crystallizing material is NH_4SCN.

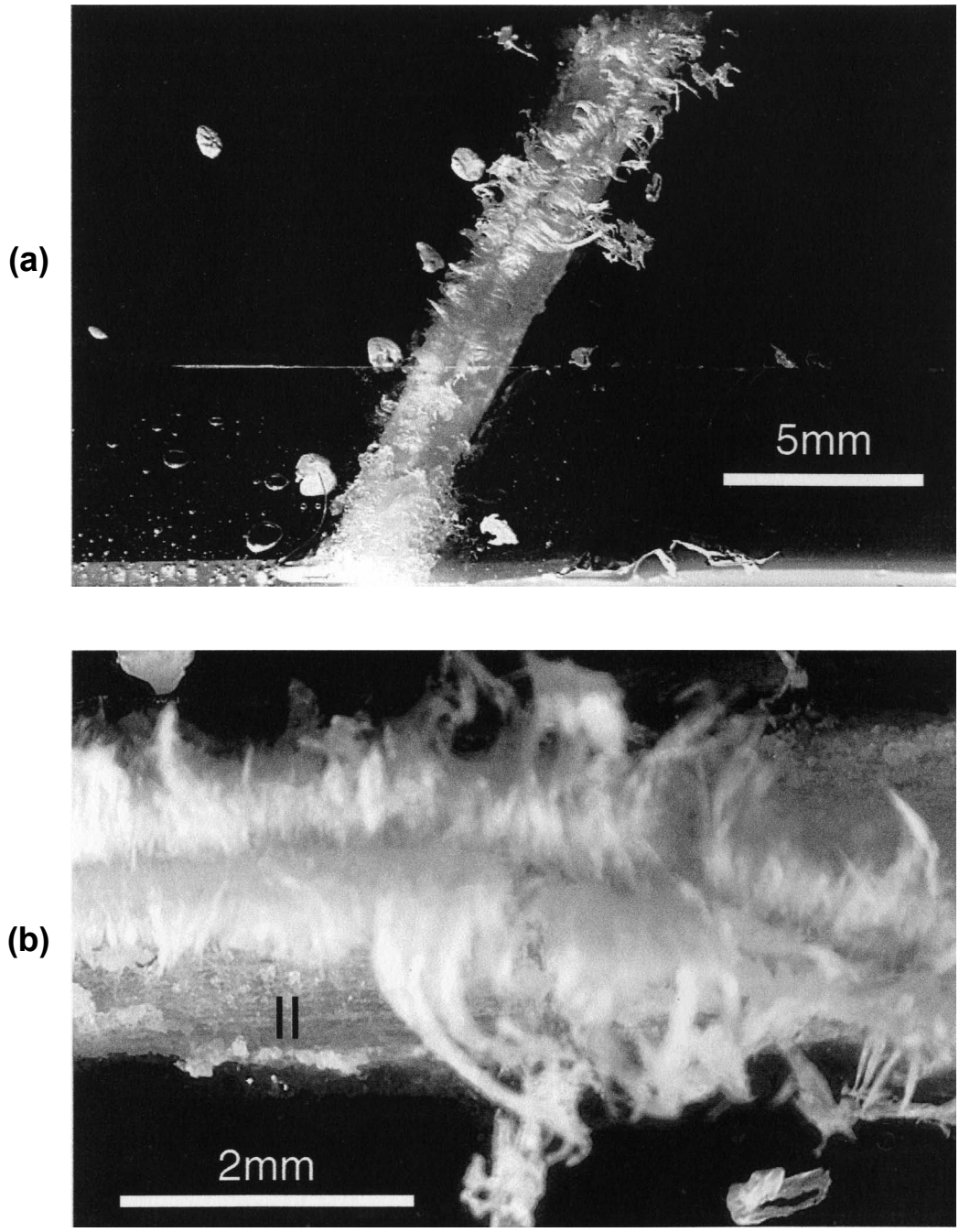

Fig. 2.50 Growth of poor fibers in constant fluid pressure experiment *CP-10* in which the fluid pressure was kept at about 1/6 of the atmospheric pressure (25 in. Hg of vacuum) and sample was exposed to the room air with relative humidities varying between 30~40%. (**a**) Photograph of a vein of poor, curled fibers grown over a period of 6 days. Vein opening by growth is obvious. (**b**) Enlarged view of the same vein at a larger power. Besides curled fibers near the center, those fibers near the edge show Type II features (**II**).

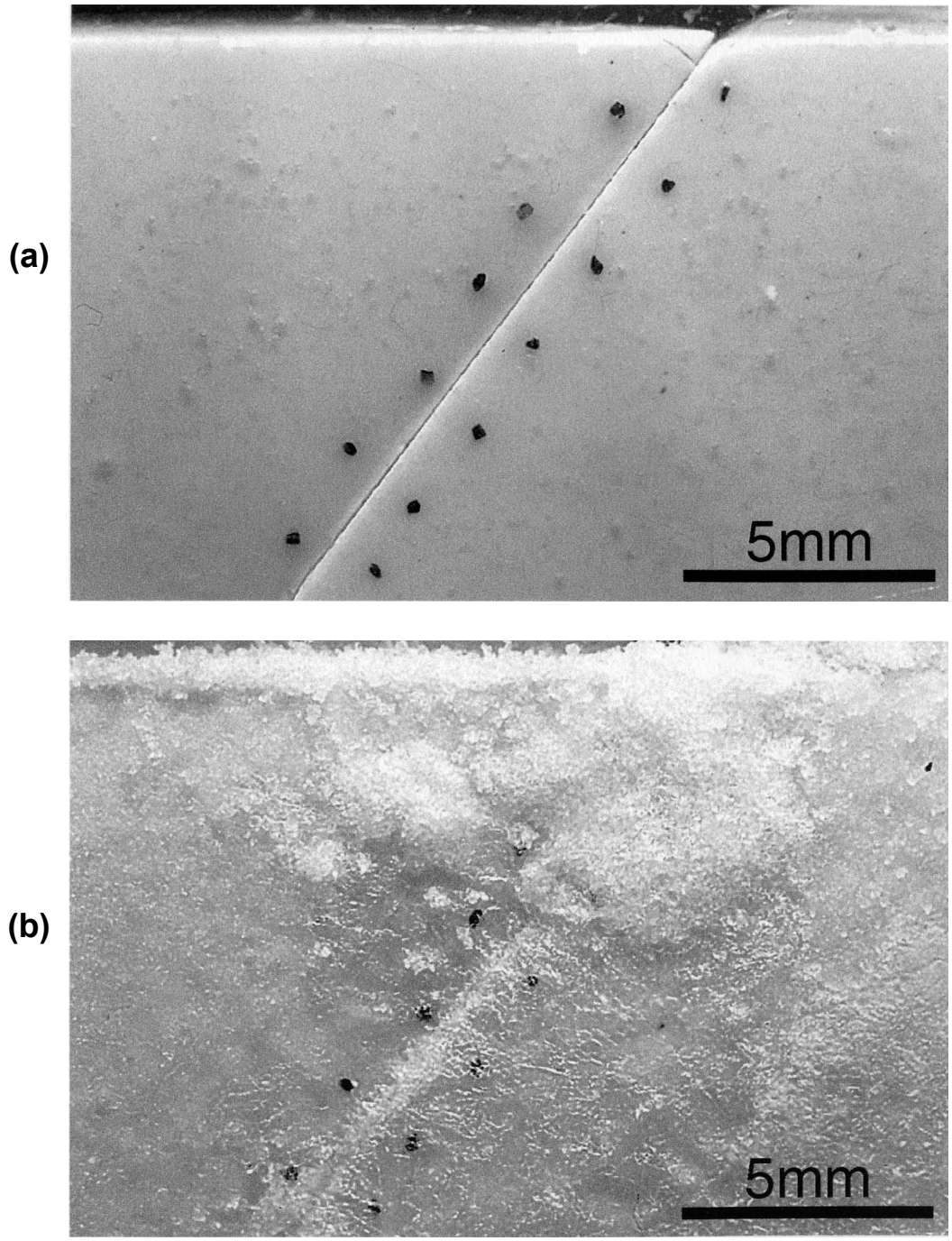

Fig. 2.51 Constant fluid pressure experiment *CP-12* (set-up as illustrated in Fig. 2.46c) showing little fiber growth and vein opening when the fluid pressure is close to the atmospheric pressure. Ceramic blocks (*Square*, coated with epoxy except on the crack side) were connected to a reservoir with a fluid pressure initially equivalent to 22 in. Hg of vacuum or 8/30 P_{atm} but actually increased to the atmospheric pressure overnight due to a leak of air in the set-up. (**a**) Initial state of sample. (**b**) Photograph of sample the next day, showing only granular growth on and beyond the crack. Crystallizing material is $NaNO_3$.

(a)

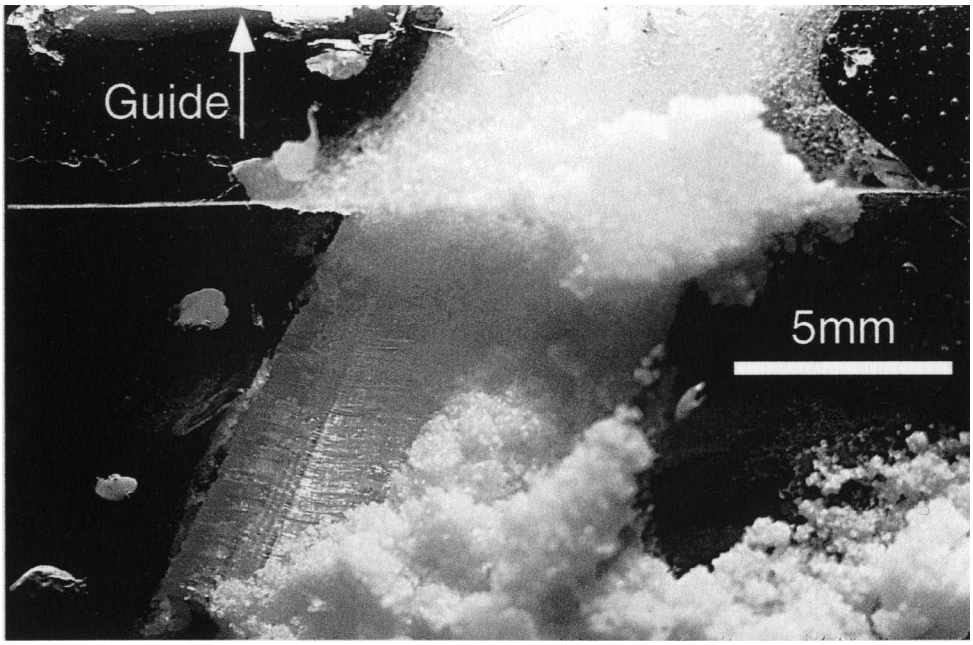

(b)

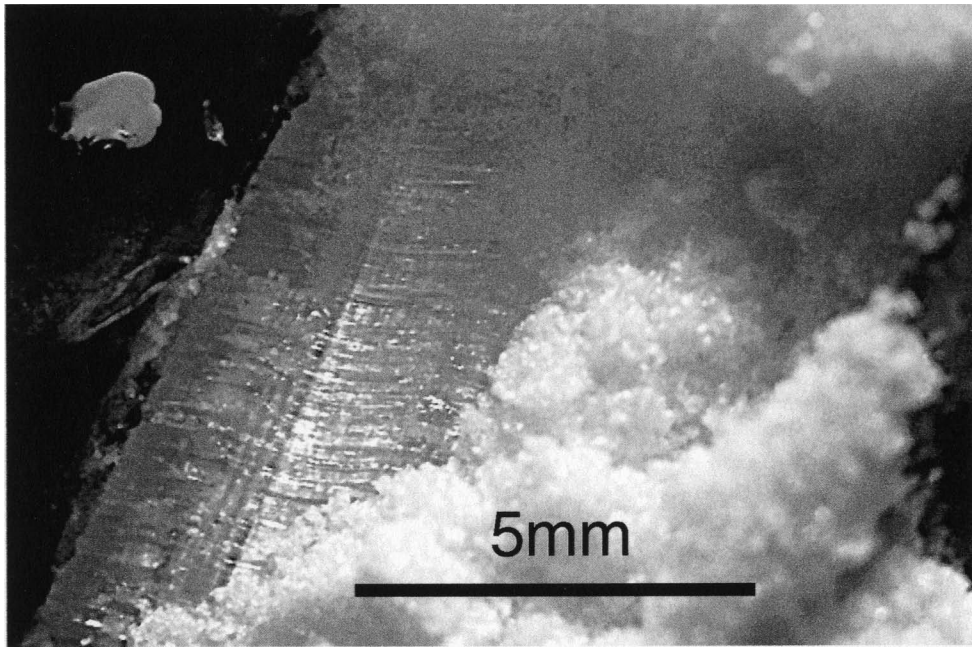

Fig. 2.52 (**a**) Growth of good fibers of NH_4SCN and large amounts of vein opening in a constant fluid pressure experiment *CP-11* in which the ceramic blocks were connected to *small* reservoirs of fluid as shown in Fig. 2.48a, the fluid pressure was kept at about 1/6 of the atmospheric pressure (25 in. Hg of vacuum) and the sample was exposed to the room air with relative humidities varying between 19-23%. Experiment started about 60 days before. The granular growth on the right side of vein suddenly appeared two days before due to a leak of air in the set-up (P_f increased to P_{atm}) and the continuous nutrient supply from the right side reservoir, while at the same time beautiful fibers grew from the left wall since the left side reservoir had been cut off by the accident. (**b**) Micrograph of the same vein at a larger power. Fibers are shown to be slightly curved, probably reflecting the ductility of a thick layer of silicone grease bewteen the left block and guide.

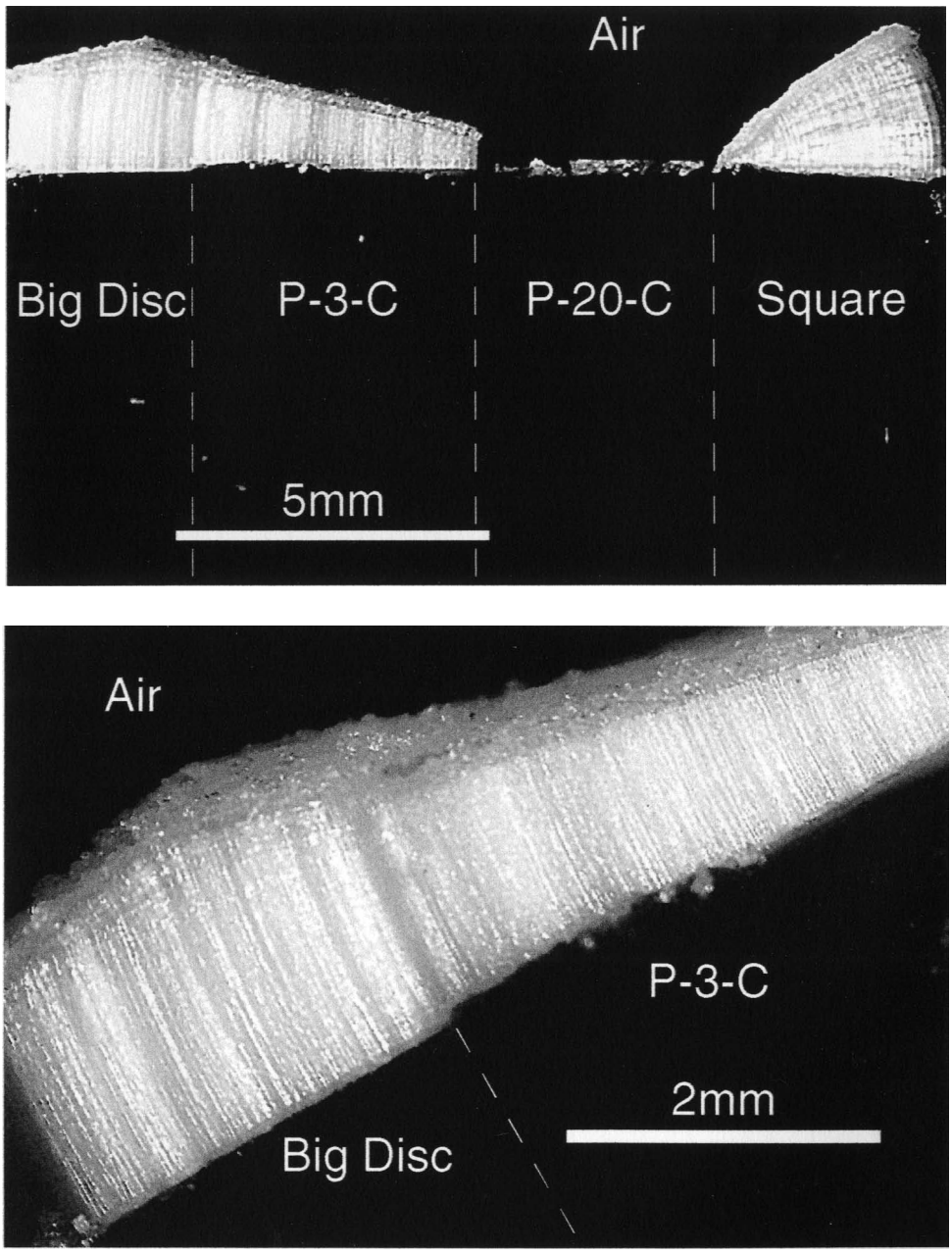

Fig. 2.53 Growth of fibers of NH_4SCN on a ceramic block made of 4 pieces of different types of ceramic glued together (*TB-14*). The integrated sample was painted black and coated with epoxy except on the growth side. Experiment was run in a closed desiccator with an ambient RH of about 15±5%. The extent and the type of each of the constituent pieces of ceramic in the block are shown accordingly in all figures. (**a**) Photograph of the whole sample after 87 hours of growth, showing good fibers grown on the edges of all types of ceramic except on that of *P-20-C* where only some granular growth occurred. Despite the different pore sizes of *Big Disc* and *P-3-C*, fibers on their edges do not show noticeable variation in size across the junction where the two ceramic pieces meet. Neither does this fiber size look significantly different from that of fibers on *Square*. Due to the zero rate of growth at the junction between *P-20-C* and *Square* fibers on *Square* are curved with Type I features radially arranged. (**b**) Enlarged view of the fibers on the *Big Disc* and *P-3-C* portion of the wall showing little difference in fiber size between the two. The average growth rate on this portion varies between 7~25μm/hr.

(c)

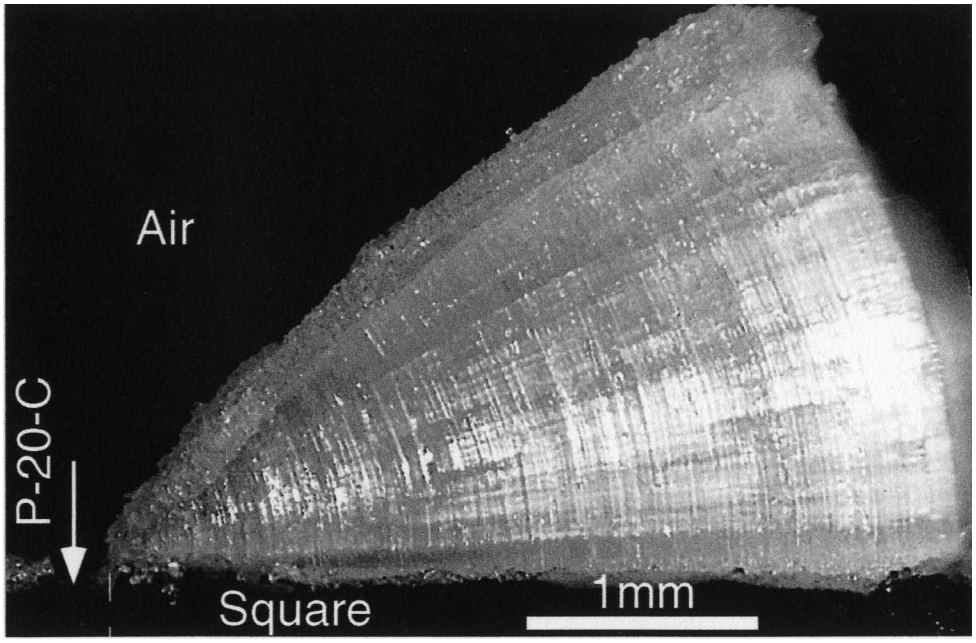

(d)

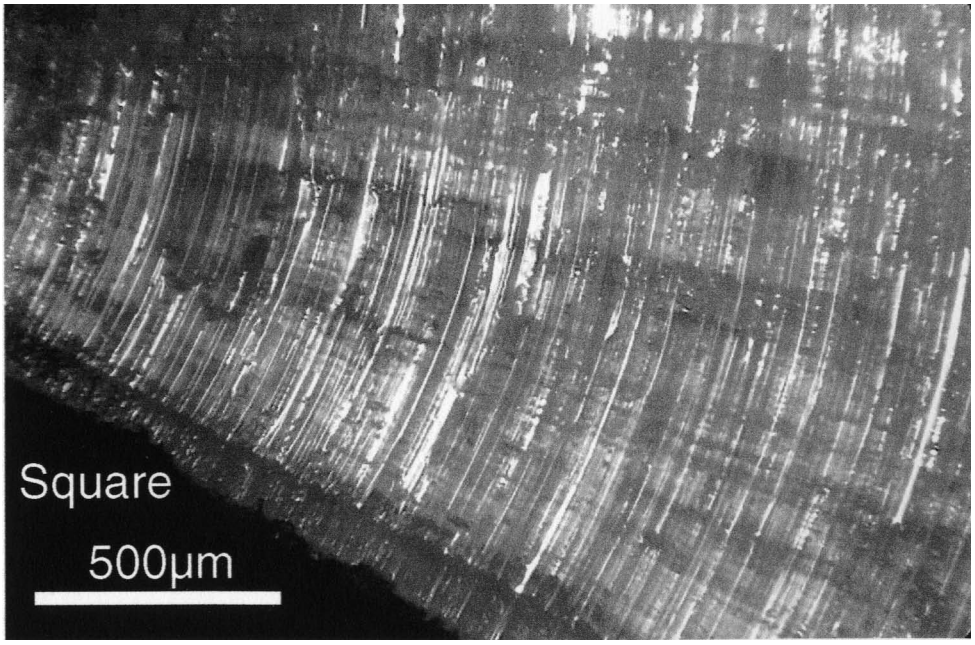

Fig. 2.53 (continued) **(c)** Enlarged view of the curved fibers on the *Square* portion of the wall showing good, clear curved fibers and their Type I features radially extending outward from the point of junction between *P-20-C* and *Square*. **(d)** Micrograph of the same fibers at a still larger power. The average growth rate on this portion varies between 0~28μm/hr.

(e)

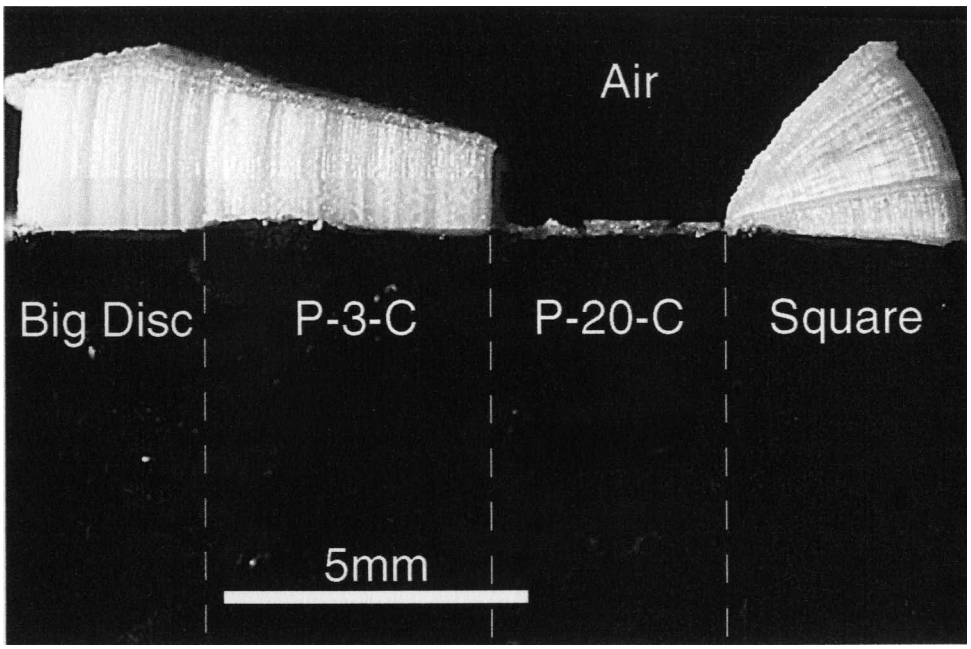

(f)

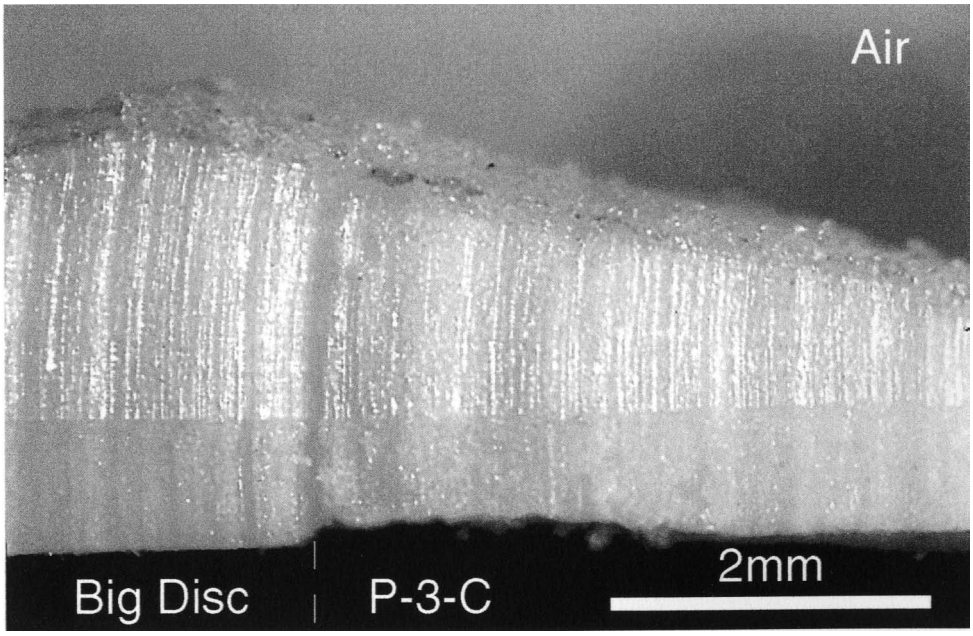

Fig. 2.53 (continued) (**e**) More growth at the base of fibers on the fine ceramic portions of the wall over the next 25 hours (with an average growth rate of 32μm/hr). The new fibers look clearly different in character from the old fibers and there is a marked Type I discontinuity across the fibers on both growth sites separating the new fibers from the old. (**f**) Close-up of the fibers on the *Big Disc* and *P-3-C* portion of the wall showing that the Type I discontinuity is really marked by a change in character of fibers rather than by a seam of granular material.

(g)

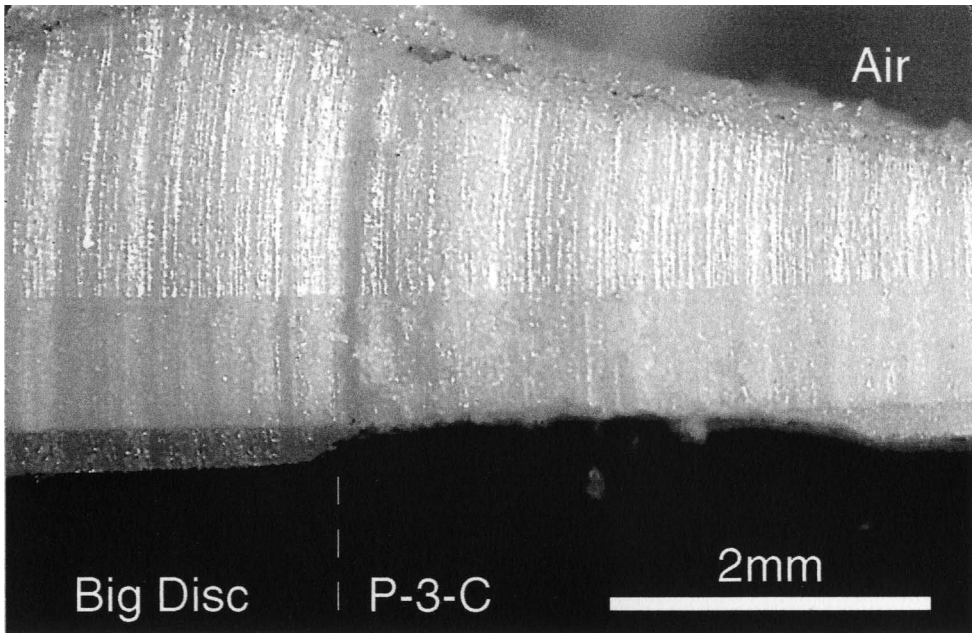

(h)

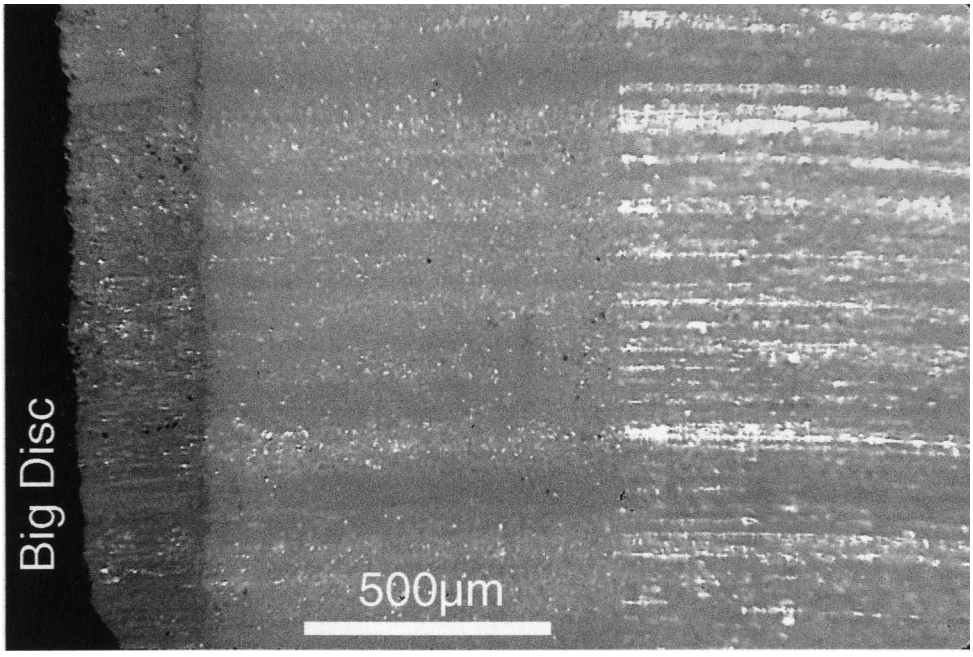

Fig. 2.53 (continued) (**g**) Very slow new growth of fibers on the *Big Disc* and *P-3-C* portions of the wall in the last stage of experiment (for about 320 hours). New fibers are clear and transparent, different in character from either the first or second phase of fiber growth, and they are again separated from the previously grown fibers by a Type I discontinuity, caused by the brief peroid of change of the humidity conditions during the last time of sample observation. (**h**) Close-up of the fibers on the *Big Disc* portion of the wall. Growth rate has been less than 1µm/hr, reflecting a greatly diminished moisture content or pore fluid pressure in sample.

(i)

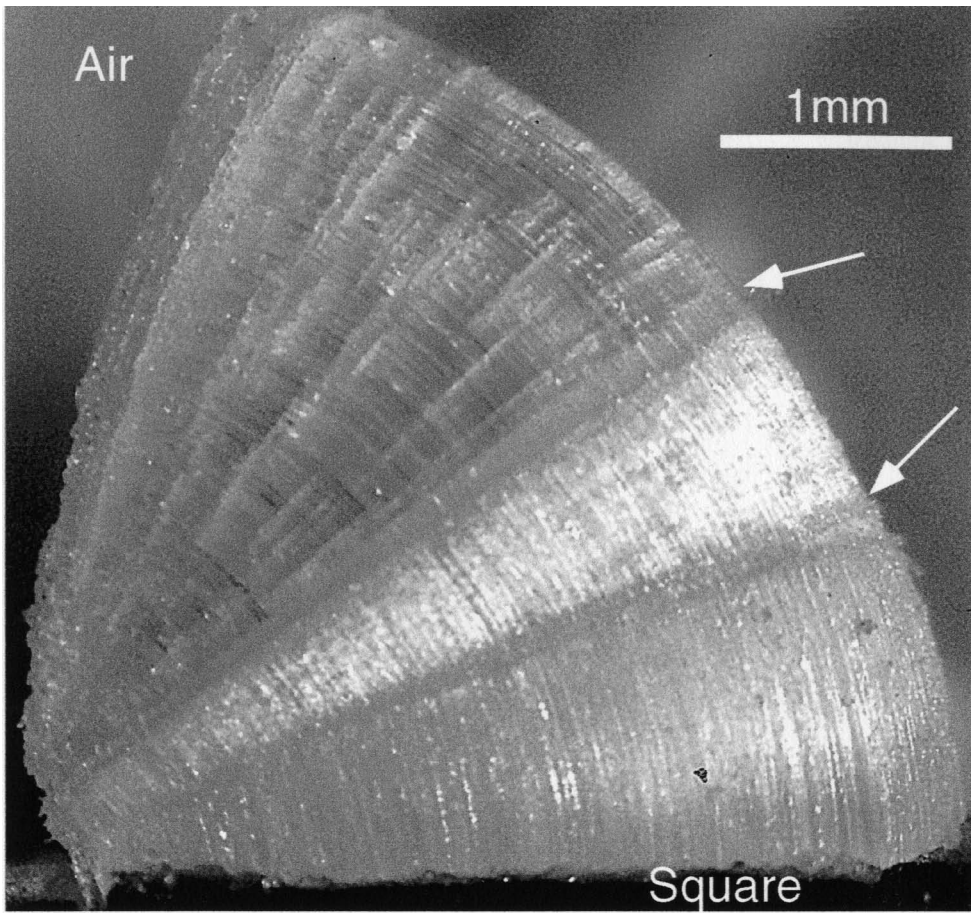

(j)

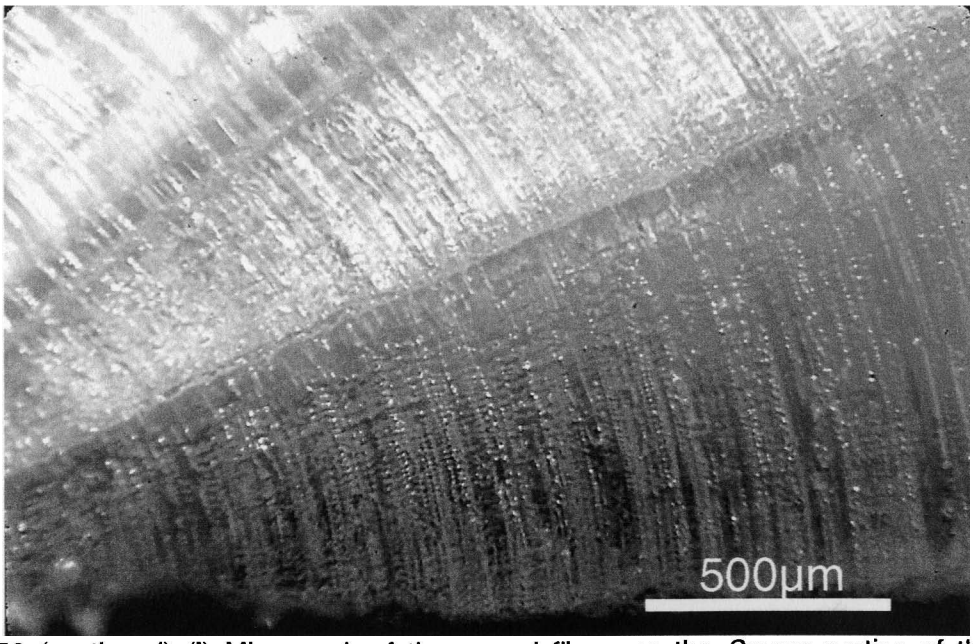

Fig. 2.53 (continued) (i) Micrograph of the curved fibers on the *Square* portion of the wall showing beautifully curved fibers and their radially arranged Type I transverse features. The two main Type I features (arrow) correspond to those shown across the fibers on the *Big Disc* and *P-3-C* portion of the wall. (j) Close-up of the same fibers showing numerous tiny Type II features in the newly grown fibers as well as the major Type I bands.

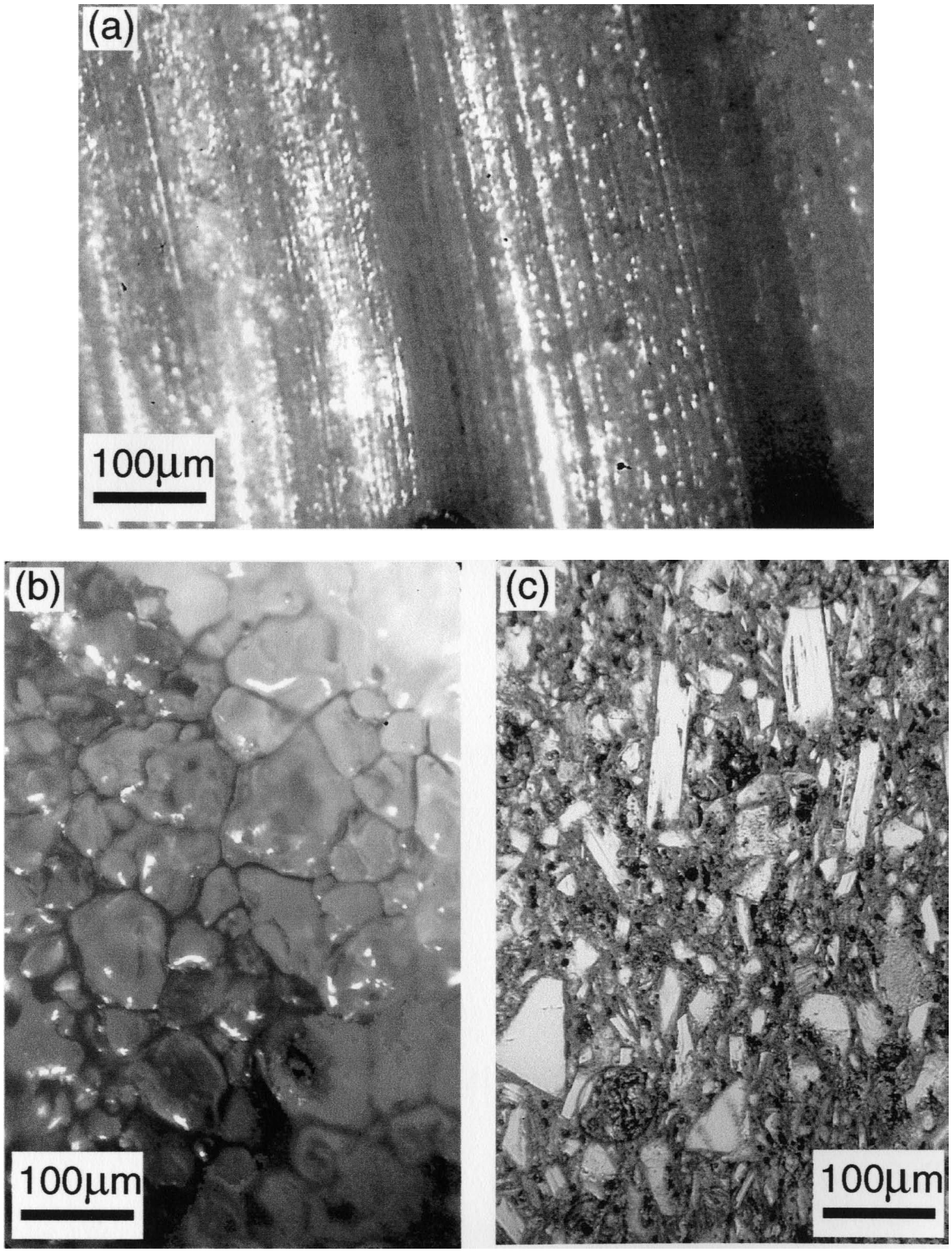

Fig. 2.54 (**a**) Photomicrograph showing good fibers of NH_4SCN grown in a single-block experiment (*NFB-07a*) with ceramic *Big Disc*. (**b**) Cross-sectional view of the fibers from the same sample as (a), obtained by detaching the fiber aggregate from the wall and then dyeing the parted surface (fiber bases) in ink, imparting clearer outlines to the grain boundaries. (**c**) Photomicrograph of the porous material used (*Big Disc*). For comparison, all three micrographs are shown at the same scale. See text for discussion.

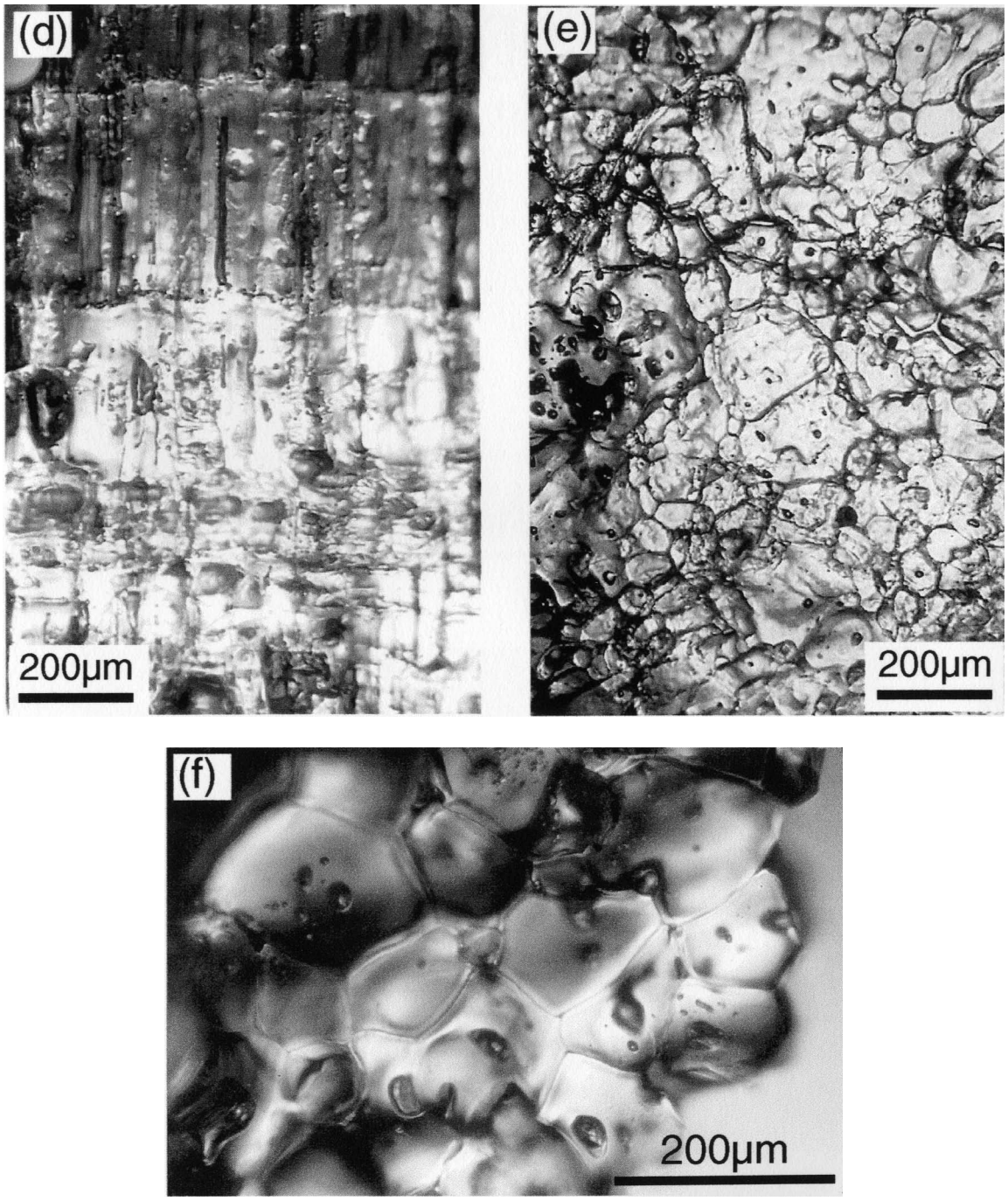

Fig. 2.54 (continued) (**d**) Photomicrograph of fibers of NH_4SCN grown in a single-block experiment (*NFB-14*) with ceramic *Big Disc*, taken in reflected light. Fibers contain abundant transverse features (both Types I and II) but fiber boundaries are only barely recognizable. (**e**) Cross-sectional view of the fibers from the same sample as (d), obtained in the same way as (b), shown at the same scale as (d) for comparison. (**f**) Close-up view of the cross sections of fibers from the same sample.

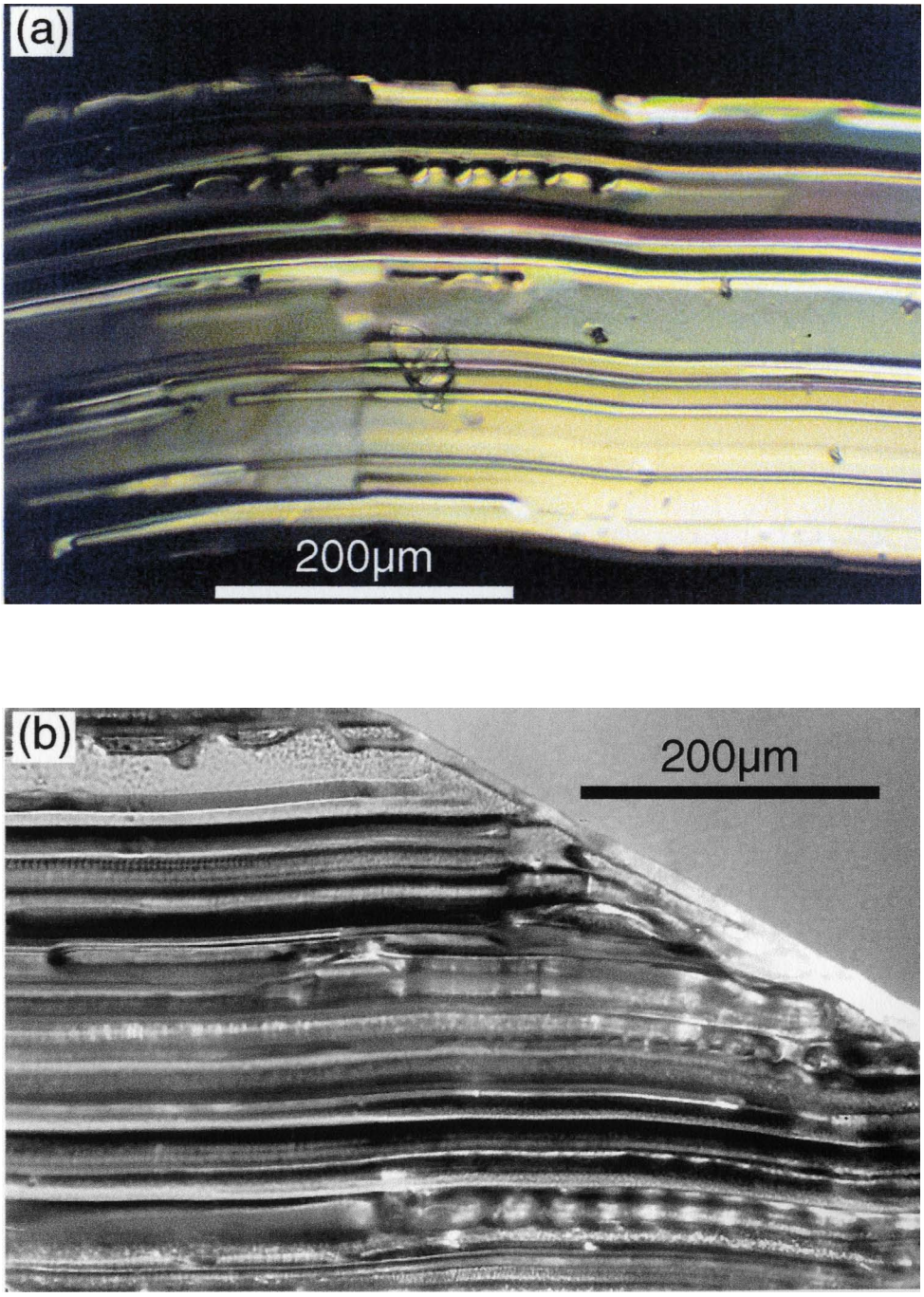

Fig. 2.55 Photomicrographs of single ribbon-shaped fiber bundles of NH_4SCN from sample *NFB-22*, grown on ceramic *Big Disc*, showing the bundled character and size of individual fibrils. (**a**) Photomicrograph of a slightly curved fiber bundle taken under crossed nicols showing presence of finer fibrils within the fiber but the whole fiber shows uniform extinction when the stage is rotated. (**b**) Another fiber bundle consisting of finer fibrils, seen in reflected and transmitted light. The fibrils are expressed as alternating ridges and grooves on the surface of the fiber, but optically, extinction occurs in all the fibrils at the same time.

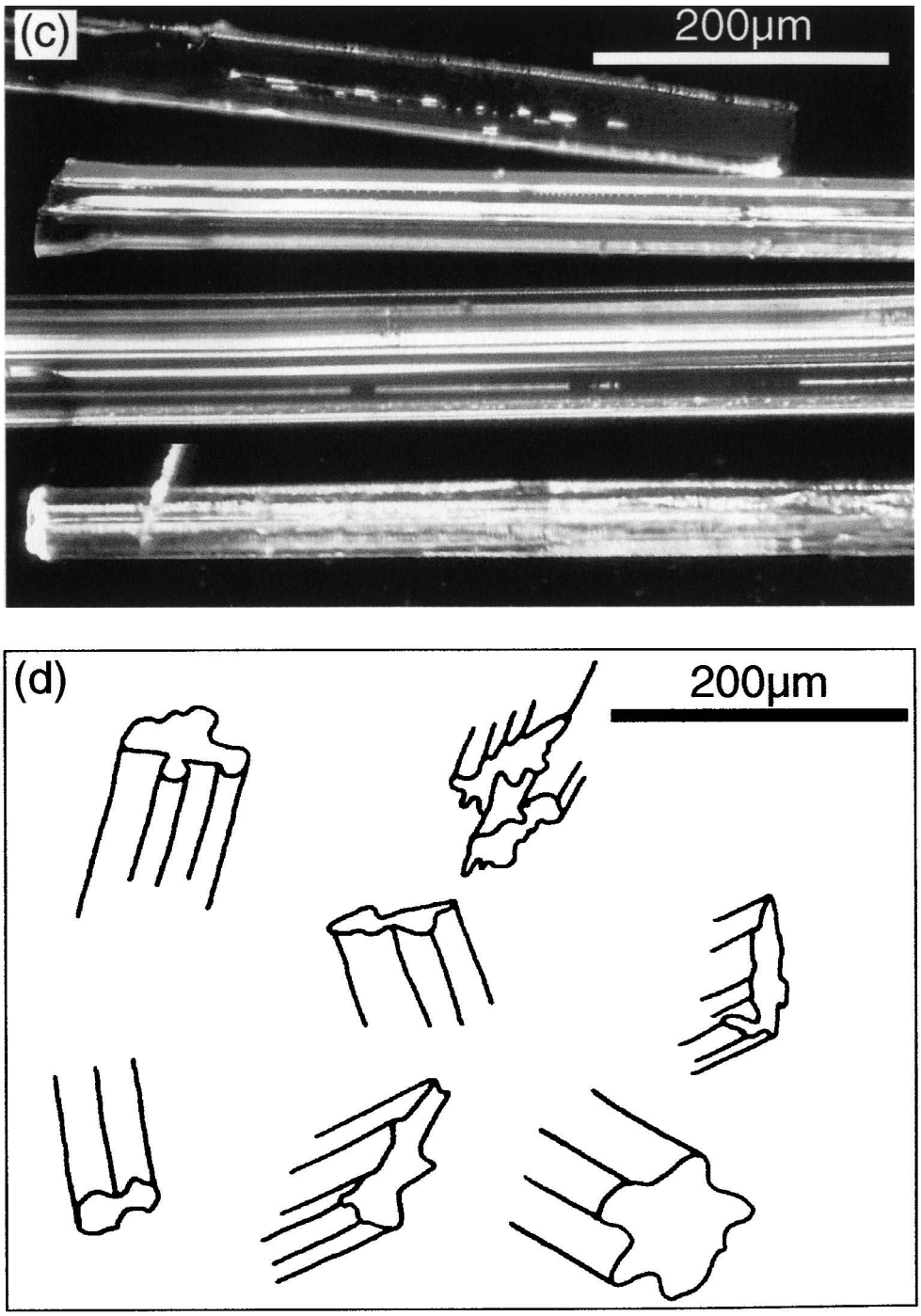

Fig. 2.55 (continued) (**c**) Photomicrograph of single rod-shaped fibers of *NH_4SCN* from sample *NFB-22*, grown on ceramic *Big Disc*, showing cylindrical or fluted morphologies of single fiber bundles which consist of finer fibrils. (**d**) Sketch of other single fibers from the same sample showing their rod-shaped morphologies and very irregularly-shaped cross sections.

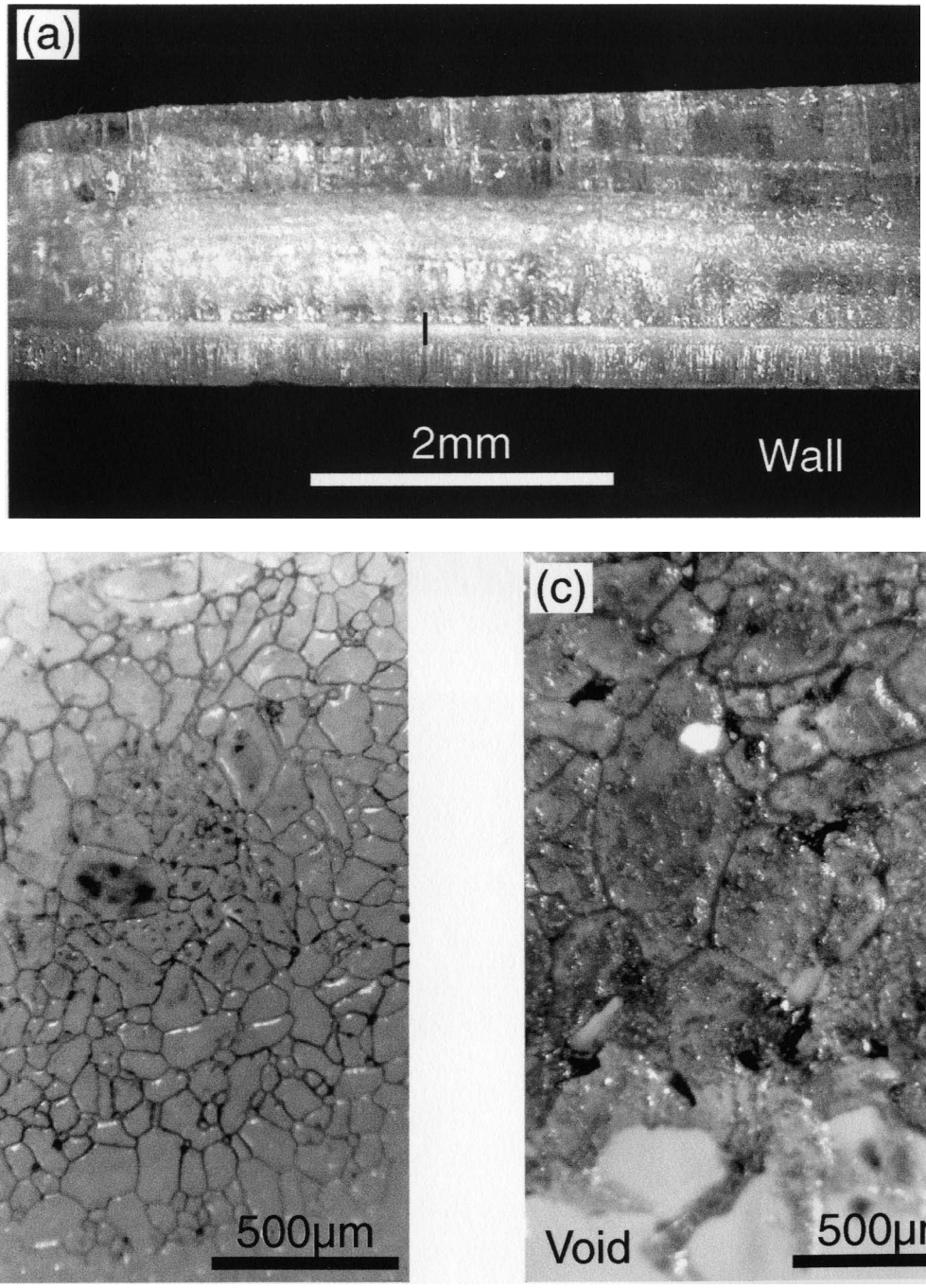

Fig. 2.56 (**a**) Good, clear fibers of NH_4SCN grown in a two-block experiment (*DW-08*) with ceramic *Square*. Growth occurred over a period of 54 days in a dessicator with an ambient relative humidity of about 10±5%. There are at least three Type I transverse features present across the fibers, one of which (**I**) is particularly conspicuous and is marked by a thick seam of milky granular growth. (**b**) Cross-sectional view of the fibers, obtained in the same way as Fig. 2.54b, showing fiber sizes in a range of 20-200µm. (**c**) Cross sectional view of the clear, loosely packed fibers at a different site, at the same scale as (b), showing still larger sizes of fiber bundles as well as voids (light-colored, near the bottom of picture).

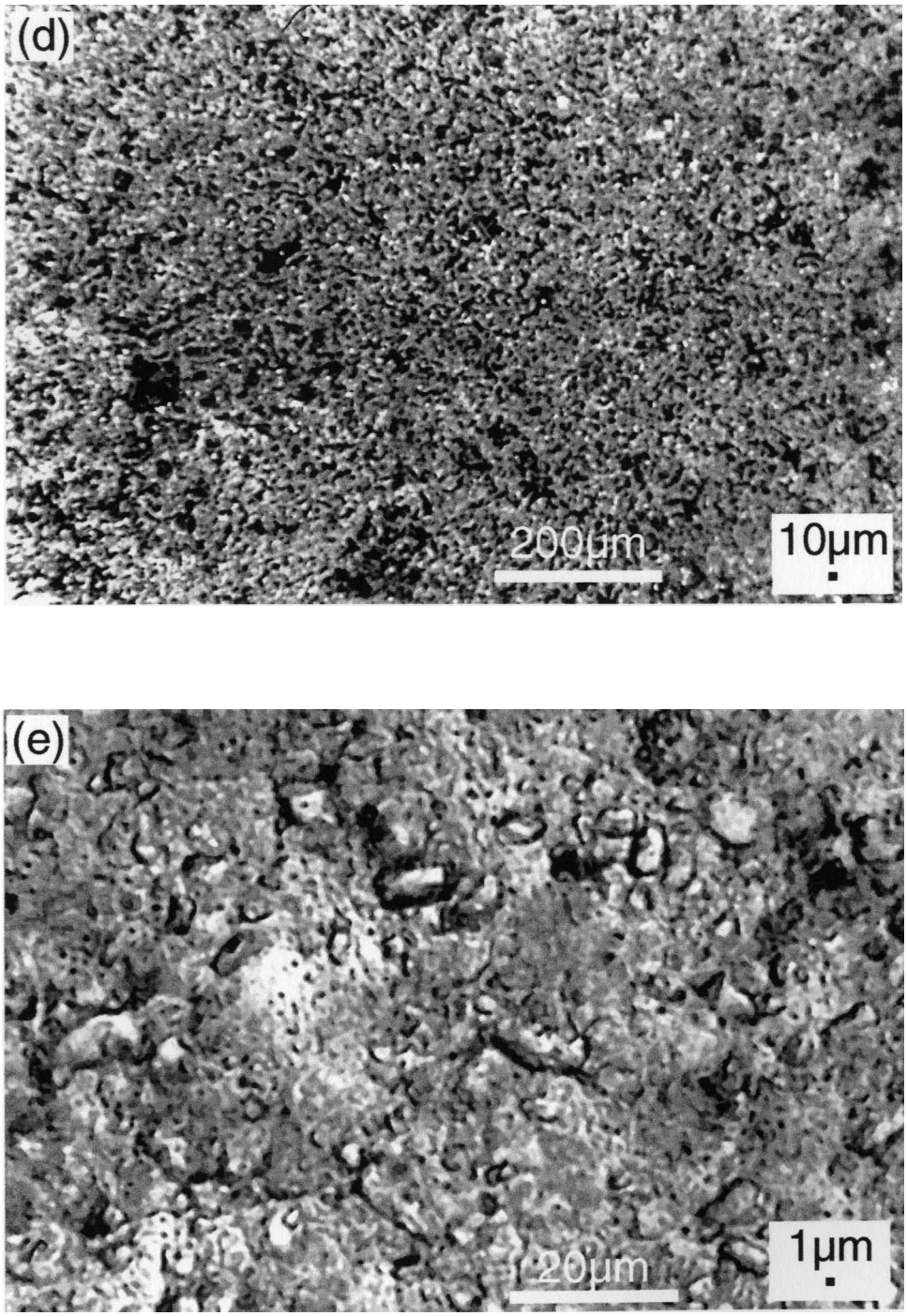

Fig. 2.56 (continued) (**d**) Cross sectional view of the tightly packed fibers on a detached surface along the milky type I feature labeled 'I' in (a), showing a much finer grain size. (**e**) Enlarged view of a thin section photomicrograph of the ceramic *Square* showing its fine pore sizes. Besides a bar scale there is also a small black dot scale in (d) and (e) for comparison. Most pores in (e) are seen to be smaller than 1 μm, while the average grain size in (d) is at least 3-5 μm across.

Fig. 2.57 (**a**) & (**b**) Photomicrographs showing fibers of $NaNO_3$ grown on ceramic *Square* in a dead-weight experiment (*DW-15*). A conspicuous type I feature separates the fibers into two parts of different character. The older part (upper) was grown over a period of 9 days under a compressive loading of about 4kg/cm^2, while the younger part (lower) grew during the last 2 days when the loading had been removed. (**c**) & (**d**) Cross-sectional views of the older fibers of *DW-15* obtained by parting the two sides of the vein near the center and dyeing the parted surface (fiber sections) in ink. While (c) shows coarse grains of the loosely packed fibers near the center of the parted surface, (d) is a view closer to the edge, showing coarse fibers passing into finer grains towards the edge.

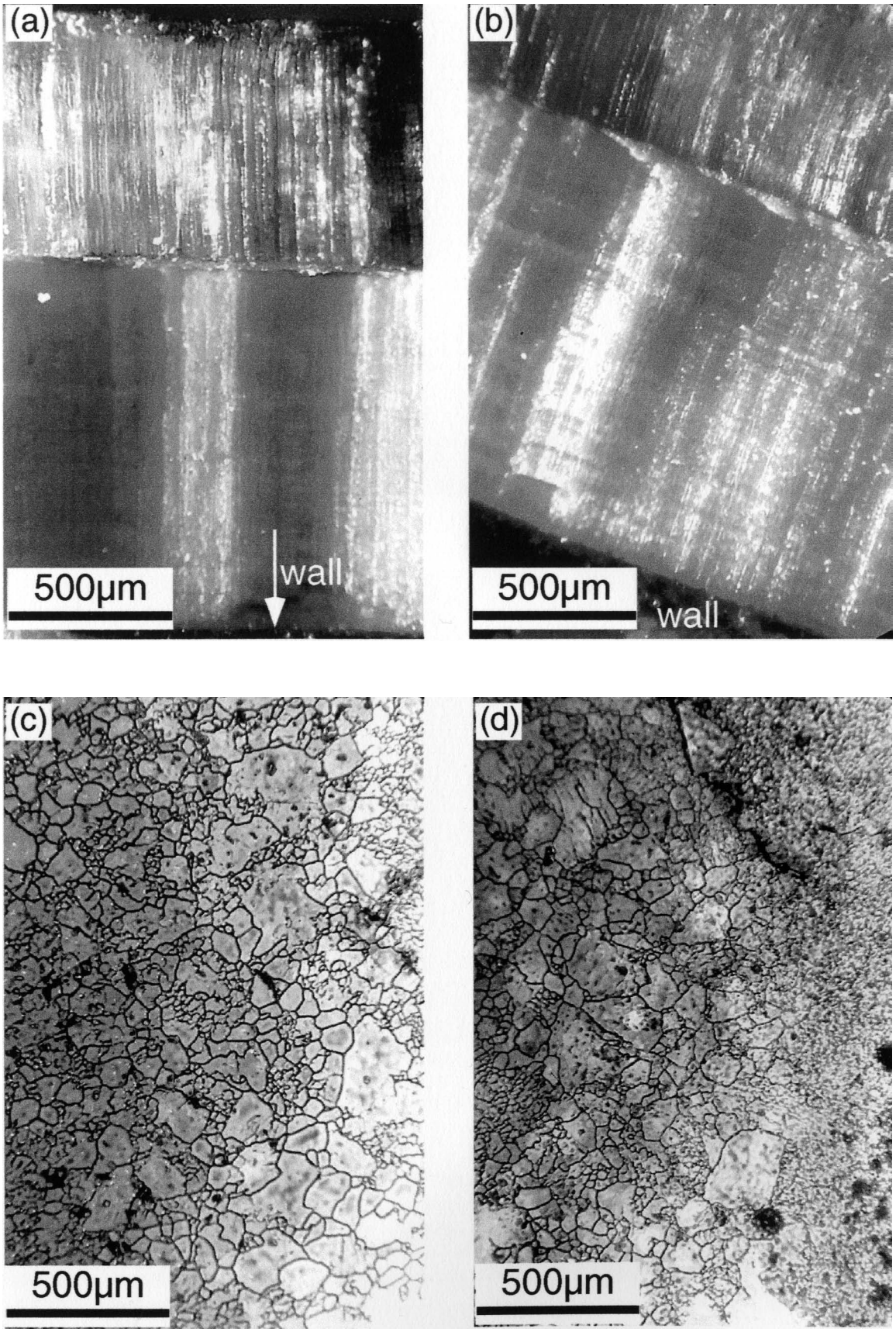
(a)
500μm
wall
(b)
500μm
wall
(c)
500μm
(d)
500μm

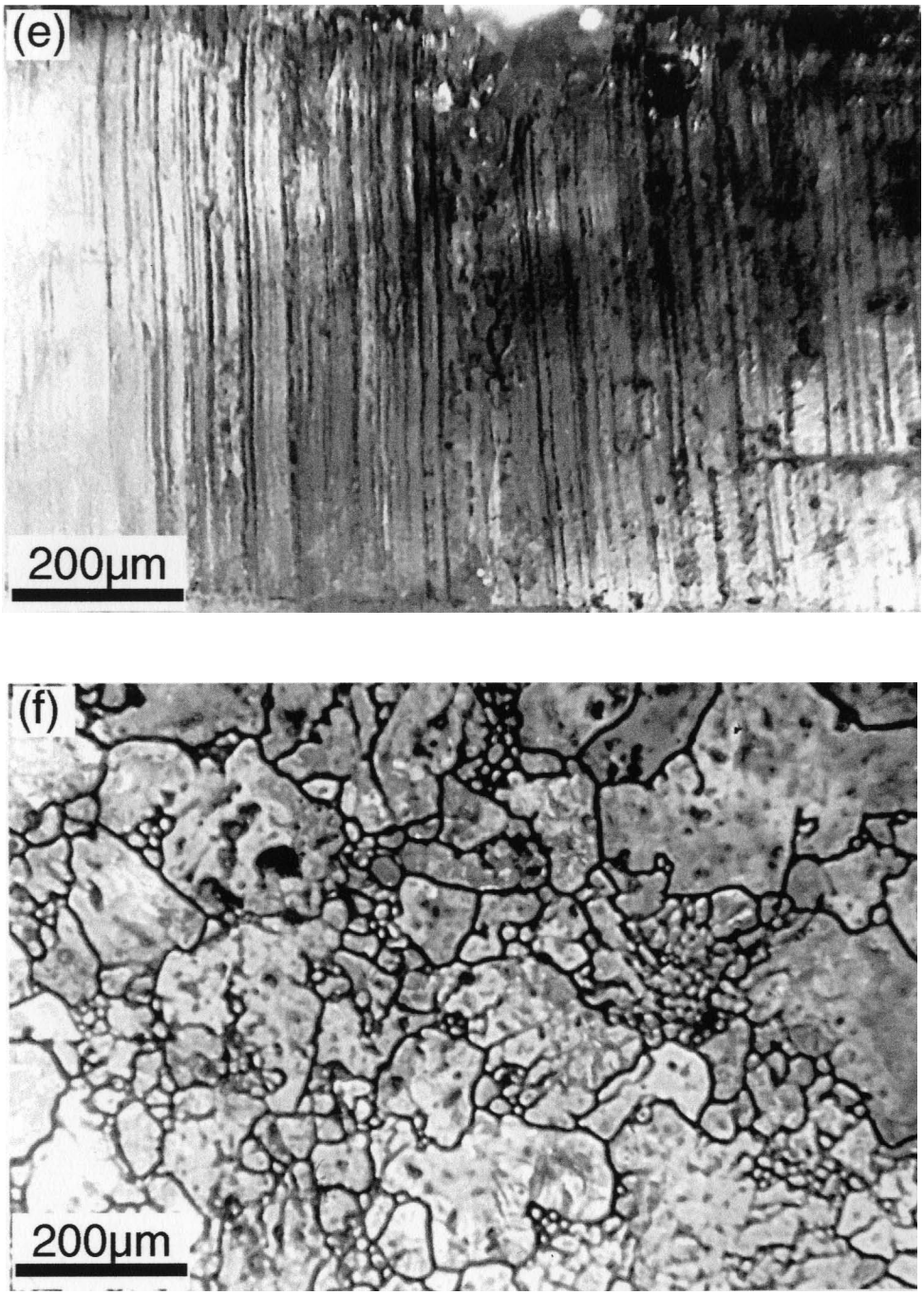

Fig. 2.57 (continued) (**e**) Enlarged view of the older fibers of *DW-15* (dyed in ink) showing fluted shapes of fibers and fiber boundaries. (**f**) Enlarged cross-sectional view of fibers shown at the same scale as (e) for comparison. The apparent larger sizes of fibers in (f) suggest that the grooves and ridges in (e) do not necessarily represent the boundaries of individual grains but may arise from the existence of irregular fibrils (shown as irregular patches within large grains in (f)) in individual fiber bundles.

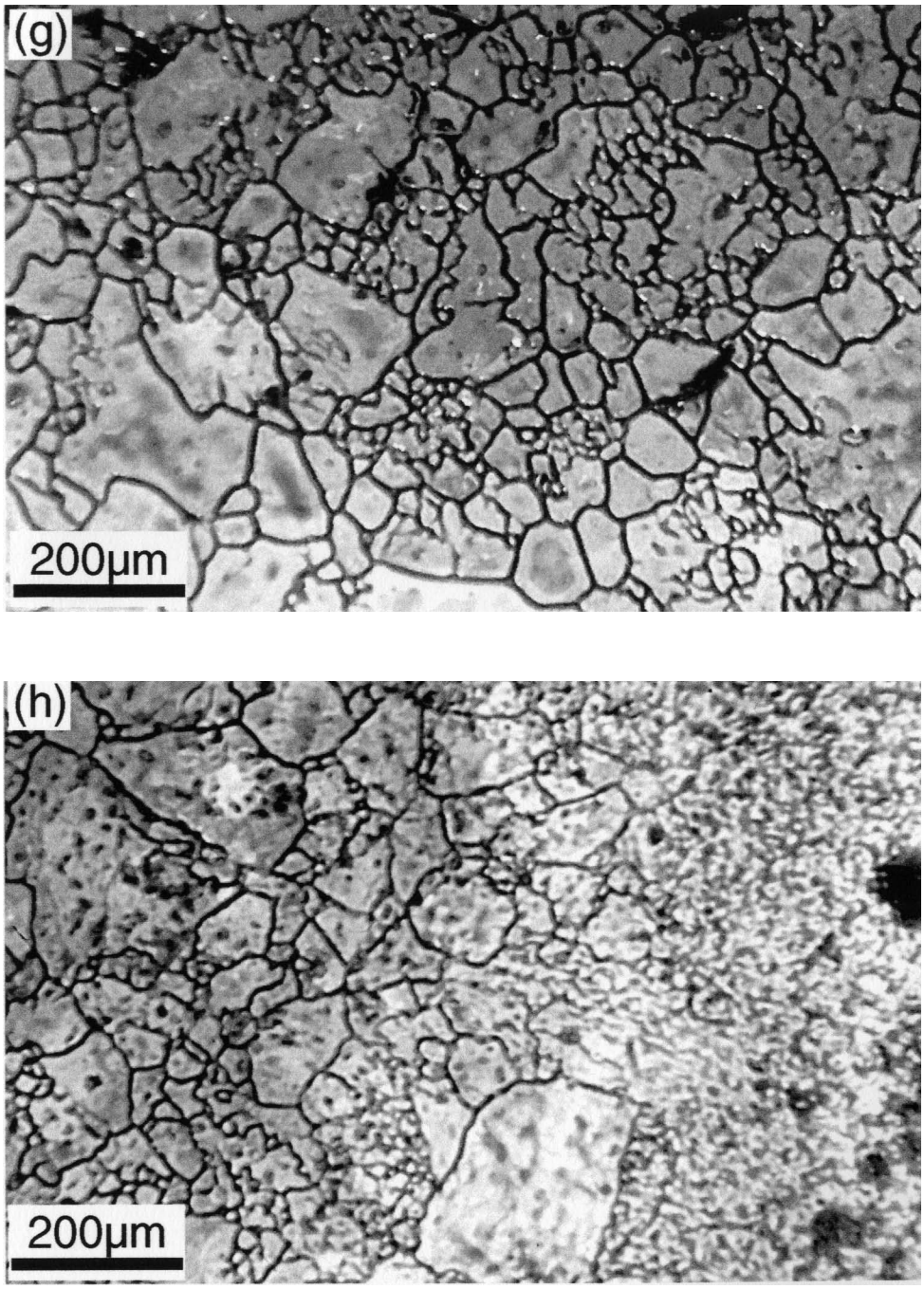

Fig. 2.57 (continued) (**g**) Another cross-sectional view of the old loosely packed fibers near the center of the parted vein surface, shown at the same scale as (e) for comparison. (**h**) Enlarged cross sectional view of the old fibers near the edge of the parted surface, at the same scale as (e), showing coarse fibers or fiber bundles passing into finer grains towards the edge (to the right).

Fig. 2.58 (**a**) Tightly packed fibers of NH_4SCN grown in a single-block experiment (T*B-10a*) with ceramic *P-3-C*. The growth occurred for about 48 hours in a dessicator with an ambient relative humidity of about 15±5%. An ink marker seen on the older fibers (which makes them darker than the newly grown fibers) was placed across the fiber-wall interface about 6 hours before. A small white box drawn near the bottom of the picture represents the size of the field of view of the porous material of (c) at the current scale. (**b**) Cross-sectional view of the above fibers at the same scale as (a), obtained by detaching the fiber aggregate from the wall after (a) was taken and then dyeing the parted surface in ink to bring out clearer outlines of the grain boundaries. As in (a), a small white box is included in the figure (upper right corner) to show the size of (c) at this scale. (**c**) SEM photomicrograph of the fractured surface of ceramic *P-3-C*.

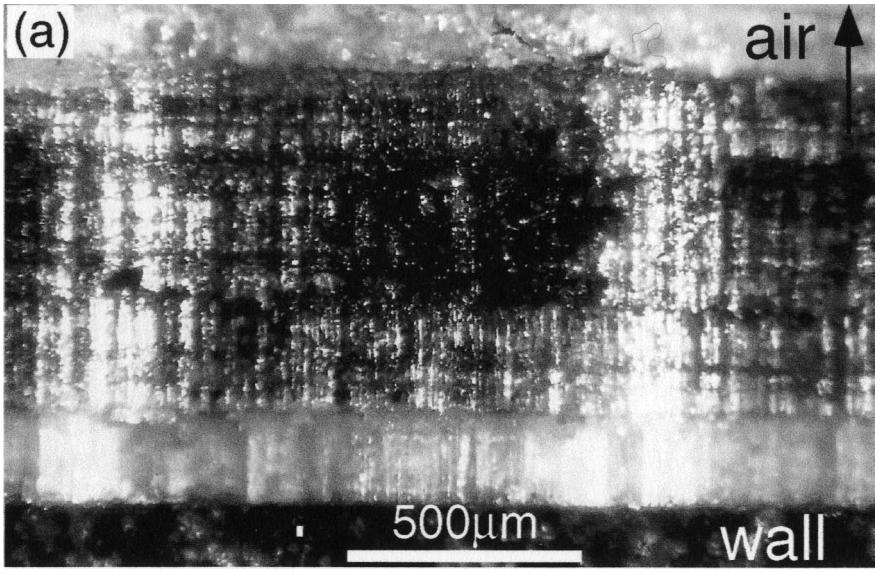
(a)
air
500μm
wall

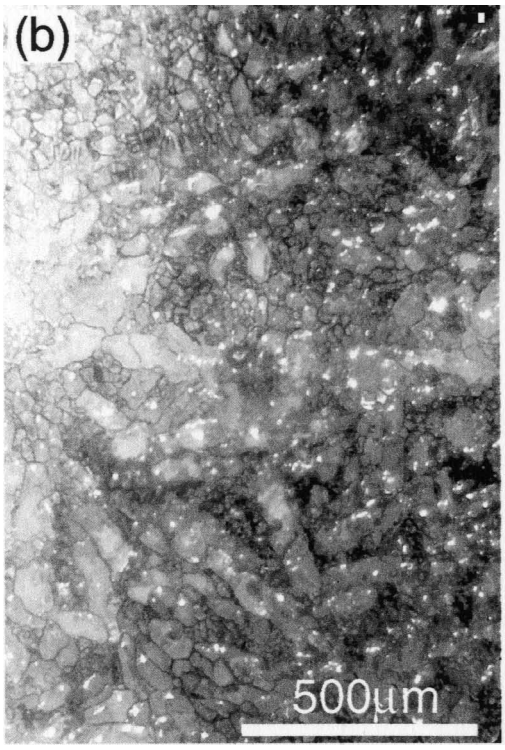
(b)
500μm

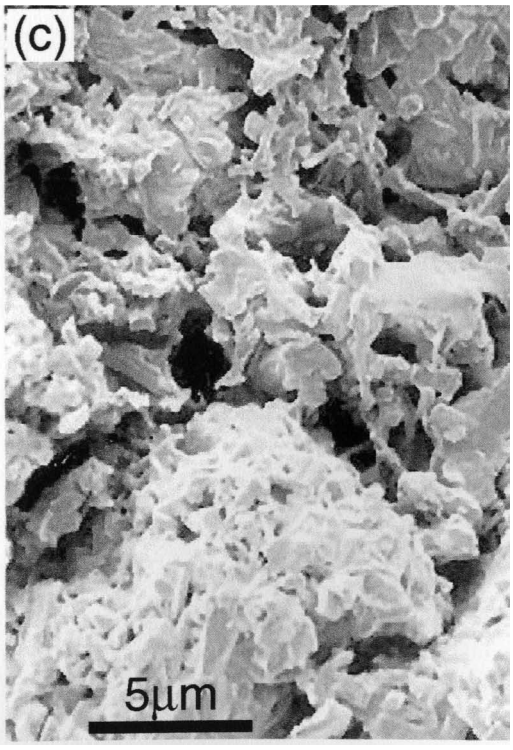
(c)
5μm

Fig. 2.59 Photomicrographs of fibers of *NH_4SCN* grown on pieces of thin cellulosic filter membrane of type *VSWP (*with a nominal pore size of 0.025µm) showing their bundled character and the larger sizes of their constituent fibrils compared with the pore size of the substrate. All photos taken under crossed nicols. (**a**) Fibers grown on *SM-03* which are slightly curved due to their loosely packed nature. Arrow indicates one fiber or fiber bundle that shows maximum extinction. (**b**) Another piece of aggregate of fibers grown on *SM-03*. Photo taken in both transmitted and reflected light. Small white dot on the left has a diameter of 2.5µm which is 100 times the nominal pore size of the substrate. (**c**) Photomicrograph of a fiber ribbon collected from sample *SM-01* showing its internal ridge-and-groove shaped fibrils and inclusion trails. Note optically this is a single fiber since extinction occurs in all the fibrils at the same time. For comparison, a small white box is drawn on the right to represent the size of the field of view of (d). (**d**) SEM micrograph of a typical Millipore filter membrane. Type is not known but pore size rating is shown to be around 0.3-0.8 µm, much larger than the pore size of the 0.025µm type. Photo courtesy of *Millipore.*

(a)

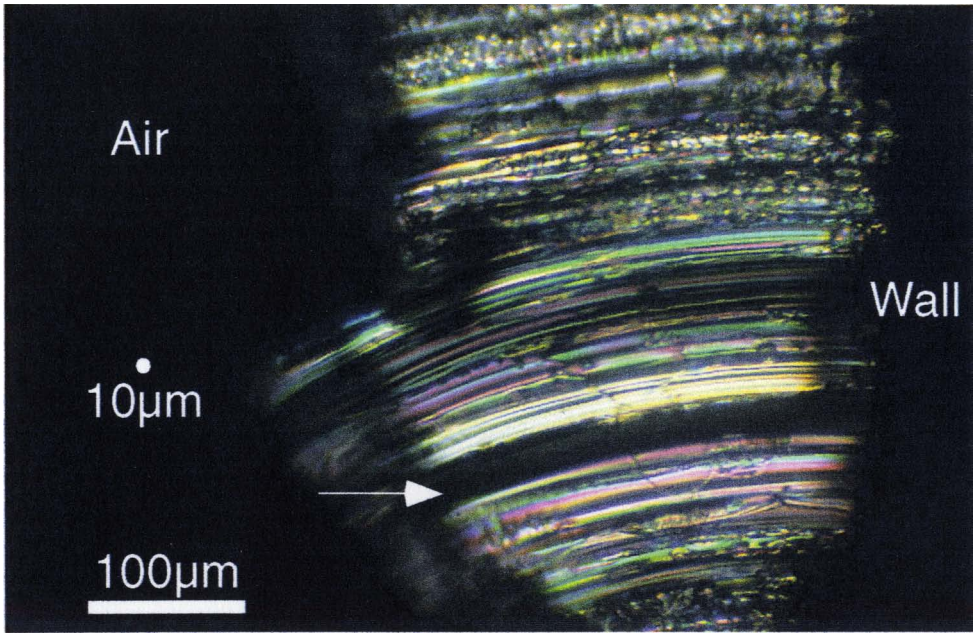

(b)

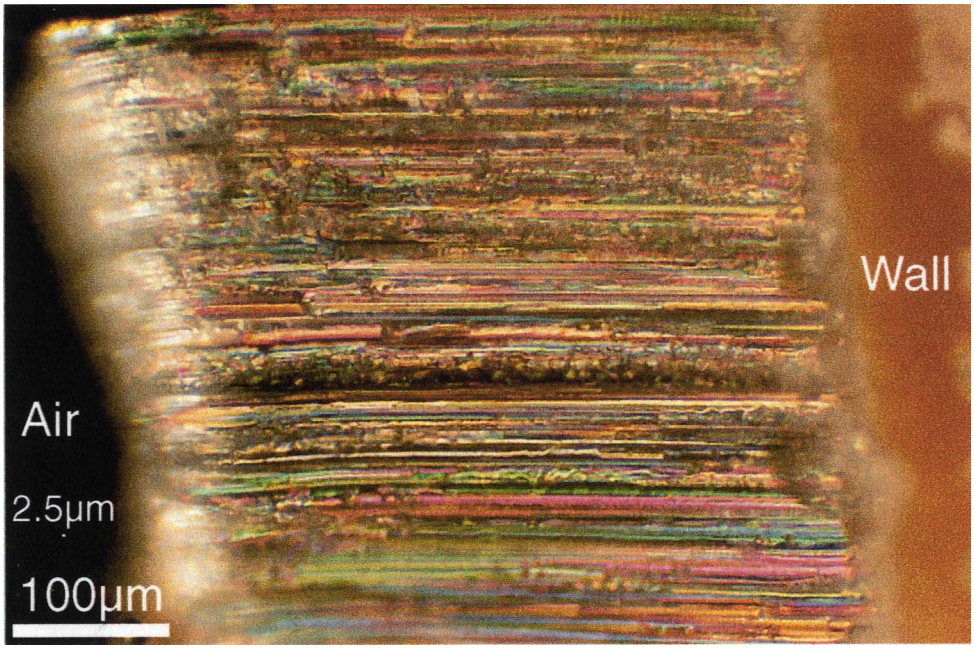

(c)

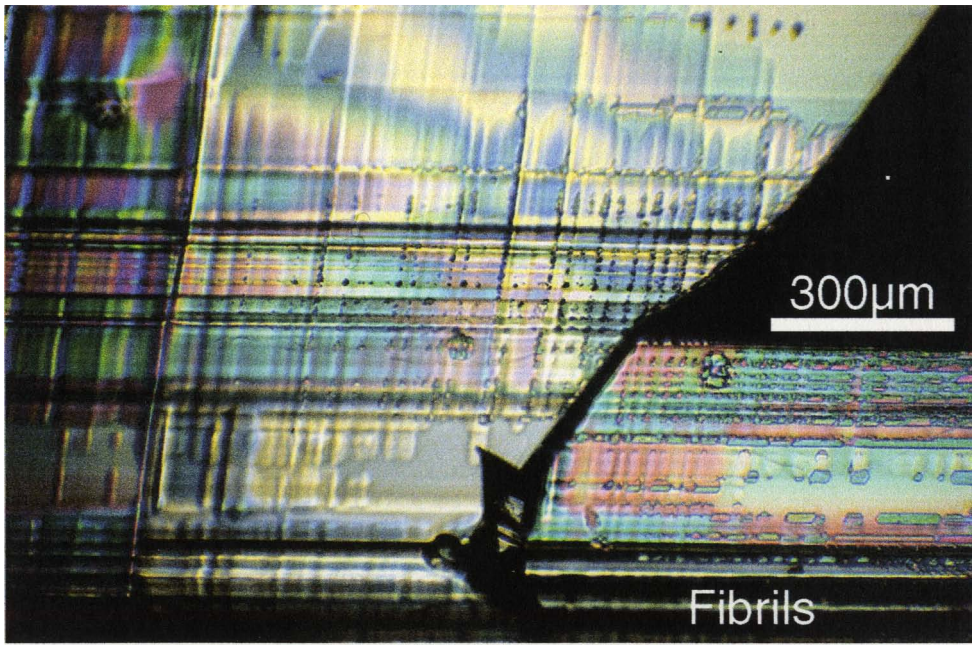

(d)

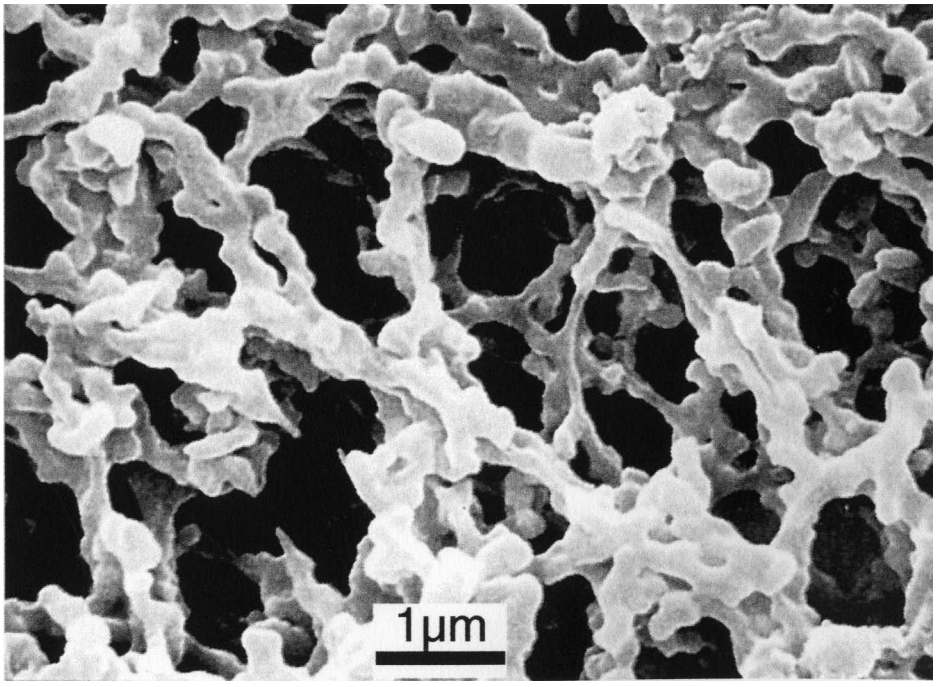

Fig. 2.60 Photomicrographs of fibers or fiber bundles of NH_4SCN collected from sample *SM-07* (grown at a relative humidity of about 35±5%) compared with the pore size of the filter membrane used (type *GSWP*, provided by *Millipore*). (**a**) Photomicrograph of a fresh fiber or fiber bundle from sample *SM-07*, taken under crossed nicols. It is one fiber since optically the whole grain shows uniform extinction, but it consists of many fine fibrils of different thicknesses with varying orders of interference colors, forming a characteristic fluted structure of fibers. The spacing of fluid inclusions in the filbrils is about 2-3 μm, about the same order of the size of fibrils. A small white box near the bottom represents the size of the field of view of (d) drawn to scale. (**b**) Another fiber bundle from sample *SM-07*. Again it gives uniform extinction but is heavily fluted with fine fibrils with varing interference colors. Notice numerous fluid inclusion trails along the fibrils as well as two conspicuous Type I transverse discontinuities across them. The spacing of inclusions ranges between 3-6 μm. A white box is drawn to scale at the bottom to show the field of view of (d). (**c**) Photomicrograph of fibers (one or several fiber bundles) grown on sample *SM-07*, taken under single nicol. Again a white box is drawn to scale at the bottom to represent the field of view of (d) for comparison. (**d**) SEM micrograph of the filter membrane of type *GSWP* (with a nominal pore diameter of 0.22μm). Photo courtesy of *Millipore*. See text for discussion.

(a)

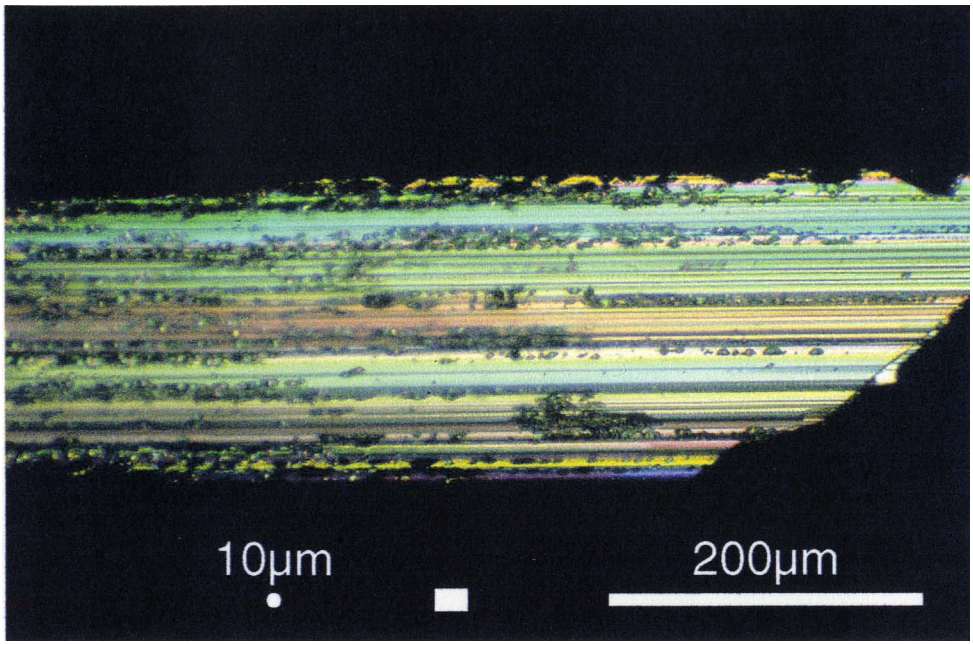

(b)

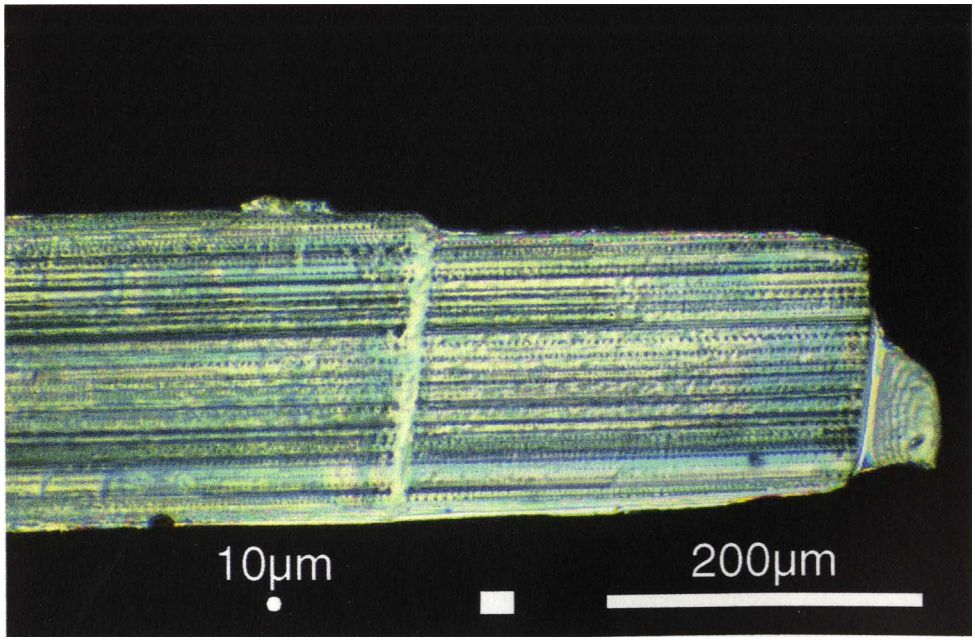

(c)

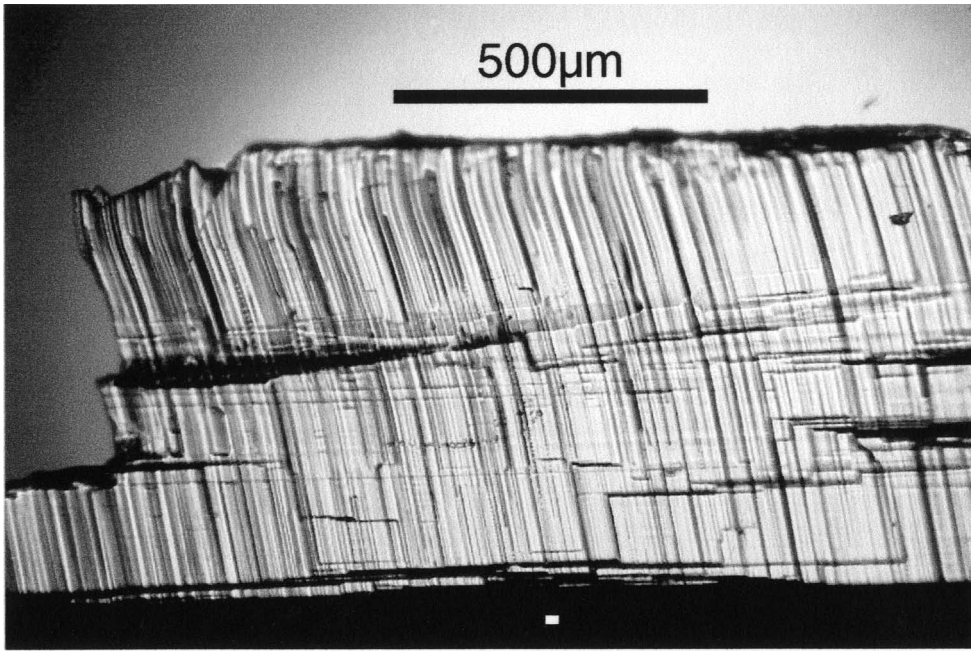

(d)

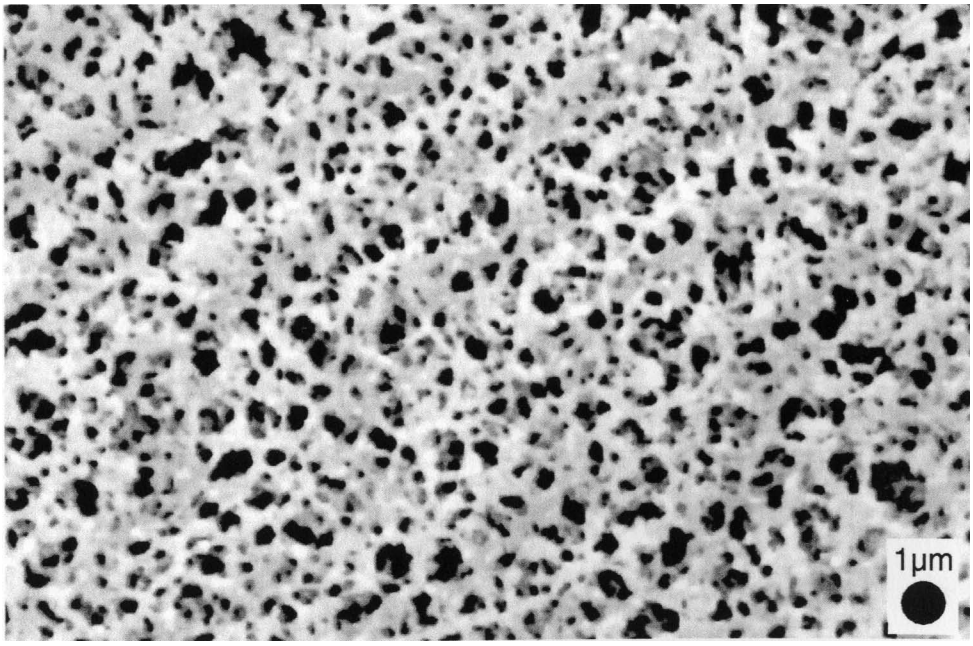

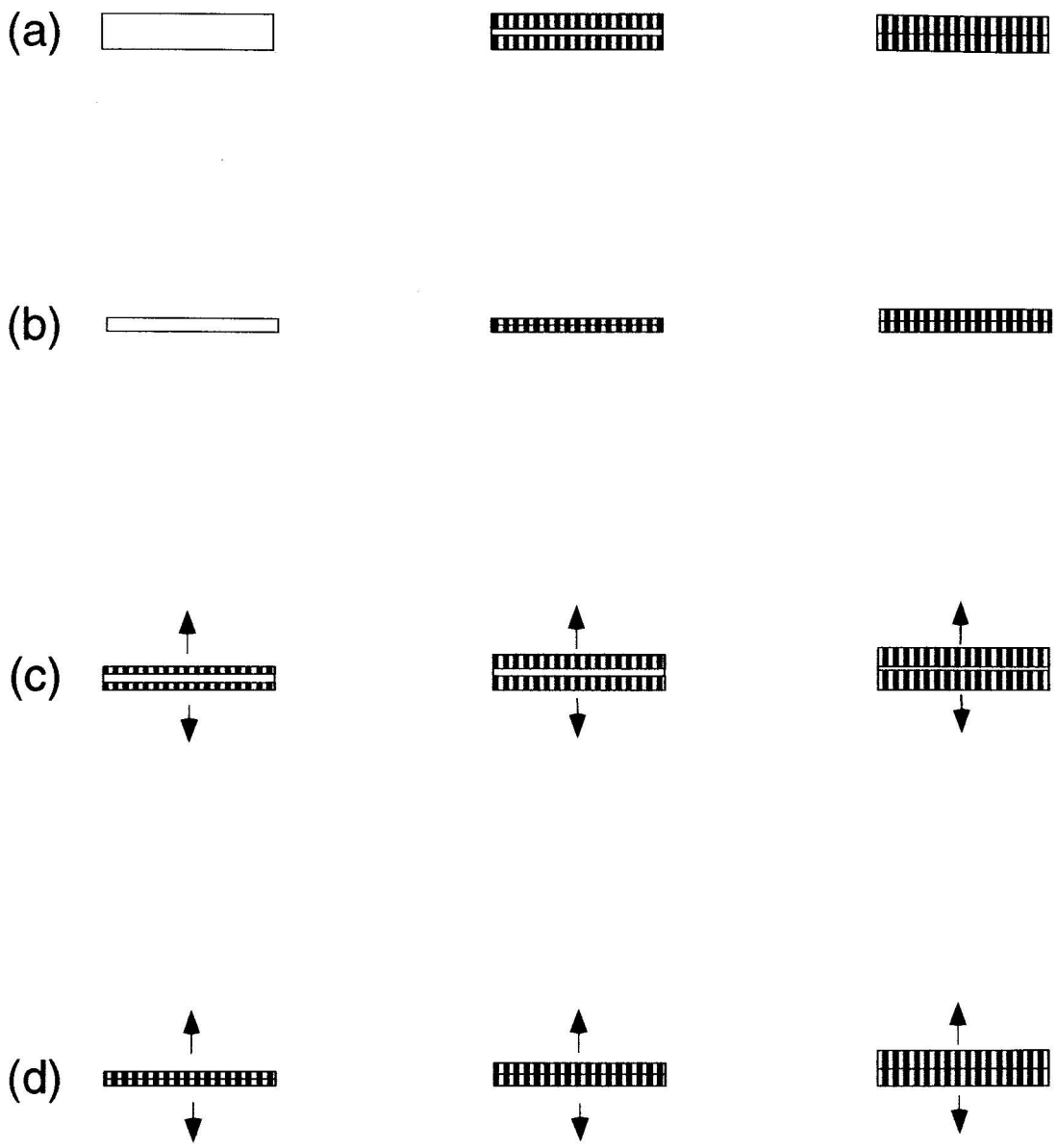

Fig. 2.61 Four different types of vein opening histories. Arrows indicate vein opening induced by tectonic deformation of the wall rocks. (**a**) Growth in a preexisting open fissure without concurrent tectonic deformation in the wall rocks. (**b**) Growth in a preexisting narrow fissure which is later widened to some extent by further growth of fibers, again without concurrent deformation in the wall rocks. (**c**) Growth in a vein that is opening faster than the growth rate as the result of concurrent tectonic deformation in the wall rocks. (**d**) Growth in a vein that would be opening more slowly if opened by tectonic deformation alone without the fibers also pushing away the enclosing walls.